ornl

ORNL/Sub/93-SM037/1

OAK RIDGE NATIONAL LABORATORY

LOCKHEED MARTIN

Innovative Grinding Wheel Design for Cost-Effective Machining of Advanced Ceramics

PHASE I FINAL REPORT

R. H. Licht
S. Ramanath
M. Simpson
E. Lilley

CERAMIC TECHNOLOGY PROJECT

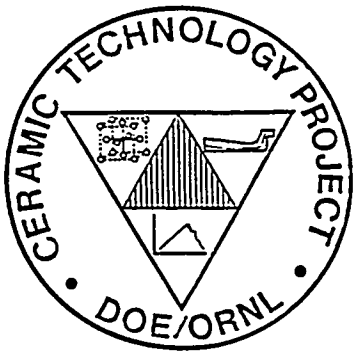

MANAGED AND OPERATED BY
LOCKHEED MARTIN ENERGY RESEARCH CORPORATION
FOR THE UNITED STATES
DEPARTMENT OF ENERGY

ORNL-27 (3-96)

DISCLAIMER

ORNL/Sub/93-SM037/1

INNOVATIVE GRINDING WHEEL DESIGN FOR COST-EFFECTIVE MACHINING OF ADVANCED CERAMICS

R. H. Licht
S. Ramanath
M. Simpson
E. Lilley

Date Published: February 1996

PHASE I FINAL REPORT

Prepared by
Norton Company
Superabrasives Division
Worcester, Massachusetts 01615-0008

Funded by
U.S. Department of Energy
Assistant Secretary for Energy Efficiency and Renewable Energy
Office of Transportation Technologies
Propulsion System Materials Program
EE 51 05 00 0

for
OAK RIDGE NATIONAL LABORATORY
Oak Ridge, Tennessee 37831-6285
managed by
LOCKHEED MARTIN ENERGY RESEARCH CORPORATION
for the
U.S. DEPARTMENT OF ENERGY
under Contract DE-AC05-96OR22464

W.B.S. Element 1.5.0.1

INNOVATIVE GRINDING WHEEL DESIGN FOR COST-EFFECTIVE MACHINING OF ADVANCED CERAMICS

Subcontract No. 87X-SM037V

FINAL REPORT
March 31, 1995

R. H. Licht
S. Ramanath
M. Simpson
E. Lilley

Norton Company
Superabrasives Division
Worcester, MA 016515-0008

Research sponsored by the U.S. Department of Energy, Assistant Secretary for Energy Efficiency and Renewable Energy, Office of Transportation Technologies, as part of the Ceramic Technology Project of the Propulsion Systems Materials Program, under contract DE-AC05-96OR22464 with Lockheed Martin Energy Research Corporation.

TABLE OF CONTENTS

1. EXECUTIVE SUMMARY

Major impediments to the commercialization of advanced ceramics are reliability and cost. Toward the objective of improving reliability and reducing manufacturing cost, the U.S. Department of Energy, Office of Transportation Technologies, under contract with Martin Marietta Energy Systems (MMES), Inc. has sponsored research as part of the Ceramic Technology Project (CTP). The goal of the CTP, managed at ORNL, is to develop highly reliable and cost-effective structural ceramics for advanced heat engine applications such as automotive gas turbine, piston and diesel engines. The Cost-Effective Ceramic Machining (CECM) Program was established as part of the CTP in recognition of the importance of machining to commercializing advanced ceramics. The CECM recognized that ceramic machining, predominantly diamond grinding, is a major cost factor in advanced ceramics manufacturing. The abrasive wheel performance significantly influences the grinding costs. Additionally, the quality of the grinding operation greatly affects ceramic surface integrity, tolerance and manufacturing yield.

The Innovative Grinding Wheel Program was performed in response to MMES Request for Proposal No. SM037-87 and was managed under the CECM Program. The objectives of the Phase 1 program were: to define requirements, design, develop and evaluate a next-generation grinding wheel for cost-effective cylindrical grinding of advanced ceramics. Innovative wheel compositions optimized for cylindrical grinding could be relatively easily optimized for other machining operations such as centerless, surface and ID grinding. The Norton team achieved the Phase 1 objectives, demonstrating an experimental metal bonded wheel with diamond superabrasive that resulted in significantly improved grinding performance over standard wheels when evaluated in cylindrical grinding of three types of advanced ceramics.

The scope of the program involved a cooperative effort involving three Norton groups. The overall program was led by Norton Company Abrasives. Under this group the Abrasives R&D group led the technical effort while wheel manufacturing and eventual wheel commercialization is the responsibility of the Superabrasives Division. Norton Company Abrasives R&D designed and developed a novel metal bond system, and performed the wheel tests at the Norton World Grinding Technology Center. The second group, Norton Diamond Film Division, conducted a parallel and complementary research and development effort that incorporated a novel design chemical vapor deposition (CVD) diamond film wheel system. The third group, the Northboro Research and Development Center (NRDC), supplied ceramic specimens for the grinding tests and evaluated surface integrity in the ground ceramics.

The program was divided into two technical tasks: 1) Analysis of Required Grinding Wheel Characteristics and 2) Design and Prototype Development.

The major work in our Task 1, analysis of required grinding characteristics, was a thorough analysis of wheel bond characteristics. There are three major bond types that hold the abrasives: resin, glass or vitrified, and metal bond. Each bond system has advantages and disadvantages for grinding ceramics. Resin bonded wheels are the most widely used as an all purpose grinding wheel for ceramics. Resin bond products are free cutting and a good starting points for grinding a wide range of advanced ceramics, but do not possess adequate life, and require frequent truing and dressing. Vitrified-bonded wheels can provide better life but need to be handled with caution because of the brittle nature and lower strength of the bond. Current or conventional metal bonds have been found to be excessively durable and consume more power in grinding fine grain size ceramics, but require frequent dressing to remove worn abrasives, and expose new sharp ones. Metal bonds have the advantage of higher strength and higher wheel speed capability. Our initial focus of bond design in this program was to work in metal bond systems with the objective of developing a system that possesses the most favorable attributes of all current bond systems. Specifically, experimental metal bonds were designed to give intermediate grinding action between standard resin and metal bonds.

A critical parameter in controlling the cost and quality in a ceramic machining operation is determining the precise point at which dressing or truing is required. Truing refers to regenerating the original profile on the wheel and also making it run concentric to the axis of rotation. Dressing is the process used to expose the abrasive grit above the bond level for efficient grinding action. Truing and dressing operations are essentially non-productive wheel wear and account for a significant portion of abrasive cost in ceramic machining. Therefore, understanding the truing and dressing characteristics of a grinding wheel is also essential to any wheel development program aimed at manufacturing efficiency.

Task 1 was also designed to determine the structural and composition requirements for next generation grinding wheels. This analysis included the mechanical, thermal and coolant absorption characteristics of the system; type and characteristics of the abrasive grit; analysis of the wheel stiffness characteristics; identification of economic targets for wheel and process costs; and development of wheel behavior models.

Our approach expanded Task 1 to include bond-only wear and strength tests. This series of tests allowed us to model the experimental bonds to give intermediate grinding characteristics between standard resin and metal bonds. Task 1 culminated in a large experimental matrix of 76-mm screening wheels, used to grind sialon disks in a cylindrical plunge test. Some experimental bonds demonstrated significant improvements over standard resin bond wheels. Additionally, the experimental metal bond demonstrated the ability to grind significantly more than standard metal bonds without loading. By using this screening test approach, we were able to test approximately 45 Superabrasive wheel variables before down selecting to the most promising bonds for the Task 2, 203-mm diameter tests.

The novel CVD diamond wheel approach was incorporated in this program as a part of Task 1. The work was designed to include a small-wheel screening test complementing the main Superabrasive metal-type bond approach. The higher risk CVD

diamond wheel approach was to be a feasibility study and was not planned for continuation into Task 2, Design and Prototype Development. The CVD approach was considered a higher risk but was considered to have a high-potential payoff in applying this new technology to machining of ceramics. The CVD diamond wheel activity was concluded in Task 1 as planned. The initial CVD wheel design was unsuccessful. A thin CVD diamond wheel was redesigned and tested. This test was designed to evaluate the basic grinding characteristics of this new CVD diamond design. Diamond thickness and preform geometry had the greatest impact on performance. While significant grinding improvements were noted from the initial screening test, the results were not promising for this type of operation compared to conventional grinding wheels. The CVD wheel approach does not appear at this stage to offer promise for cost-effective cylindrical grinding of ceramics. Other possible abrasive applications for this approach will be explored.

Task 2 was intended to design and construct prototype wheels and evaluate grinding performance on at least two commercial grades of silicon nitride rods. Grinding characteristics include surface roughness, spindle power, grinding forces, wheel dressing characteristics, wheel loading characteristics, wheel wear, vibration characteristics, and coolant compatibility. There were two major considerations in selecting the ceramic materials used for assessing the grinding performance of new wheels in this program. The first was the relevance of the material to transportation technology components. The second criterion was that the materials must be commercial and have reduced volume flaw characteristics so as not to mask severe grinding damage that could be produced with new grinding products or incorrect dressing. Saint-Gobain/Norton Industrial Ceramics Corporation's NC-520 sialon, NCX-5102-HIP'ed Si_3N_4 and AZ67H-20% ZTA meet the above criteria and were chosen for Task 2.

In Task 2, a series of the most promising metal bonds from Task 1 were scaled up to 203-mm (8-in.) diameter test wheels. An improved Superabrasive metal-bond specification for low-cost machining of ceramics in external cylindrical grinding mode was demonstrated. The 203-mm diameter test wheel made in this bond contained 75 concentration diamond abrasives of size U.S. mesh 270/325. The wheels were tested on a CNC instrumented cylindrical grinder in both plunge and transverse test conditions. The experimental wheel successfully ground three types of advanced ceramics, sialon, HIP'ed Si_3N_4 and ZTA, for extended time without the need for wheel dressing. The spindle power consumed by this wheel during test grinding of NC-520 sialon is as much as to 30% lower than with a standard resin-bonded wheel with 100 diamond concentration, that is typically used in this application. The wheel wear with this improved metal bond was an order of magnitude lower than the resin-bonded wheel, which would significantly reduce ceramic grinding costs through fewer wheel changes for retruing and replacements. The projected manufacturing cost of this experimental wheel is not appreciably different from standard resin- and metal-bonded superabrasive wheels, and therefore this experimental wheel would have a significant cost advantage in grinding ceramics.

An essential element to our approach was to quantify surface integrity and assess surface damage caused by the new products. Grinding wheel performance should be evaluated by not only grinding system factors such as force, power, wheel wear, cut rate, G-ratio, and dressing characteristics; but also on ceramic surface integrity considerations such as retained strength, surface finish, surface damage and residual stress. It was essential that a next-generation grinding wheel that could significantly reduce machining costs would not compromise surface integrity on the machined ceramic parts.

In the Task 1 small-wheel screening test, we performed optical examination and C-ring compression tests of selected sialon disks. For the C-ring compression tests, corner breaks and the limited number of data points made comparative conclusions suspect. However, the experimental results did not show evidence of unusual grinding damage to the ceramic disks. More comprehensive flexure testing was planned and done for the Task 2 rods. Stresses generated during flexural testing was normal to the grinding direction, which resulted in a more meaningful cylindrical grinding damage evaluation. Therefore, the C-ring test in Task 1 was determined to have limited usefulness as a qualitative assessment of grinding damage.

For the Task 2 large-wheel test, optical examination and flexure test of three types of ceramic rods ground by experimental metal-bond wheels and standard resin wheels did not show any unusual grinding damage. The sialon rods had strengths similar to the resin-bonded wheel flat-ground MOR specimens and there was no noticeable difference between the resin- and metal-wheel ground specimens. This indicates that the innovative experimental wheel did not create unusual or excessive machining damage compared to the standard resin-bond product while retaining its enhanced performance and cost effectiveness.

2. LIST OF TABLES

3. LIST OF FIGURES

INNOVATIVE GRINDING WHEEL DESIGN FOR COST-EFFECTIVE MACHINING OF ADVANCED CERAMICS

R.H. Licht, S. Ramanath, M. Simpson, and E. Lilley
Norton Company, Worcester and Northboro, Massachusetts

4. ABSTRACT

Norton Company successfully completed the 16-month Phase 1 technical effort to define requirements, design, develop, and evaluate a next-generation grinding wheel for cost-effective cylindrical grinding of advanced ceramics.

This program was a cooperative effort involving three Norton groups representing a superabrasive grinding wheel manufacturer, a diamond film manufacturing division and a ceramic research center. The program was divided into two technical tasks, Task 1, Analysis of Required Grinding Wheel Characteristics, and Task 2, Design and Prototype Development. In Task 1 we performed a parallel path approach with Superabrasive metal-bond development and the higher technical risk, CVD diamond wheel development.

For the Superabrasive approach, Task 1 included bond wear and strength tests to engineer bond-wear characteristics. This task culminated in a small-wheel screening test plunge grinding sialon disks. Task 1 screening tests demonstrated experimental bonds that performed significantly better than both standard resin- and standard metal-bond wheels. The use of this screening test approach allowed for many wheel variables to be evaluated before down selecting to the most promising bonds for Task 2.

In Task 2, an improved Superabrasive metal-bond specification for low-cost machining of ceramics in external cylindrical grinding mode was identified. The experimental wheel successfully ground three types of advanced ceramics without the need for wheel dressing. The spindle power consumed by this wheel during test grinding of NC-520 sialon is as much as to 30% lower compared to a standard resin bonded wheel with 100 diamond concentration. The wheel wear with this improved metal bond was an order of magnitude lower than the resin-bonded wheel, which would significantly reduce ceramic grinding costs through fewer wheel changes for retruing and replacements. The projected manufacturing cost of this experimental wheel is not appreciably different from standard resin- and metal-bond superabrasive wheels, and therefore this experimental wheel would have a significant cost advantage in grinding ceramics. Evaluation of ceramic specimens from both Tasks 1 and 2 tests for all three ceramic materials did not show evidence of unusual grinding damage.

The novel CVD-diamond-wheel approach was incorporated in this program as part of Task 1. The important factors affecting the grinding performance of diamond wheels made by CVD coating preforms were determined. Diamond thickness and preform geometry had the greatest impact on performance. While significant grinding

improvements were noted during the Task 1 investigation, the results were not promising for this type of operation compared to conventional grinding wheels. The CVD wheel approach does not appear at this stage to offer promise for cost-effective cylindrical grinding of ceramics.

5. INTRODUCTION

Ceramic machining, predominantly diamond grinding, is a major cost factor in advanced ceramics manufacturing. The abrasive wheel performance significantly influences the grinding costs. Additionally, the quality of the grinding operation greatly affects ceramic surface integrity, tolerance and manufacturing yield.

5.1 CERAMIC MACHINING MARKET

Beginning with ceramic pottery that required no machining, today we have ceramics that are ground to surface finishes typically a few hundred nanometers down to several angstroms. Finishes in the range of 0.1-0.3μm (4-12μin) are required for most wear and engine components while finer finishes are required for parts such as silicon wafers, ceramic mirrors and ceramic bearing components. Advanced ceramic materials are inorganic, usually covalent-bonded polycrystalline structures, that are strong, refractory, and have high hardness. Therefore they are inherently difficult to machine or polish. Typically, the finishing of ceramics into useful components requires an abrasive (~70% of the time) or a non-abrasive machining process. The worldwide ceramic grinding market for resin-bonded wheels is approximately $271 million and for metal-bonded wheels is approximately $280 million[1]. These markets may be classified into four major segments: industrial ceramics, electronic ceramics, technical ceramics, and advanced ceramics. The advanced ceramics market (ceramic bearings, engine components, etc.) are characterized by the key requirements of close tolerances, good retained strength after grinding and good surface finish. Even though the advanced ceramics market is small, the growth rate is the highest. The most common method for finishing of ceramic components has been using diamond abrasive wheels. The primary reason for the widespread use of diamond is its high hardness required by the hardness of the workpiece.

5.2. INDUSTRY REQUIREMENTS - COST AND QUALITY CONSIDERATIONS

5.2.1. DOE Cost-Effective Ceramic Machining Initiative

Advanced ceramics posses unique properties of high temperature durability, corrosion resistance, strength, hardness, stiffness and wear resistance. These properties make advanced ceramics attractive to many applications in the transportation, energy, military, and industrial markets. Major impediments to the commercialization of advanced ceramics are reliability and cost. Toward the objective of improving reliability and reducing manufacturing cost, the U.S. Department of Energy, Office of Transportation Technologies, under contract with Martin Marietta Energy Systems (MMES), Inc. has sponsored research as part of the Ceramic Technology Project (CTP). The goal of the CTP, managed at ORNL, is to develop highly reliable and cost-effective structural ceramics for advanced heat engine applications such as automotive gas turbine, piston and diesel engines. The Cost-Effective Ceramic Machining (CECM) Program was established as part of the CTP in recognition of the importance of machining to commercializing advanced ceramics. The CECM led a series of workshops to identify industry and government needs. Two ORNL workshops identified abrasives and grinding wheels as a major issue and opportunity[2,3]. While ceramic machining can involve several abrasive and non-abrasive techniques, the majority of advanced ceramic machining operations involve diamond grinding operations. This program was performed in response to MMES Request for Proposal No. SM037-87 and was managed under the CECM Program. The RFP emphasized cylindrical grinding of silicon nitride and other advanced ceramics. Norton believes this emphasis on silicon nitride and cylindrical grinding is consistent with the majority of transportation component needs. We are also confident that innovative wheel compositions optimized for cylindrical grinding of advanced ceramics can be relatively easily optimized for other machining operations such as centerless, surface and ID grinding.

5.2.2. Ceramic Machining Cost Considerations

It is widely recognized in the advanced ceramics community that the machining operation is the largest single manufacturing cost category. A survey of all Norton industrial ceramic businesses showed that typical machining costs range from 20% - 70% of the total cost of manufacturing depending on product requirements[2,4]. Advanced ceramic manufacturers such as Norton Advanced Ceramics (NAC) identified machining cost as a major impediment to widespread use of ceramic engine components. The reasons for the high machining costs are: 1) it is capital and labor intensive, 2) expensive diamond abrasive is consumed, and 3) production rates are relatively low. The requirement for wheel dressing has also been identified as a significant factor in abrasive cost.

5.2.3. Reliability - Ceramic Surface Integrity

In addition to cost considerations, the second major challenge to introducing a new grinding wheel system is maintaining ceramic quality and surface integrity. For example, relatively economical cut rates can be accomplished by grinding in the brittle mode of material removal. However, for some applications it may be necessary to change to finer grit size wheels and much lower removal rates in order to work in the ductile mode and minimize sub-surface damage. Unfortunately the sub-surface median cracks are extremely difficult to see so that parts damaged by machining can not be picked out by inspection.

It is critical to have close cooperation and support between the grinding wheel manufacturer and the ceramic material supplier. Norton Company, with both abrasive and industrial ceramics branches, could take advantage of a customer-supplier relationship within the same parent organization, which maximized the synergy of this program.

An essential element to our approach was to quantify surface integrity and assess surface damage caused by the new products. Grinding wheel performance should be evaluated by not only grinding system factors such as force, power, wheel wear, cut rate, G-ratio, and dressing characteristics; but also on ceramic surface integrity considerations such as retained strength, surface finish, surface damage and residual stress. It was essential that a next-generation grinding wheel that could significantly reduce machining costs would not compromise surface integrity on the machined ceramic parts.

Surface integrity assessment was an essential part of confirming that an acceptable new grinding wheel was developed. Budget considerations in this Phase 1 program limited the scope of the surface integrity characterization to selected samples ground by standard and the best performing experimental wheels. The characterization included surface finish, microscopic surface examination, C-ring compression tests on disks and ceramic rod flexure strength. In a Phase 2, independent wheel validation program, it is recommended that more extensive retained strength be done to quantify grinding damage, and that residual stress in the ground surface be characterized and compared to standard grinding conditions. Residual stresses left behind from machining at and below the surface can influence the final mechanical properties of the workpiece[5-7]. Meaningful residual stress distribution measurements on curved surfaces is a procedure that requires some development.

5.2.4. Grinding Wheel Dressing Considerations

The requirements of any typical advanced ceramic component manufacturer are to produce quality components of acceptable tolerances, part geometry, surface finish, and part strength at cost viable material removal rates. This implies that there are several requirements that have to be satisfied simultaneously. It is possible, for example, to hold the tolerance by using strong diamond types. However the resulting part strength may

decrease because of the damage caused by grinding with "flattened" and worn abrasive particles.

One of the most critical parameters in controlling the cost and quality in a ceramic machining operation is determining the precise point at which dressing or truing is required. Truing refers to regenerating the original profile on the wheel and also making it run concentric to the axis of rotation. Dressing is the process used to expose the abrasive grit above the bond level for efficient grinding action.

Acceptable upper and lower control values for tolerance, finish, part strength, spindle power, etc., should be set in any grinding operation. Typically, a freshly trued and dressed wheel should meet all requirements simultaneously. As more components are ground, there would be a point in time when one of the requirements is not met, and the wheel must be trued and dressed. A schematic of the dressing operation control limits is shown in Figure 1. At time, $t = t_o$, the acceptable tolerance, finish, strength, power values are set based on component performance requirements. During grinding, time, $t = t_n$, represents the point when one of the grinding limits (in this example spindle power) is exceeded. This indicates that it is time to either dress or true the wheel (depending on set grinding factors).

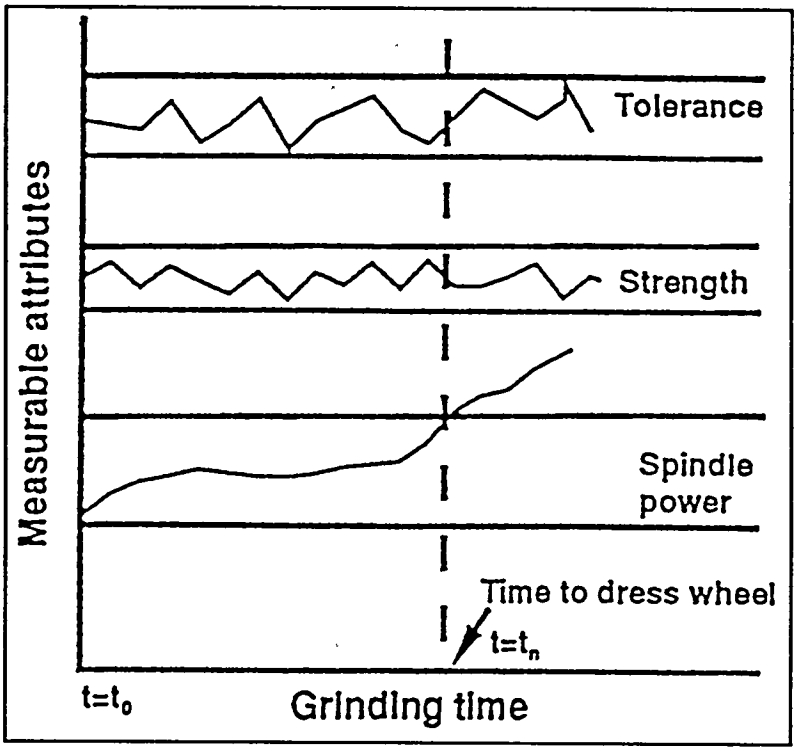

Figure 1. Schematic figure of measurable attributes of a grinding process versus time showing the need for dressing.

Truing and dressing is essentially non-productive wheel wear and this accounts for a significant portion of the abrasive costs in ceramic machining. Understanding the truing and dressing characteristics of a grinding wheel is essential to any wheel development program.

5.2.5 Wheel Bond Selection

There are primarily three major bond types that hold the abrasives: resin, glass or vitrified, and metal bond[8,9]. Each existing bond system has advantages and disadvantages for grinding ceramics. Table 1 summarizes the characteristics of these bond systems.

Resin-bond products are good starting points for grinding a wide range of advanced ceramics, producing quality surfaces with good part strength. However, the resin-bonded wheels do not possess adequate life, and require frequent truing and dressing. Resin-bonded wheels are the most widely used, all purpose wheel for grinding ceramics. Vitrified-bonded wheels can provide better life but need to be handled with caution because of the brittle nature and lower strength of the bond. Vitrified-bond products also pose considerable limitations for use in higher-speed grinding. Conventional metal bonds have been found to be exceptionally durable and consume more power in grinding fine grain size ceramics, requiring frequent dressing to remove the worn abrasives, and expose sharp ones. However, metal bonds have the advantage of higher strength and higher wheel speed capability. High-speed grinding has shown significant potential for ceramic grinding[10]. Metal bonds also have the ability to be dressed by new, electrodischarge techniques, such as Electrolytic In-Process Dressing (ELID)[11].

Our initial focus of bond design in this program was to work in metal-bond systems with the objective of developing a system that possesses the most favorable attributes of resin and metal bonds. Further discussion of bond material characteristics is described in the results section, 7.1, Analysis of Grinding Wheel Requirements.

In order to understand the grinding process, we need to look at the interactions at the grinding zone as shown in Figure 2. They include abrasive/work, bond/work, chip/work and chip/bond interactions. While abrasive-work interaction leads to material removal, the other three result in rubbing and energy loss, which lead to adverse surface quality. The bond/work energy loss may be reduced by lowering the contact area between bond and work through experimental modification of the bond. This was one of our approaches in this program. The chip/bond interaction leads to wear of the bond. The size of the chip is very important and could be controlled by changing the grinding parameters like wheel speed, depth of cut and wheel parameters like abrasive size and combination. For efficient grinding, we need sharp cutting points, good chip clearance, strong abrasive retention and self-sharpening abrasive in a bond matrix that is resistant to attritious wear yet possesses good lubricating properties. We believe all these requirements can be designed into a metal bond.

Table 1. Bond Types and Their Characteristics

RESIN (Polymer Matrix)	VITRIFIED (Glass Matrix)	METAL (Metal Matrix)	
Multilayer	Multilayer	Multilayer	Single Layer
• Easy to use • Inexpensive • Easy to true/dress • Freeness of cut • Range of ceramic work materials • Good finish	• Controlled porosity • Free cutting • Easy to true • May not need dressing • Intricate forms • High contact areas (creepfeed) • Holds form longer	• Durable • High stiffness (thin wheels okay) • Good form holding • Good heat removal • High speed potential • Withstands abuse • Electro-discharge dressing	• Free cutting • High stock removal • High accuracy forms • High abrasive density
• Low life • Poor form holding • Not high removal rates	• No chemical bond • Speeds limited • Not for thin cut-off wheels • Prone to cracking due to misuse	• Existing bonds are difficult to dress	• Low life due to single layer • Not trueable

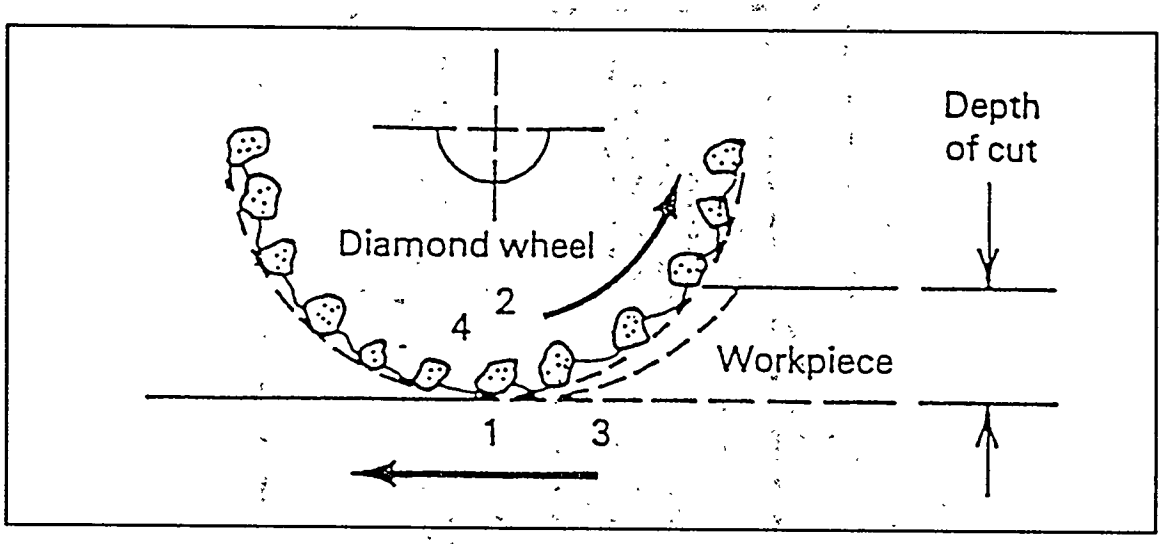

Figure 2. Schematic illustrating interactions in the grinding zone of a grinding wheel/workpiece interface. 1. Abrasive/work interface; 2. Chip/bond interface; 3. Chip/work interface; 4. Bond/work interface.

5.2.6 Ceramic Material Selection

There were two major considerations in selecting the ceramic materials for assessing the grinding performance of new wheels in this program. The first was the materials' relevance to transportation technology components. The second criterion was that the materials must be commercial and have reduced volume flaw characteristics so as not to mask severe grinding damage that could be produced with new grinding products or incorrect dressing.

The intent of the RFP was to develop a wheel for cylindrical grinding of components such as engine valve stems. Currently Norton Advanced Ceramics (NAC) produces sialon valves, and sialon is the base material for NAC's program in Advanced Ceramic Manufacturing under the DOE/ORNL CTP. Therefore we selected NRDC's NC-520 sialon as the primary material for both Tasks 1 and 2 grinding tests. The second material selected was NRDC's NCX-5102, which is a HIP'ed Si_3N_4 - 4% Y_2O_3 developed for high temperature (1371°C) gas turbine applications. NCX-5102 was developed by NRDC to demonstrate high ceramic reliability under a CTP contract[12]. It was desirable to evaluate the new grinding wheel products on an oxide ceramic. The third material selected was AZ67H zirconia toughened alumina (ZTA). This material is an 80% Al_2O_3 transformation toughened with a second phase tetragonal zirconia polycrystal (TZP). AZ67H has shown promise in ceramic roller follower tests[13,14] and is currently produced by Norton Advanced Ceramics for several wear component applications such as metal-forming dies.

All three materials are considered fully dense and contain reduced flaw populations so that any severe grinding damage produced by new wheels would not be hidden. As an example, for NCX-5102, the DOE sponsored Program in Advanced Processing[12] has shown that as volume flaws in silicon nitride are reduced, failure will occur from grinding-related surface breaks, even in tensile testing of large-volume, longitudinally-ground specimens[15,16].

6. OBJECTIVE/SCOPE

The objectives of the Phase 1 program were: to define requirements, design, develop, and evaluate a next-generation grinding wheel for cost-effective cylindrical grinding of advanced ceramics. The objectives are divided into two technical tasks:

1. Analysis of Required Grinding Wheel Characteristics - This task objective was to determining the structural and composition requirements for grinding wheels for cylindrical grinding of silicon nitride and other ceramic parts. The analysis was to include the mechanical, thermal, and coolant absorption characteristics of the system; type and characteristics of the abrasive grit; analysis of the wheel stiffness characteristics; identification of economic targets for wheel and process costs; and development of wheel behavior models.

2. Design and Prototype Development - This task objective was to design and construct prototype wheels and evaluate grinding performance on at least two commercial grades of silicon nitride rods. Grinding characteristics include, surface roughness, grinding forces, wheel dressing characteristics, wheel-loading characteristics, wheel wear, vibration characteristics and coolant compatibility. This task was to culminate in the delivery of six duplicate wheels of the optimized grinding wheel to MMES.

The scope program involved a cooperative effort involving three Norton groups. This effort had the following approach and division of responsibilities. The overall program was led by the Norton Company Abrasives R&D Division. Wheel manufacturing and eventual wheel commercialization will be the responsibility of the Norton Company Superabrasives Division. Norton Company Abrasives R&D designed and developed a novel metal-bond system, and performed the wheel tests at the Norton World Grinding Technology Center. The second group, Norton Diamond Film Division conducted a parallel and complementary research and development effort that incorporated a chemical vapor deposition (CVD) diamond film wheel system. The third group, the Northboro Research and Development Center (NRDC), supplied ceramic specimens for the grinding tests and evaluated surface integrity in the ground ceramics. Norton Diamond Film and NRDC are divisions of Saint-Gobain/Norton Industrial Ceramics Corporation (SGNICC), which is a subsidiary of Norton Company. Figure 3 illustrates the overall Innovative Grinding Wheel Program Plan and shows the interaction of the three research groups.

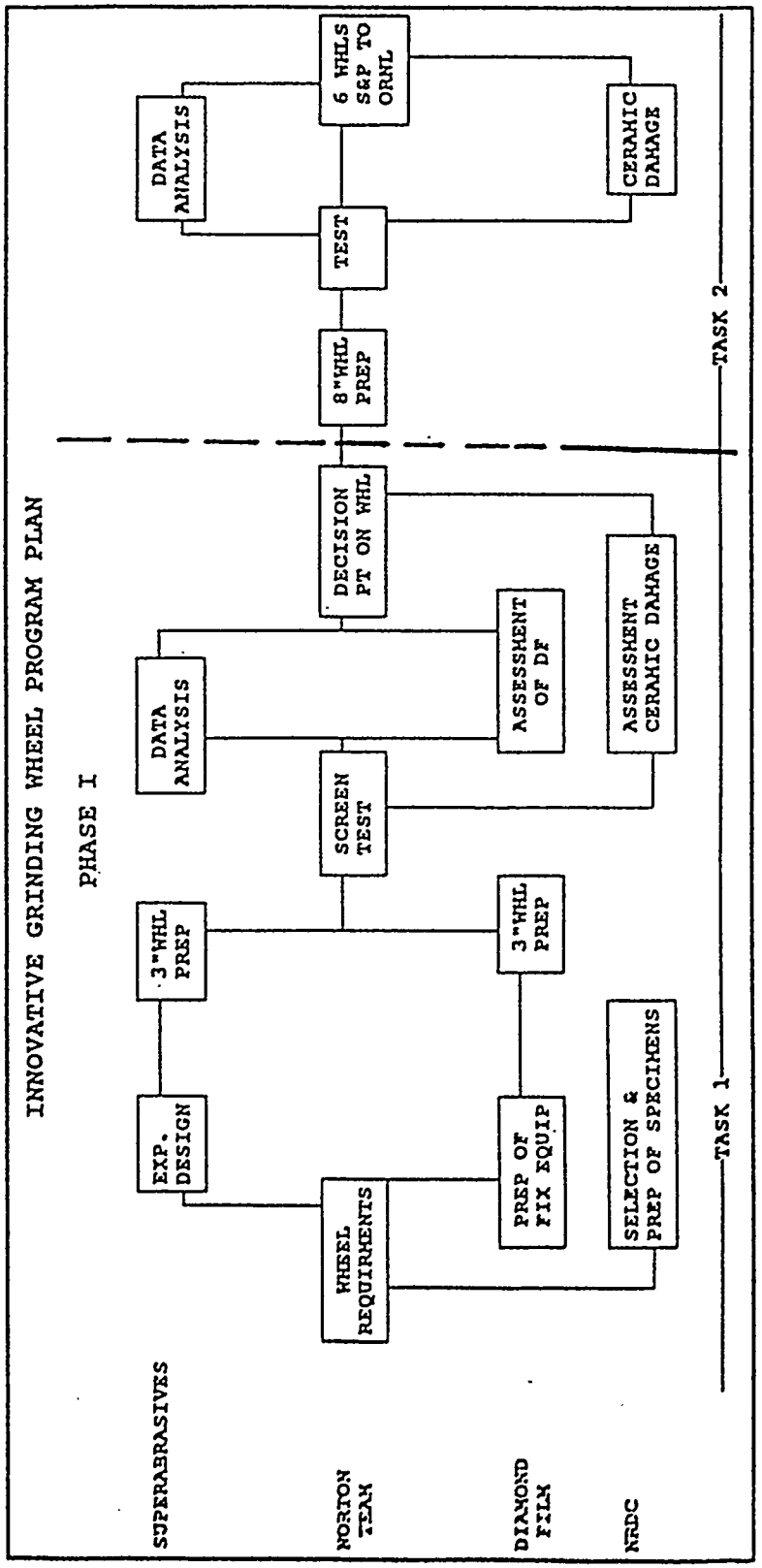

Figure 3. Innovative Grinding Wheel Program Plan

The parallel-path approach was carried out in Task 1, Analysis of Required Grinding Wheel Characteristics. This task involved the design of the bond with respect to mechanical and thermal characteristics, and the selection of the diamond grit. To better achieve the analysis requirements of Task 1, we proposed and completed significant experimental testing of new bond compositions and completed a large grinding test matrix. Task 1 culminated in this small-wheel (76mm diameter) screening test involving controlled feed plunge grinding of sialon test disks.

Task 2, Design and Prototype Development, we down-selected to a few wheel types for further design and optimization. The manufacturing process was scaled up from the 76-mm (3-in.) wheels to 203 mm wheels. These 203-mm (8-in.) diameter prototype wheels were tested in a cylindrical mode, grinding ceramic rod specimens similar in geometry to valve stems. Grinding wheel performance was assessed on three types of ceramic specimens: NC-520 sialon, NCX-5102 HIP'ed silicon nitride and AZ67H zirconia toughened alumina. Wheels were evaluated for grinding parameters such as material removal rate, wheel wear, G ratio, normal force, tangental force, and grinding power. Additionally, the grinding wheel influence on ceramic surface integrity characteristics such as surface finish, damage, and retained strength were selectively evaluated.

The best performing wheel specification was selected after testing in Task 2. Six duplicate wheels of this metal bond, 203-mm wheels were fabricated and delivered to Oak Ridge National Laboratory at the end of the Phase 1 contract for validation testing.

Norton Company has proposed a Phase 2 option that would include manufacturing scale-up to a 356-mm (14-in.) diameter wheel commonly used in cylindrical grinding of ceramics. This manufacturing scale-up would probably include further optimization of the wheel specification. The Phase 2 program would culminate with independent product testing at leading U.S. ceramic manufacturers ceramic machine shops.

7. RESULTS

7.1. ANALYSIS OF GRINDING WHEEL REQUIREMENTS -- TASK 1

7.1.1. Task Overview

This task involved the design of the bond with respect to mechanical and thermal characteristics and the selection of the diamond grit. Task 1 was expanded to include initial bond-only (no diamond) wear and strength tests. Task 1 culminated in a small-wheel screening test involving controlled feed plunge grinding of sialon disks. This test allowed us to evaluate numerous wheel variables before down-selection to the most promising bonds in Task 2. Task 1 also contained the parallel path CVD diamond wheel activity.

7.1.2. Requirements Definition and Experimental Design -- Task 1.1

7.1.2.1. General Wheel Design and Description of Bonds. Advanced ceramic components such as silicon nitride valves for automotive engines are machined to final shape and size predominantly by precision grinding, using wheels containing diamond and/or occasionally cubic boron nitride abrasives (superabrasives). The requirements of cost-effective grinding wheels include the ability to grind work material at high-removal rates, consume low levels of power, maintain low power levels for extended periods, produce quality work pieces with surface integrity, and have sufficient wheel durability to maintain its form (if any) for extended periods, thereby requiring infrequent "truing" and "dressing" operations. Truing refers to an operation that makes the wheel surface run concentric to its axis of rotation. If the wheel has a profile or form, truing also includes regenerating the profile on the wheel as per drawing. Dressing refers to a procedure that exposes the abrasive grits above the bond surface for cutting action.

There are primarily three major bond types that hold the abrasives: resin, glass or vitrified, and metal bonds. Resin-bond products are good starting points for grinding a wide range of advanced ceramics producing quality surfaces of good strength, but they do not possess adequate life, requiring frequent truing and dressing. Vitrified-or-glass bonded products can provide better life but need to be handled with caution due to the extremely brittle nature and low strength of the bond matrix. They also pose considerable limitations for use in high-speed grinding, a technology that is currently evolving. It is extremely difficult to process them into wheels thinner than .125 in. (3 mm) with current methods of manufacture. Conversely, conventional metal bonds have been found to be exceptionally durable, consume more power in grinding fine grain size ceramics, and require frequent dressing to remove the worn abrasives, and expose sharp ones. The dressing process of conventional metal bonds is time consuming and not

desired by the operator. Hence, the focus of bond design is to identify metal systems that possess the desirable characteristics of current resin and metal bonds. Wheels with a single abrasive layer bonded on to steel cores are also included under metal products. Table 1 summarizes the different bonds and their characteristics.

7.1.2.2. Superabrasive Bond Development; Bond-Only Wear and Strength Tests. For optimum performance of the wheel, the wear rates of the abrasive grits during its use must equal that of the bond holding it. This allows a continuos exposure of sharp, new abrasive grits to the work piece for efficient grinding action. Typically, abrasives wear by fracture, attrition and/or pull-out from the bond. For a given grinding condition, the wear rate of the abrasive grits is controlled by factors such as their type, size, amount and the abrasive - bond strength. On the other hand, the bond wear rate is governed by factors such as its strength, hardness, type and amount of fillers, and its microstructure.

A wear test was set up that would simulate the wear of the bond during grinding. Differences in bond wear between the fast-wearing resin bond and durable metal bond were determined. This information was used as a basis in designing other metal bonds. The test consisted of forcing a bond sample, 6.25 x 6.25 x 25 mm, containing no abrasives, against the side of a rotating disk at constant load. The rotating disk contained silicon carbide abrasives of size U. S. mesh 170/200. A resin-bonded sample (Norton DB70), which is used in wheels for grinding silicon nitride and similar advanced ceramics, was tested first. The wear (by weight) of the resin bond sample (DB70) for a given amount of time (15 seconds) was determined. The experiment was repeated several times and the cumulative wear was determined. The wear test was then repeated with the standard metal-bonded samples, DM17 and DM112. Due to their low-wear rate, the weight loss was measured every 45 seconds. The disk was refurbished with new silicon carbide abrasives frequently to counter the effect of its wear on the test results. Figure 4, shows the normalized cumulative wear of the resin and metal bonds as a function of time. The resin bond wore at a significantly higher (up to 5 or 6 times) than either one of the metal bonds. Since these metal bonds are too durable and resin bond wears too fast, the metal bonds for improved grinding wheels must possess wear rates that lie between the two.

A series of metal bond compositions possessing abrasive wear and strength between the resin bond DB70 and metal bonds DM17 or DM112 were designed and manufactured. Some of these bond compositions contained different levels of pore inducers in a DM17 bond. Pores in bonds not only weaken them to desired levels but serve several purposes in a grinding wheel. Porosity lowers the wheel-work contact area thereby reducing friction and spindle power drawn, provides a space for the ground ceramic chips ("chip clearance") and improves application of grinding fluid, essential for lubrication and heat transfer. Figure 5 shows the cumulative wear data versus time for metal bond DM17 with 20-, 40- and 60-volume percent of pore inducer PI2 in the wear test against an abrasive disk at constant load. The cumulative wear rate increased with the percentage of pore inducer PI2. The wear rate is shown to almost equal that of resin bond DB70 at 60-volume percent levels.

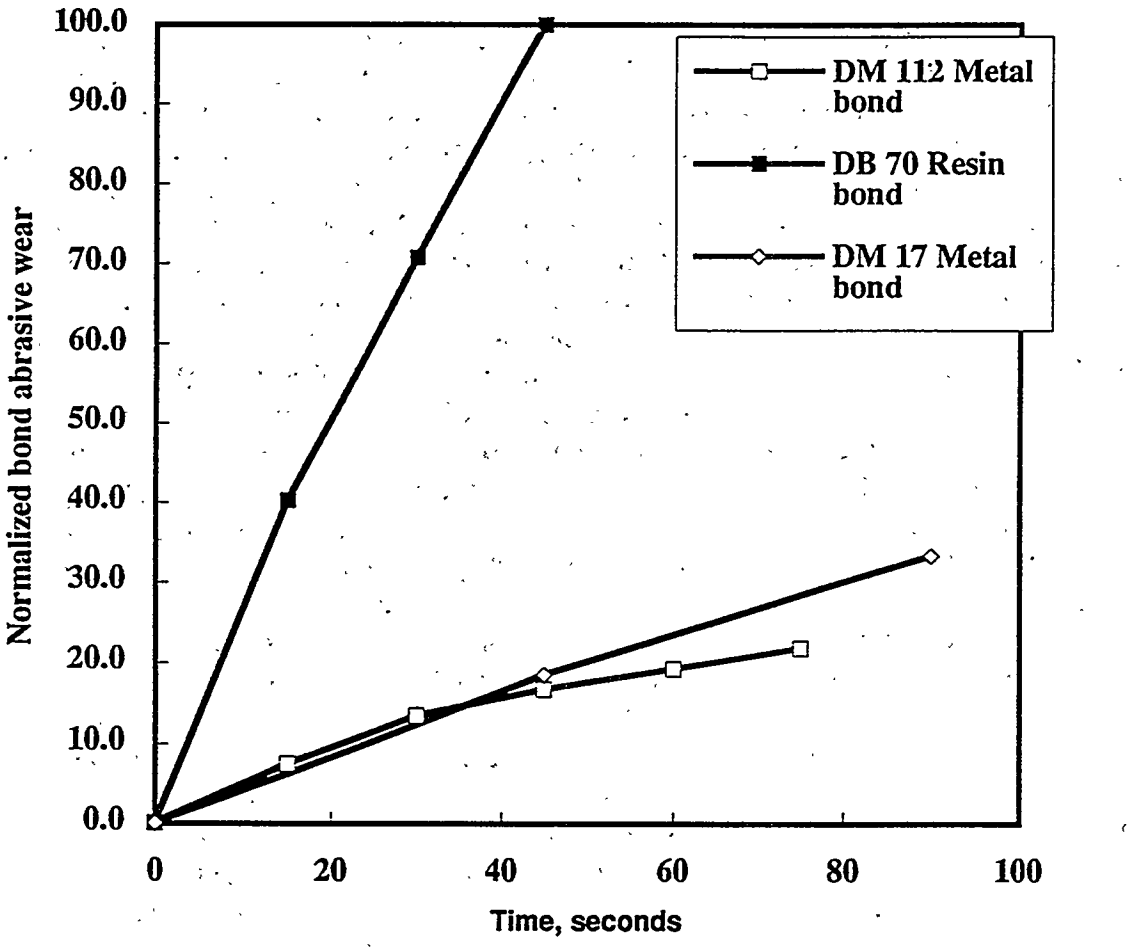

Figure 4. Normalized cumulative wear of resin and metal bonds, containing no abrasives, plotted as a function of time. The resin bond (Norton DB70) is typically used to grind advanced ceramics today and metal bonds Norton DM17 and Norton DM112 represent conventional metal bonds that are considered too durable for this application. The resin bond wore up to five times faster than either of the two metal bonds. The wear test was designed to simulate bond wear during grinding process.

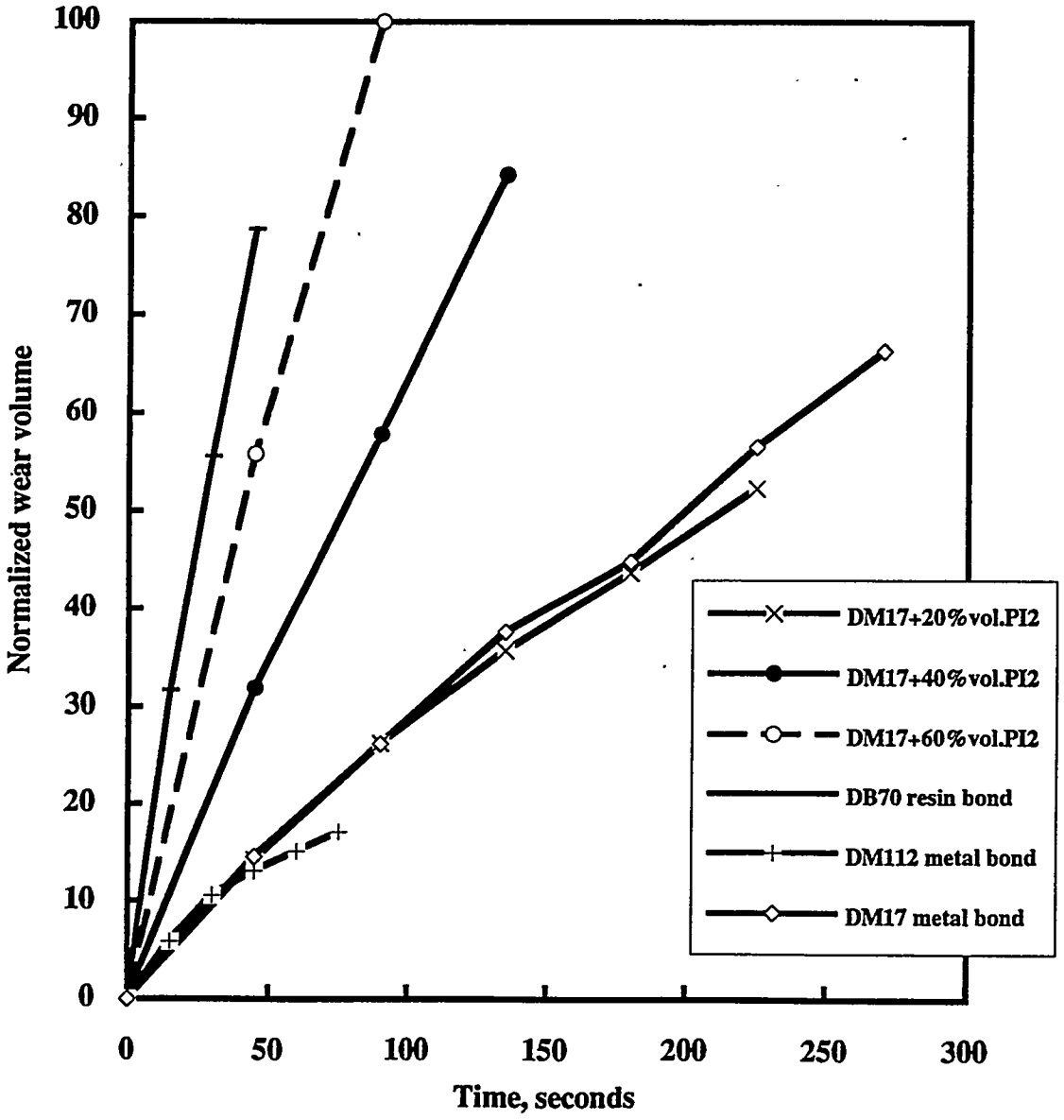

Figure 5. Normalized cumulative wear versus time of three experimental wheel bonds, without abrasives. The bonds were fabricated by introducing 20, 40, and 60% by volume of pore inducers, PI2, in Norton DM17 metal bond. It is possible to increase the wear rate DM17 bond this way to match that of the abrasive grits, which is essential for optimum grinding performance in a wheel. Standard metal bonds DM17 and DM112 and resin bond DB70 are also shown for reference.

Figures 6a and 6b show similar wear plots for the three pore inducers PI1, PI2 and PI3, at 40- and 60-volume percent levels, respectively. Other approaches to introduce porosity were abandoned after poor results.

The 3-point bend strength values of the resin bond (DB70) and metal bonds (DM17 and DM112) with no abrasives present in them were determined subsequently. Since abrasive wear of any material is a strong function of its strength, the design strength of the proposed metal bond must lie somewhere between the values obtained for the resin (DB70) and metal bond (DM112). Bond samples measuring 3 mm (0.12 in.) x 6.3 mm (0.25 in.) x 38 mm (1.5 in.) were manufactured and broken in 3-point bend strength at a cross-head speed of 5 mm (0.2 in.) per minute. The results, shown in Figure 7, indicate that the normalized bending strength values of the conventional metal bond is nearly twice that of the resin bond.

Test bars of another patented metal bond family under the trade name, Norton Alzan, have also been made and tested. Figure 8 shows the three-point bend strength of this bond with different levels of porosity. The resin bond, DB70 has been included as a reference. The strength of the Alzan bond samples was lower than that of resin bond DB70 and decreased further with increasing porosity. The wear tests of the Alzan bonds, simulating the grinding process, indicated excessive wear, even more than DB70 resin bond. Hence, Norton Alzan, or its variations including porosity were not be expected to provide adequate wheel life for grinding of ceramics and not pursued further.

In summary, the bond wear and strength tests suggest that it is possible to alter the characteristics of metal bonds close to that of resin bonds. The extent of change could be better predicted based on grinding tests.

7.1.2.3. CVD Diamond Wheel. The general concept behind the CVD wheels is illustrated in Figure 9. Preforms are coated with diamond by CVD, are assembled together into a wheel and then are impregnated with epoxy resin. The wheel is then trued and operated as a conventional wheel.

The preform thickness was chosen to be about 25um, which gave a tooth size approximately equal to 320 grit, which was the base grit size chosen for all wheels in the program.

After consulting with Prof. Howes, at UConn, we agreed that the continuous nature of the diamond on the preform would provide much higher heat transfer than a conventional wheel and therefore coolant absorption would not be as important an issue as for conventional resin-bonded wheels. No effort was therefore made to induce porosity in any of the wheels tested.

The major unknown factor in this concept was the durability of the CVD diamond on its preform. We needed to know whether the teeth on the diamond-coated preform would act as single grits, or whether they would wear faster. Emphasis was therefore placed on direct testing.

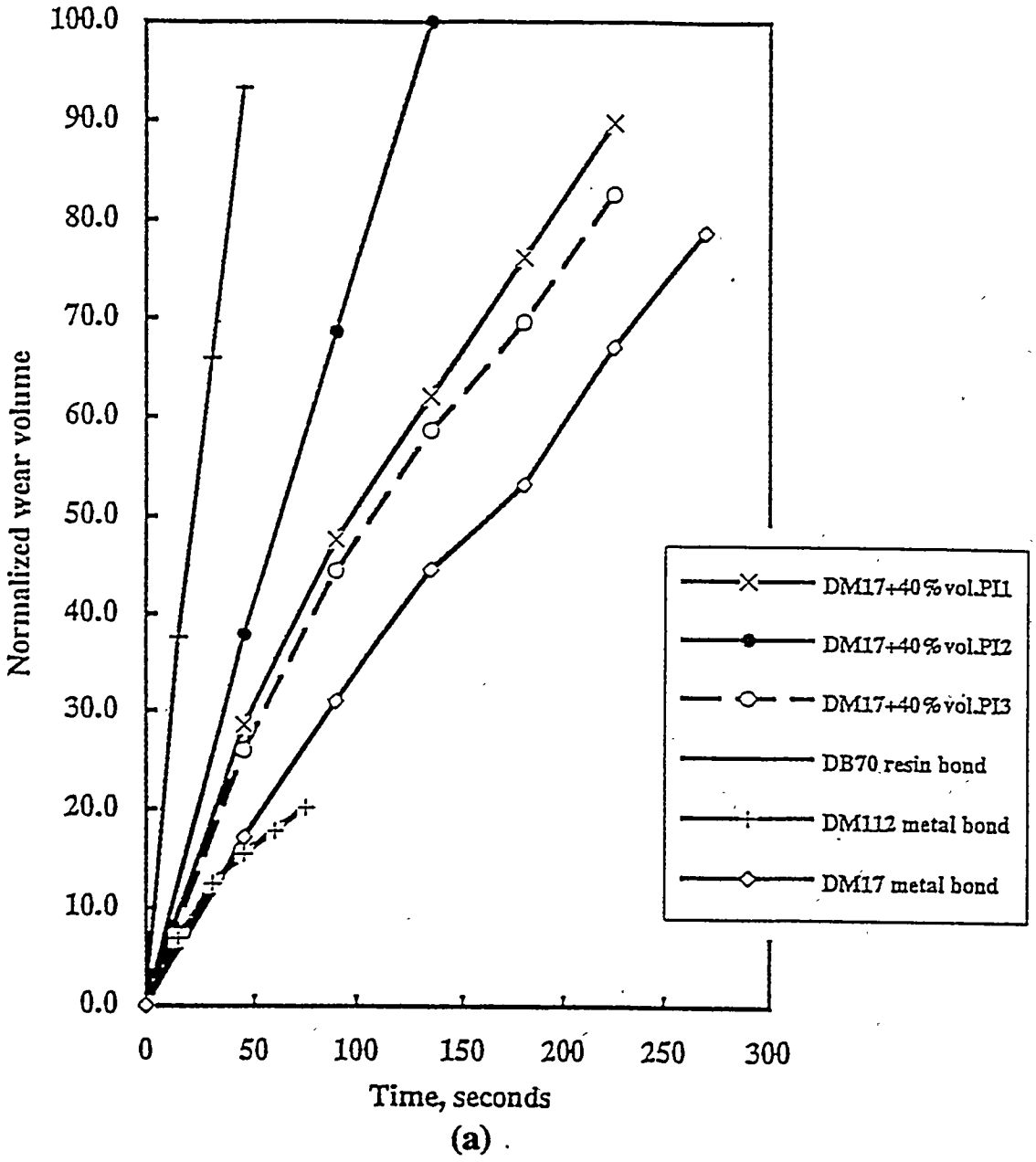

(a)

Figure 6a. Bond wear plots comparing three types of pore inducers PI1, PI2 and PI3 at 40% volume levels. All three types of pore inducers increased the wear rates of DM17 bond. Standard resin and metal bonds are shown for comparison.

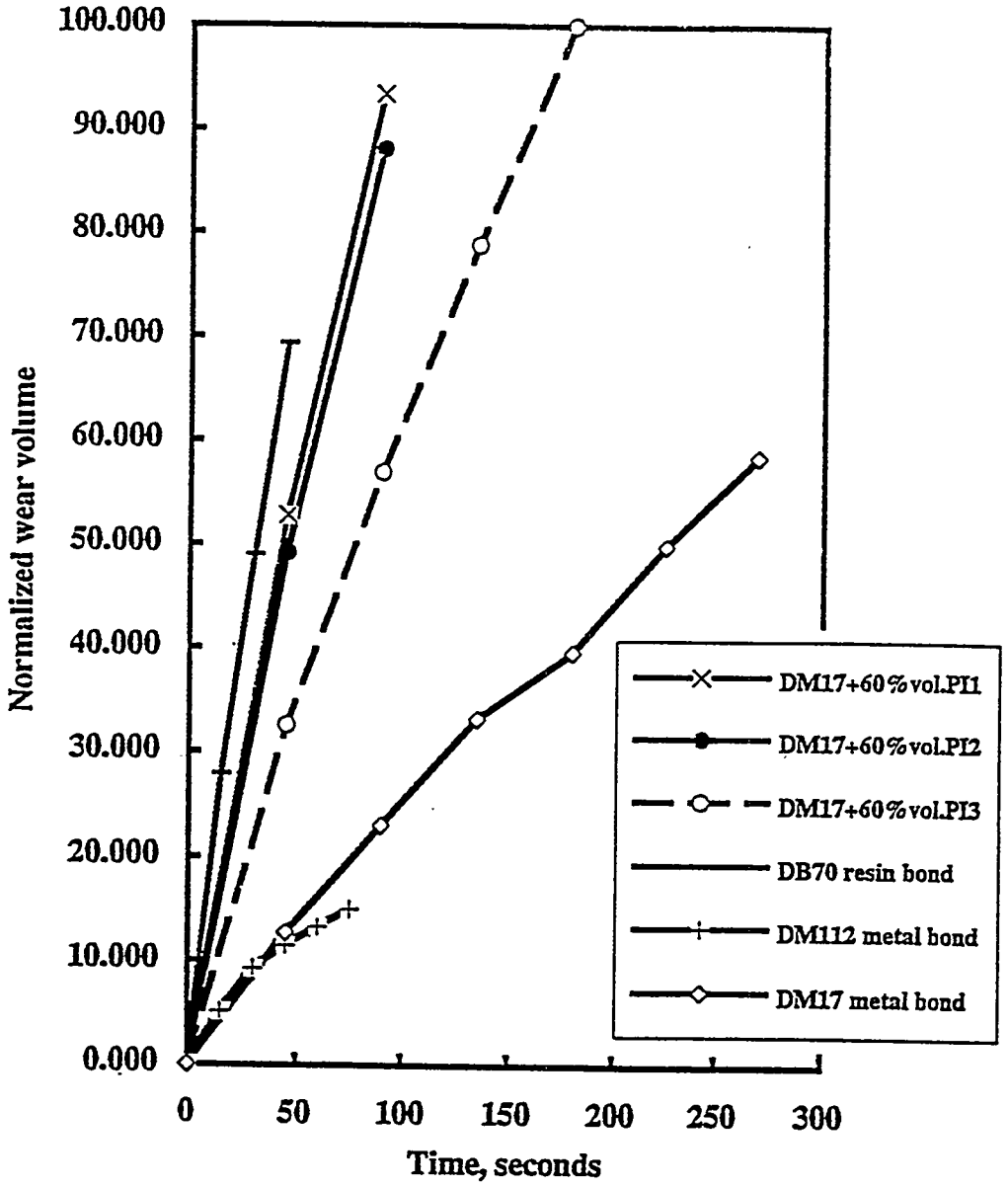

(b)

Figure 6b. Bond wear plots comparing three types of pore inducers PI1, PI2 and PI3 at 60% volume level. All three types of pore inducers increased the wear rates of DM17 bond. Standard resin and metal bonds are shown for comparison. The rate of wear of bond containing 60% pore inducer was greater than the one containing 40% pore inducer with all three types.

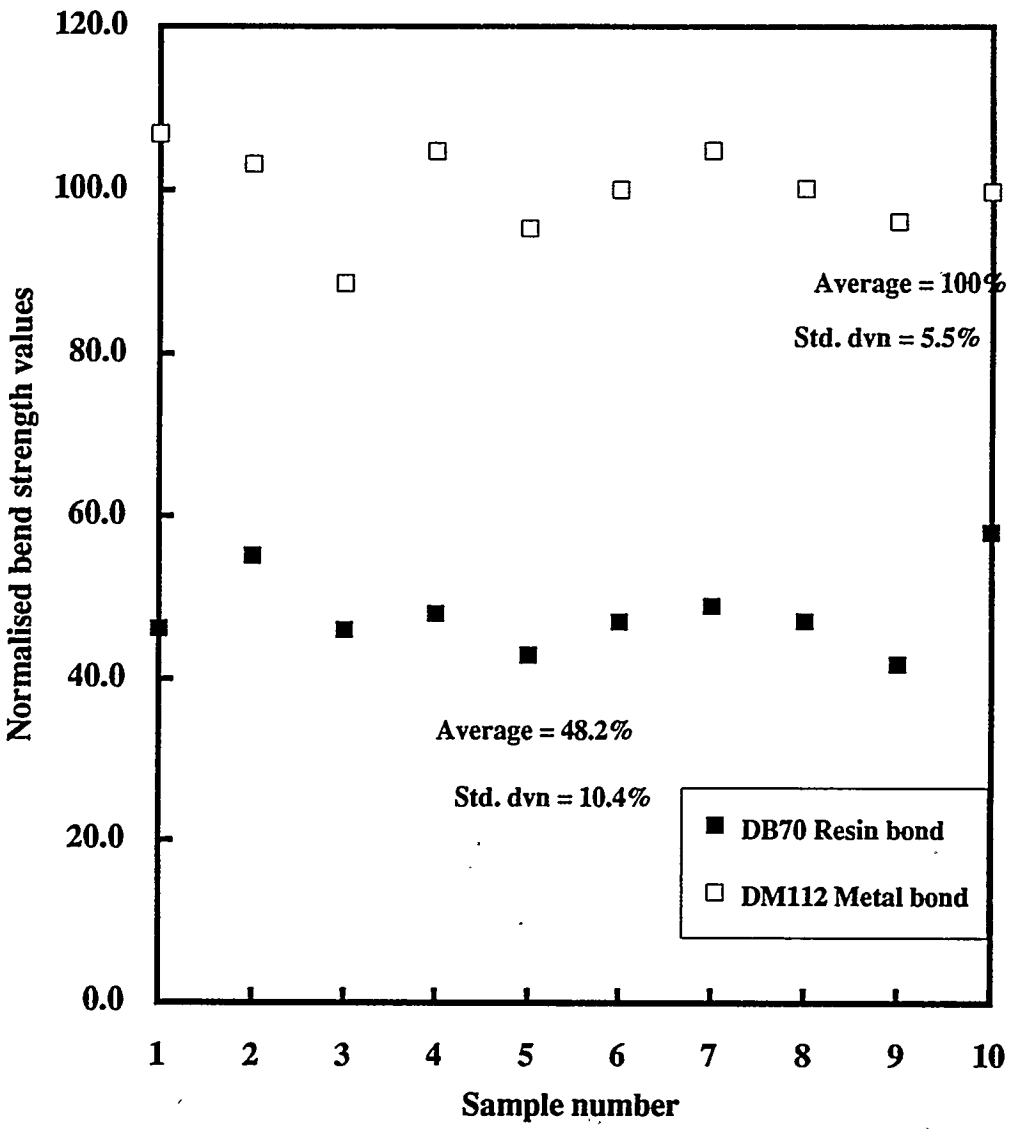

Figure 7. The normalized 3-point bend strength of Norton metal bonds DM112 and resin bond DB70. The average value of strength for resin bond is 48.2% of the metal bond. The hardness values of the resin bond are similarly lower providing an explanation for the higher bond wear in the simulated test.

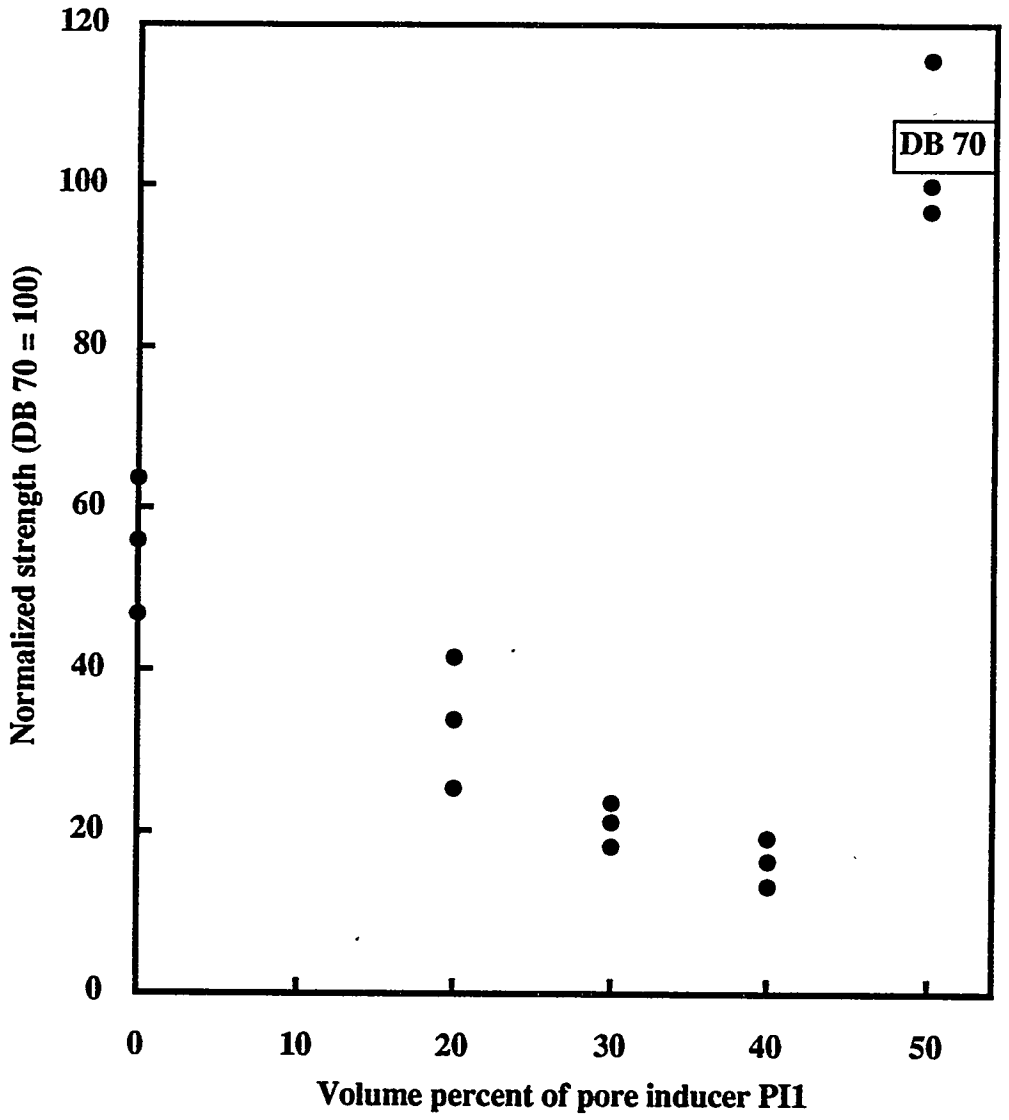

Figure 8. Normalized 3-point bend strength of another patented metal bond (Norton Alzan) with different levels of pore inducer, PI1. Although originally included as a potential candidate, this approach was abandoned due to the poor strength values, even compared to resin bond DB70.

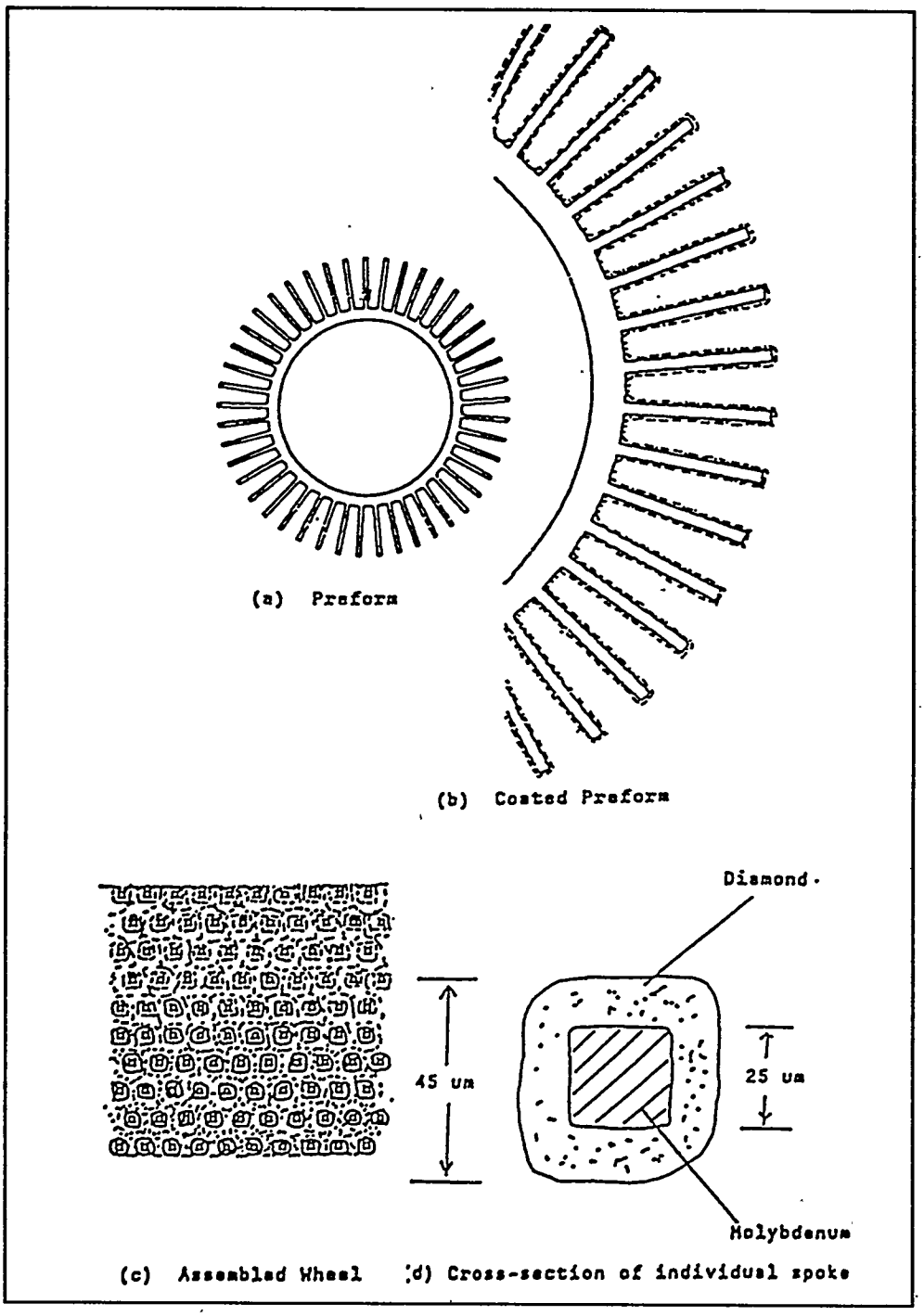

Figure 9. Steps in making the CVD diamond wheel

7.1.2.4. Selection of Abrasive Type, Size, and Concentration. The next important consideration in wheel design, after the bond type, is the selection of appropriate abrasives. This includes determination of abrasive material, type, size and amount. Because of the high hardness values of advanced ceramic materials typically ranging from 750 to 3000 kg/mm^2, diamond with a hardness of 7000 to 9000 kg/mm^2 was chosen as the abrasive material. One of the requirements in grinding of advanced ceramics into finished components is to generate low levels of surface damage. This could be accomplished through the use of sharp abrasives, which narrowed down the choices of abrasive types that are commercially available. The abrasives are also required to be sharp during their entire life in order to maintain low damage levels from component to component. This could be achieved if the grinding forces on a grit, which increases as it dulls, causes the grit to fracture. This fracture generates new sharp cutting points. Wear flats on abrasives are akin to dull edge on a knife and grinding with them produce more damage to the ceramic work piece. Hence, friable and weak types that would fracture periodically were selected in this program. Diamond abrasive grits of size U.S. Mesh 270/325 (Norton 320 grit) were selected for initial screening wheel tests. This range of abrasive sizes is recommended by our application engineers for reducing damage while maintaining acceptable levels of material removal rates in general purpose rough-to-intermediate grinding of ceramics. Abrasive specifications for finish grinding would depend on individual application needs of surface finish, part geometry, tolerances, etc. The other important factor in abrasive specification is the amount of abrasives in the wheel, defined through the term "concentration". A 100-concentration diamond abrasive wheel contains 72 carats per cubic inch of abrasive bond volume. This closely translates to 25 percent by volume of diamond in the abrasive-bond volume. Most of the test wheels contained 100 concentration diamond. The concentration values ranged from 75 to 125 in our study.

7.1.3. Screening Test Wheel Manufacturing -- Task 1.2

7.1.3.1. Superabrasive Wheels. The bond wear studies were followed with design and development of a grinding test to screen wheels made in different compositions. The goal of this task was to identify a few bond-abrasive combinations that, when made into grinding wheels, would draw low power, generate low forces and provide acceptable wheel life with no wheel "loading" tendencies in external cylindrical grinding of advanced ceramics such as sialon and Si_3N_4. Wheel "loading" refers to a phenomenon in grinding when material removal action of the wheel virtually ceases. It takes place in the following four instances: (1) the abrasive grit wear rate is comparably higher than the bond wear rate resulting in lack of grits projecting above the bond, (2) abrasive grits are released from the bond prematurely, leaving a wheel surface with no cutting points, (3) the area in and around the grit is covered due to plastic deformation of the bond, and (4) the area adjacent to the grit is filled up with work piece swarf or chips preventing the grit's participation in the grinding process. Material removal action is restored through wheel dressing in which a glass bonded stick containing abrasives is

applied to the wheel surface under pressure. This leads to wear of the bond in instances (1), (2) and (3) and clears the wheel of any chips in case (4). The dressing process with conventional metal-bonded wheels is time consuming and laborious and hence not desirable. During the design of test wheel specifications, a "Systems Approach" that looks at machine tool parameters, work material properties, wheel selection and operational factors simultaneously, was pursued with the goal of providing an optimum solution for that combination and grinding conditions. The test wheels measured 76 mm diameter x 13 mm thick x 22 mm bore diameter (3 in. x 0.5 in. x 0.875 in.) and were made in a range of compositions. Factors such as type of pore inducers, their levels, bond composition, diamond type, diamond concentration, wheel processing methods and processing conditions were evaluated. A total of nearly 70 wheels were molded and about 45 of them were evaluated. Based on results grinding tests of these 45 wheels and certain issues associated in manufacturing them, the remaining 25 or so wheels were not tested. The manufacturing issues included adhesion of wheel core and its rim as well as extrusion of bond.

7.1.3.2. CVD Diamond Wheels. A general view of the wheel used in the first grinding test is shown in Figure 10. It consists of abrasive elements arranged azimuthally and axially around the periphery of a 7.5-cm diameter grinding wheel. Axial spacing of each element was approximately 50 μm and the total assembly produced a wheel approximately 8-mm thick. Figure 11 shows a view of the teeth on one of the elements. The element was photochemically machined from 30-μm molybdenum sheet and were held in place by an epoxy impregnation after the wheel was assembled. The teeth were each 25-μm wide at the OD with a slight taper, and coated on all surfaces with approximately 10-μm thick CVD diamond using a dc plasma torch. Thus, abrasive elements of approximately 45-50 μm cross sections were created, simulating a 320-grit wheel.

For the second round of tests, the wheel substrate was modified from an array of segments back to a full wheel rim preform as shown in Figure 10.

Several preforms were made using different diamond thicknesses. We hoped to test the preforms as a thin wheel, thereby reducing the complication of the test. Unfortunately this did not prove to be possible, as the unsupported preforms were too weak and too warped by the coating process. Accordingly, a wheel segment was fabricated by laminating two parts of a wheel on top of each with Duralco 4525 epoxy.

7.1.3.3. Ceramic Disk Fabrication. One hundred four sialon (NCX-520) disks were fabricated at the Northboro Research and Development Center (NRDC) of Saint-Gobain/Norton Industrial Ceramics Corporation by cold isostatic pressing, core drilling and sintering. The sialon ceramic workpieces were ground finished to 112-mm diameter rings x 70-mm ID x 6-mm thick. Figure 12 shows the ceramic disk on the top right with the test holding fixture on the bottom and left.

Densities of the disks were all within standard Norton specification. These disks were visually inspected for cracks and abnormalities before the screening test.

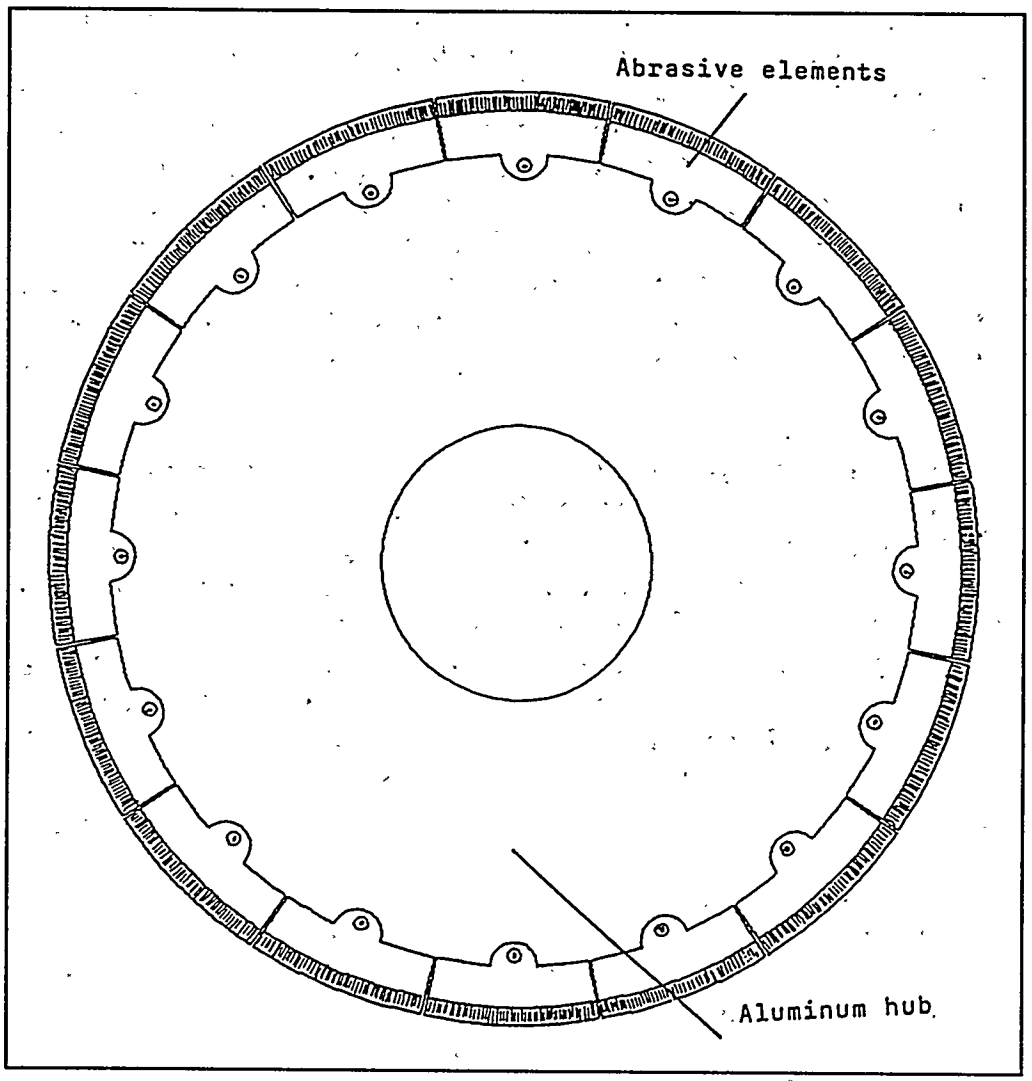

Figure 10. The first CVD wheel design.

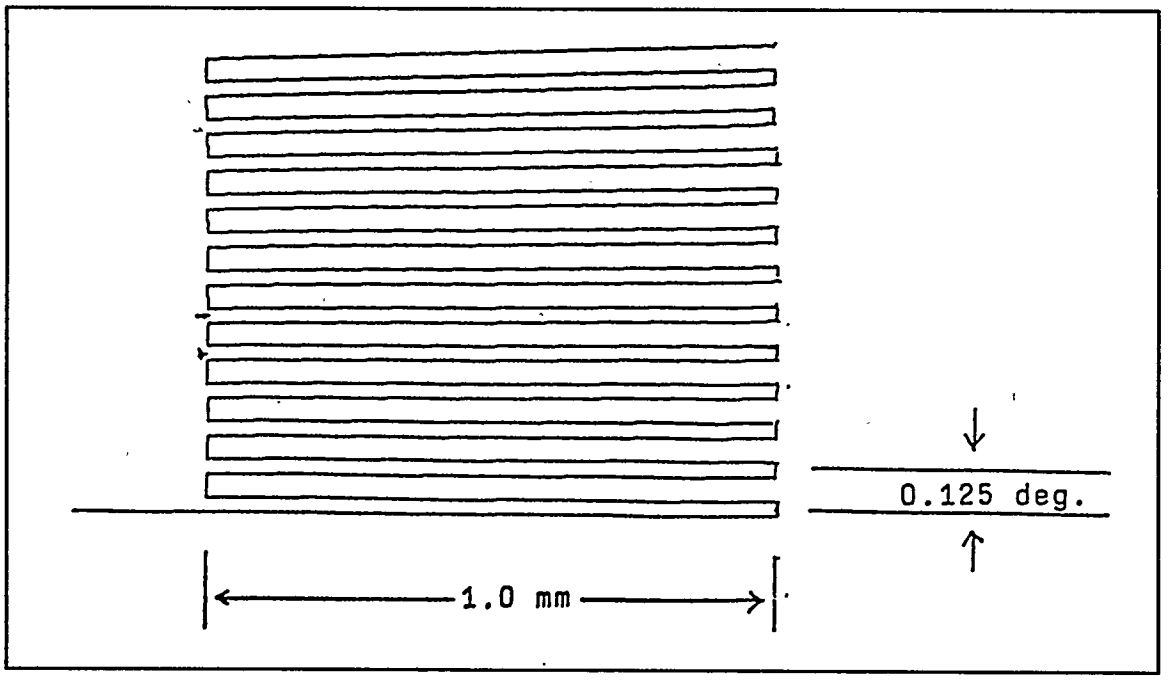

Figure 11. Detail of the teeth of the first CVD wheel design

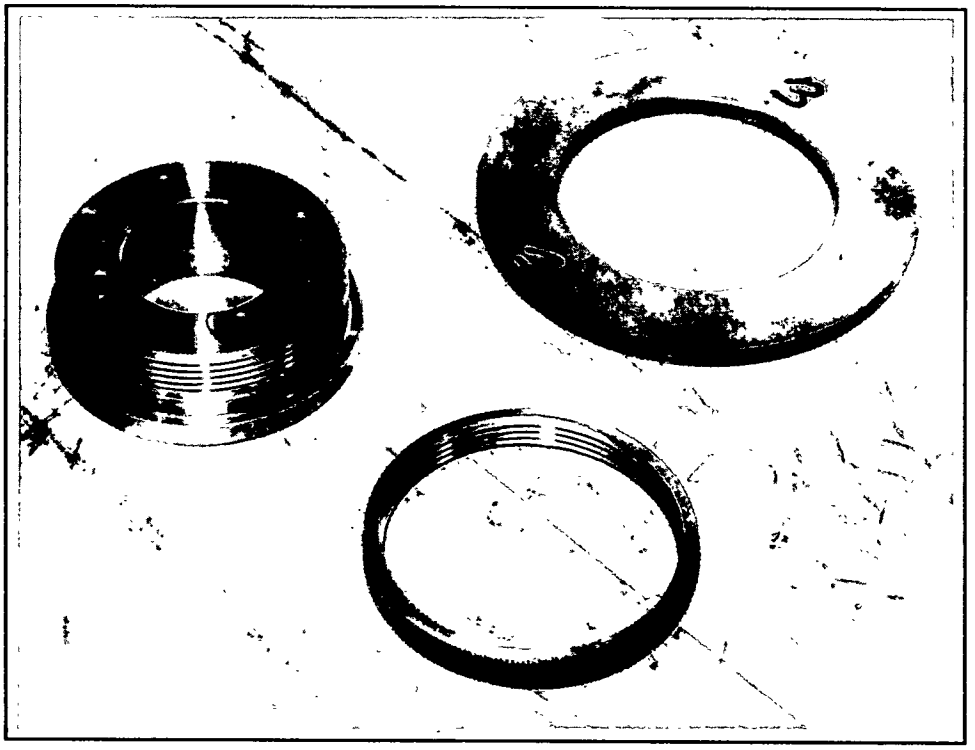

Figure 12. Sialon test disk (top right) with holding fixture assembly.

7.1.4. Screening Wheel Grinding Test and Data Analysis -- Task 1.3

7.1.4.1. Grinding Test Description. The grinding test consisted of plunging 76-mm diameter x 13-mm thick x 22-mm hole grinding wheels into samples of sialon disks measuring 112-mm diameter x 6-mm thickness x 70-mm hole at preset removal rates in external cylindrical grinding mode. Figure 13a is a schematic of the test configuration. Figure 13b is a photograph of the set-up consisting of grinding wheel and Sialon workpiece on an instrumented Okuma CNC cylindrical grinder. The sialon ceramic workpiece (Figure 12) was mounted on a specially designed and manufactured arbor that in turn was located precisely and held on the machine. It was thus possible to remove the workpiece together with the arbor for periodic examination of the ground surface and mount it back on the machine, precisely. To improve the efficiency of testing, short grinds at two material removal rates of 4.3 and 8.6 $mm^3/mm/sec.$ (0.4 to 0.8 $in^3/in./min.$) were conducted on all wheels, followed by longer runs on selected wheels. The wheels were trued to run concentric with the axis of rotation using a silicon carbide abrasive wheel of specification 37C220IVK mounted on a precision dresser device. Using 37C320KV abrasive sticks, the wheels were then dressed to expose the abrasives. The grinding fluid used in all our tests was Trimcool, a water-based coolant with rust inhibitor.

Measurements included spindle power drawn, wheel wear for known amount of work material removed, normal and tangential forces generated during grinding, and surface finish of the workpiece. Noise levels were monitored qualitatively to determine wheel loading and subsequent effectiveness of remedial wheel-dressing operation.

Wheel wear was determined through precise micrometer measurements of wheel diameter before and after a grinding cycle. The thin sialon disk workpiece produced a wear zone in the middle of the wheel face, so a depth micrometer was used the measure the diametrical change. The volume of the wheel wear was calculated from the diametrical wear and the width of the wear zone, which corresponded exactly to the width of the sialon disk workpiece.

Using the measurements, the grinding ratio values, spindle power and grinding forces per unit wheel width were calculated. Grinding ratio by definition is the volume of material ground over the volume of wheel consumed. The measured spindle power and forces in grinding were converted to values per unit wheel width in order to nullify the effect of wheel thickness. Such a calculation, generally done in grinding studies, enables the comparison of performances of wheels of different thicknesses. Data was normalized as needed and plotted.

In order to determine the stiffness of the system consisting of machine tool, wheel and work piece, a harmonic response test, "hammer test" of the Okuma cylindrical grinder was conducted with the help of the University of Connecticut. The objective was to determine the susceptibility of the machine to produce chatter on ground workpiece and make any modifications if needed. Chatter is caused by a grinding machine that is too compliant for a given operating condition. The harmonic response test determines the stability limit defined by the equation,

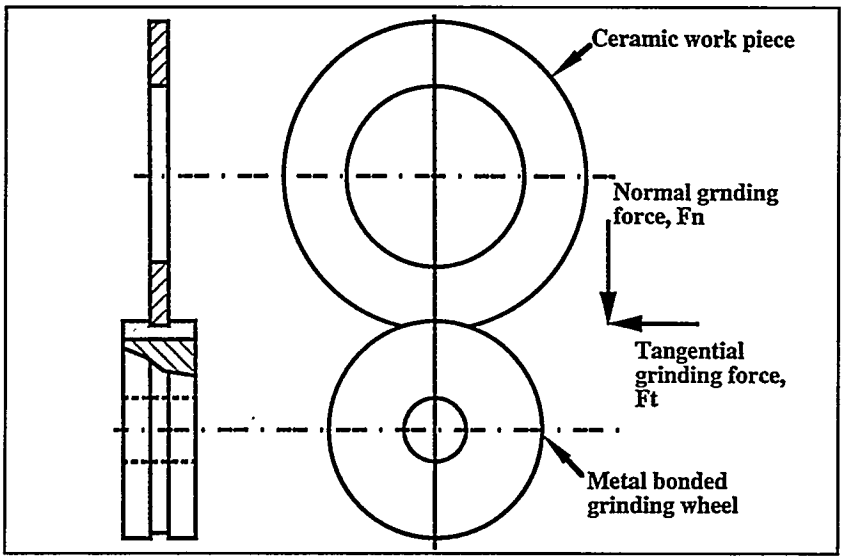

Figure 13a. Schematic of the 76-mm diameter wheel screening test.

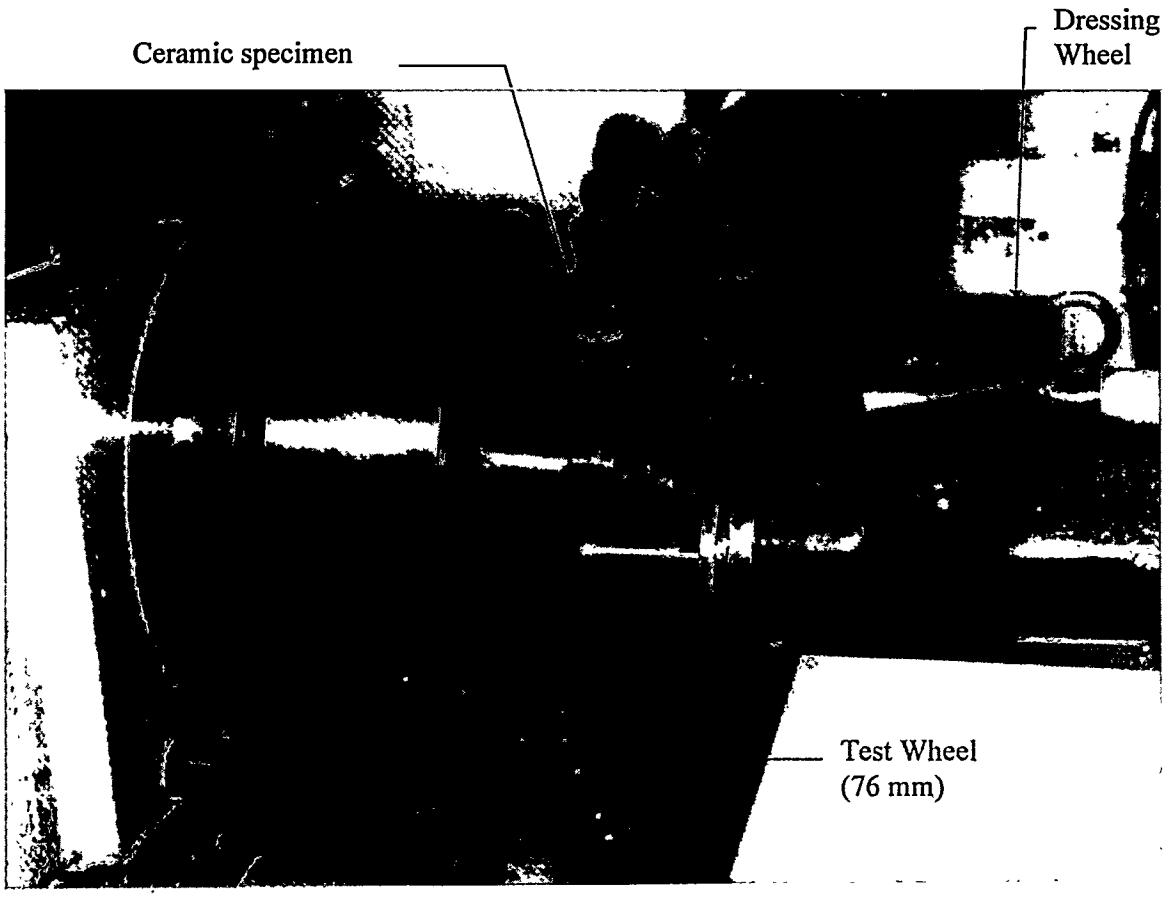

Figure 13b. Okuma cylindrical grinder plunge screening test.

$$-(1/2\ k_W + 1/2\ k_S + 1\ k) = R_{em}$$

where k_W is the cutting coefficient, k_S is the wear coefficient and k is the contact stiffness and R_{em} is the maximum negative real point on the machine compliance curve.

The **cutting coefficient, k_w,** is the force required to remove a unit depth of work piece material. This value may be estimated by measuring the cutting force and dividing it by the actual depth of workpiece removed.

The **wear coefficient, k_s,** is the force required to cause a unit depth of grinding wheel wear. For large grinding ratios, this coefficient is several orders of magnitude larger than k_w. Therefore the wear coefficient makes a negligible contribution to the equation and could be safely neglected.

The **contact stiffness, k,** is the stiffness between the grinding wheel and workpiece. This stiffness is highly nonlinear, however it could be linearized about the cutting force. The grinding wheel is much more compliant than the workpiece due to the structure of grains, bond, and porosity. The value of k can be estimated by pressing a representative workpiece against a stationary wheel. The normal force generated over the distance traversed gives the value for k.

The **negative real point, R_{em},** on the machine compliance curve is determined using the "hammer test". Knowing both sides of the equation, one could then determine if the system is stable or not. A stable system requires that the right hand side of the equation is greater than the left hand side. This type of stiffness test was performed to determine the acceptability of our specific machine tool-wheel system. Similar tests can be done to assess the wheel stiffness compatibility for other machines. For the example of an insufficiently stiff machine tool -- where it is determined that the right hand side of the equation is less than the left -- the experimental bond would need to be modified to reduce the wheel stiffness. This bond modification could be accomplished with a minor grade or composition modification to our experimental metal bond system.

For our specific grinding test system, "hammer test" results indicated that the grinding system consisting of machine tool, wheel, and work piece had adequate stiffness in all directions for testing with 76-mm (3 in.) diameter wheels. No visible chatter on the work piece was detected in all our tests. The University of Connecticut submitted their report on the "hammer test". The test indicated that the spindle stiffness is very high in two directions, and is adequate in one direction. However, in this direction the stiffness is of acceptable value, as evidenced by the lack of chatter on the workpiece in all our tests at up to 8 mm^3/sec/mm (0.8 in^3/in./min.).

7.1.4.2. Superabrasive Wheel Screening Test Grinding Results. Figure 14a graphs the spindle power consumed, normalized to unity, versus cumulative material removed per unit wheel width during grinding with 76-mm (3 in.) diameter wheels at a removal rate of 8.6 mm^3/sec/mm (0.8 in^3/min./in.). All wheels were made with U.S. mesh 270/325 diamond abrasive grits in 100 concentration. Wheels containing pore inducer, identified as PI1, at three different levels (20, 30 and 40%) were evaluated. Norton's DM112 metal bond, considered as durable for grinding of ceramics was

modified with different levels of PI1 for this test. Pores were expected to increase the bond wear rate thereby matching it to that of abrasive wear rate. The power consumed by resin bonded (DB70) wheel with the same type, size and concentration of diamond is also shown for comparison in Figure 14a. The results showed an increase in power drawn with pore inducer levels. Based on noise levels heard during grinding, all wheels showed tendencies for loading. Such wheels are generally not accepted by the end user for production grinding. Figure 14b plots the normalized grinding ratio as a function of cumulative material removed per unit wheel width for the same set of wheels. The dimensionless parameter, grinding ratio, represents the volume of material removed per unit volume of wheel consumed. Due to excessive wear, wheels with high pore inducer levels produced lower the grinding ratio values, similar to the results obtained in simulated wear test results conducted earlier. The normal grinding force values produced in using these wheels on NC-520 sialon versus cumulative material removed per unit wheel width are shown in Figure 14c . All three metal-bonded wheels in this group generated lower grinding forces than the resin-bonded wheel. However, the tendency for rising normal grinding force levels together with high noise levels heard suggested potential for wheel loading in these wheels. Figure 14d shows the tangential force values generated during grinding with these wheels. Since tangential force times wheel speed equals spindle power consumed, and all tests were performed at the same wheel speed, their trends were similar to spindle power. Similar but less pronounced results were obtained at a lower 4.3 $mm^3/sec/mm$. (0.4 $in^3/min./in.$) of material removal rate. Among the three pore inducer levels tested, the metal-bonded wheel containing 20% by volume of pore inducer PI1 could be considered as the best performer. However, its wheel loading tendencies required periodic wheel dressing with abrasive sticks.

In an attempt to reduce the wheel loading tendencies, other sets of bond compositions were tested by modifying the constituents and pore inducer levels in Norton's DM17 bond. This lowered the ductility and altered strength and hardness values. Within a given set, wheel performances were evaluated, based on spindle power drawn, grinding ratio, grinding force levels and wheel loading tendencies, for different levels of pore inducer PI2. Some of these compositions could not be manufactured above 30% PI2 levels. Figure 15 shows the test data on 3 sets of bond compositions in pore inducer levels shown. Due to extremely high wear rates, wheels in other compositions could not be tested extensively. Figure 15 also shows the grinding results using metal bond (Norton DM17) and resin bond (Norton DB70). Norton DM17 was considered too durable and Norton DB70 too wear-prone for cost-effective ceramic machining. Due to wheel loading and consequent high frictional forces between bond and work piece, the power and forces generated by the standard metal bond Norton DM17 went up abruptly, after grinding approximately 48 cm^3/cm (7.5$in.^3/in.$) of NC-520 sialon. Such abrupt increases could lead to damage levels in ceramic components after grinding to levels that would make the component unreliable in service. Closer examination of the wheel revealed most of the abrasive grits were worn down to the bond level and not projected above the bond level required for grinding. Possibly, the bond wear rate was lower than the abrasive wear rate for this event to occur at this juncture.

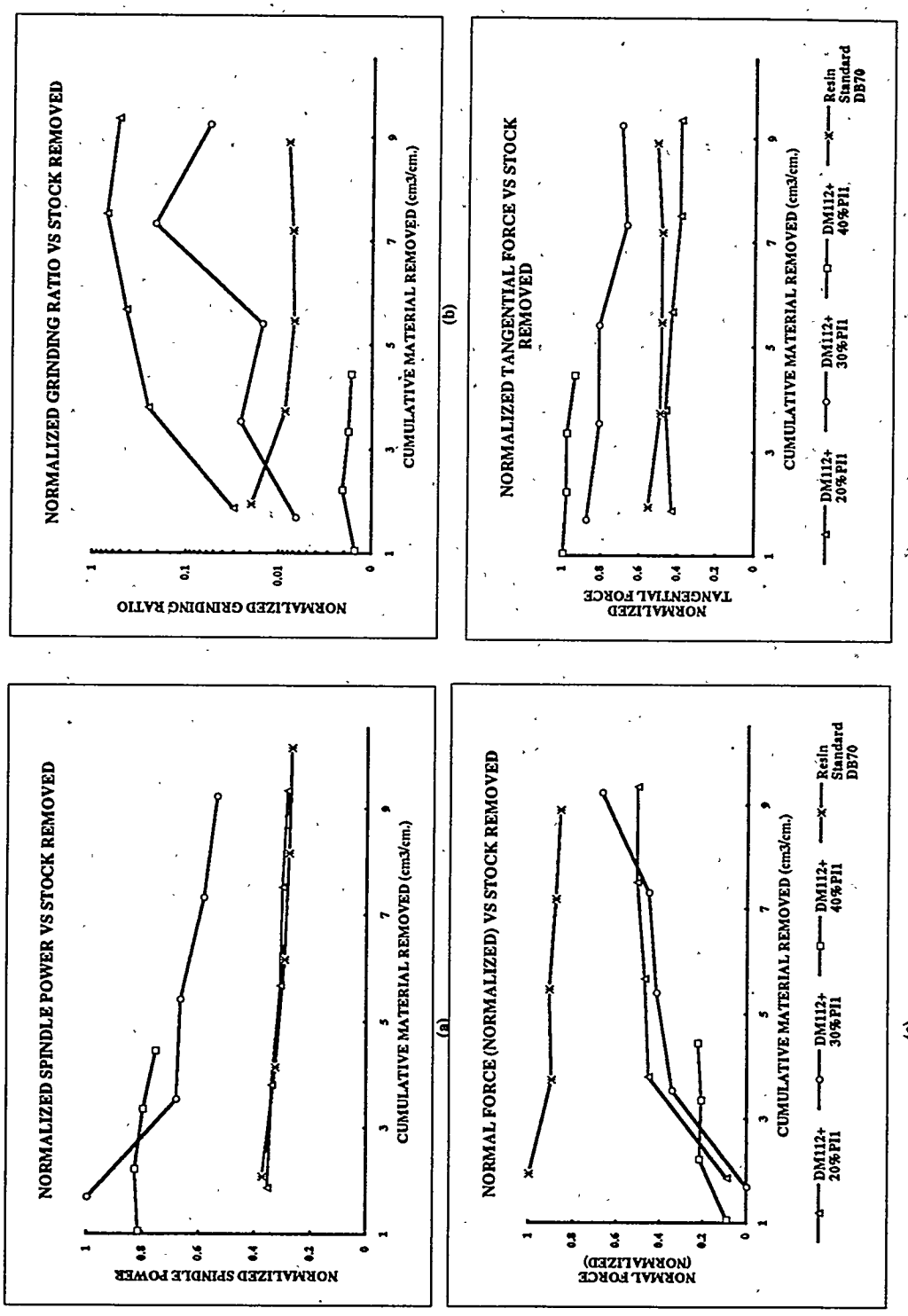

Figure 14a-d. Normalized spindle power consumed, grinding ratios obtained, normal and tangential forces generated in external cylindrical grinding of 111-mm sialon disks with a 76-mm (3-in.) diameter wheel versus cumulative material removed per unit wheel width are plotted. Metal bond DM112 with 20-, 30-, and 40-volume percents of pore inducers in them are compared indicating potential for metal bonds with desirable characteristics. All wheels contained friable 270/325 U.S. mesh diamond abrasive grits at 100 concentration.

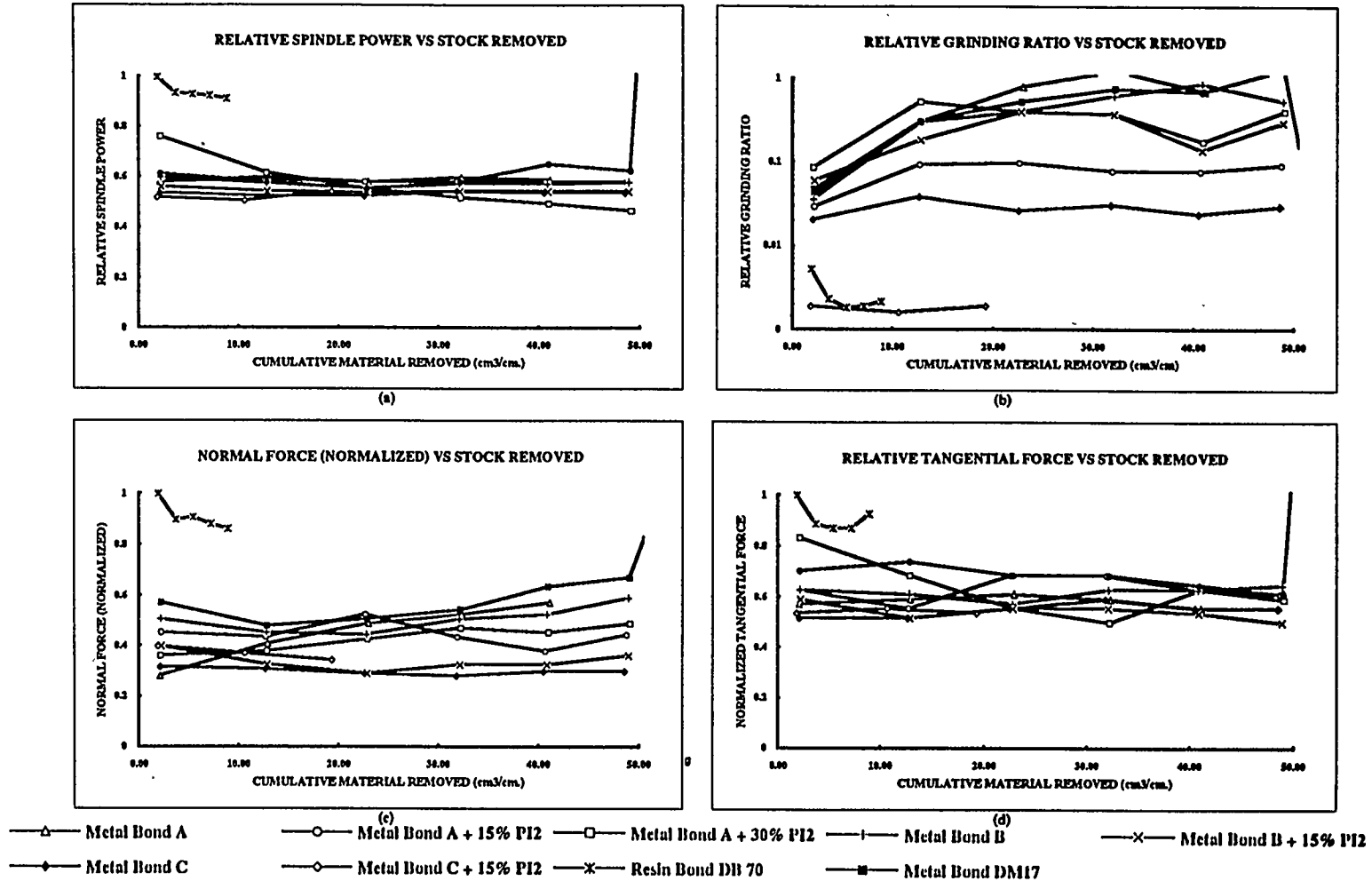

Figure 15. Other metal-bond compositions with and without pore inducers are compared for identifying compositions of wheels that would grind consuming low power, providing high grinding ratios, generating low grinding forces and minimum tendency for wheel loading. The wheel loading tendency of DM17 metal bond is evident with sudden increase in power and forces after grinding about 50 cm3/cm of wheel width. Metal bond C was identified as a promising composition for future tests.

From Figure 15 it is also evident that there are wheels in several different metal-bonded compositions that grind using low power, generating low forces and resulting in high grinding ratios. These are potential candidates for an improved metal bond. Based on other considerations such as noise levels in grinding and ease of wheel dressing, the selection was narrowed down further. Test wheel made of metal bond identified as "C" was considered as an optimal performing wheel among all specifications tested. This bond showed no signs of loading and broke down at a controlled and uniform low rate. The spindle power was about 50% lower than the resin-bonded wheel, while the wear rates were significantly lower than the resin bonded wheel. This bond also did not contain any pore inducers.

Wheels made in the promising metal bond C specification with other friable diamond types in 100 diamond concentration were tested subsequently, to determine optimum diamond abrasive type for grinding ceramics. The performances of wheels containing different diamond types were compared based on power, forces and wear during grinding. As shown in Figure 16a, wheel made with diamond type D3 consumed the most power and generated the highest forces in grinding. A test wheel containing diamond type D1 resulted in substantial (up to 50%) decrease in normal grinding forces based on Figure 16b. Wheels containing diamonds types D2 and D3 showed evidence of wear flats on grits after grinding and could explain the higher normal forces due to absence of sharp cutting points. Among the three wheels tested, the one containing diamond type D3 also wore the least for unit volume of material removed and hence resulted in the highest grinding ratios values as shown in Figure 16c.

Values for grinding ratio obtained with the wheel with D1 type diamond abrasives were the lowest, which may or may not be acceptable for cost-effective grinding of ceramics. Based on this test data, the final choice of diamond type was deferred until the grinding tests with larger 203-mm (8-in.) diameter wheels were conducted.

The effect of abrasive concentration on wheel performance was studied through the manufacture and subsequent testing of three wheels with 75-, 100-, and 125-concentration levels of D1-type diamond. Due to fewer number of cutting points in action at any given time and wheel-work contact area, lower diamond concentration wheels generally consume lower and desirable spindle power. However, lower abrasive content and consequent higher force per grit increases their wear rate, sometimes to unacceptable levels. Based on tests conducted using wheels that contain D1 type diamond the effect of abrasive concentration on grinding ratio was determined and plotted in Figure 17. Grinding ratio, considered a measure of wheel performance, increased exponentially with an increase in diamond concentration.

Several other compositions were proposed with different levels of hexagonal boron nitride and graphite as solid lubricants. There were manufacturing issues and/or poor, unacceptable grinding performance results and further tests on such compositions were discontinued. Test wheels were made in various diamond types in other metal bond systems for evaluation. Once it was determined that when using diamond type D1, such bonds have a tendency for loading, the comparison tests with wheels containing other diamond types in such bonds were not conducted.

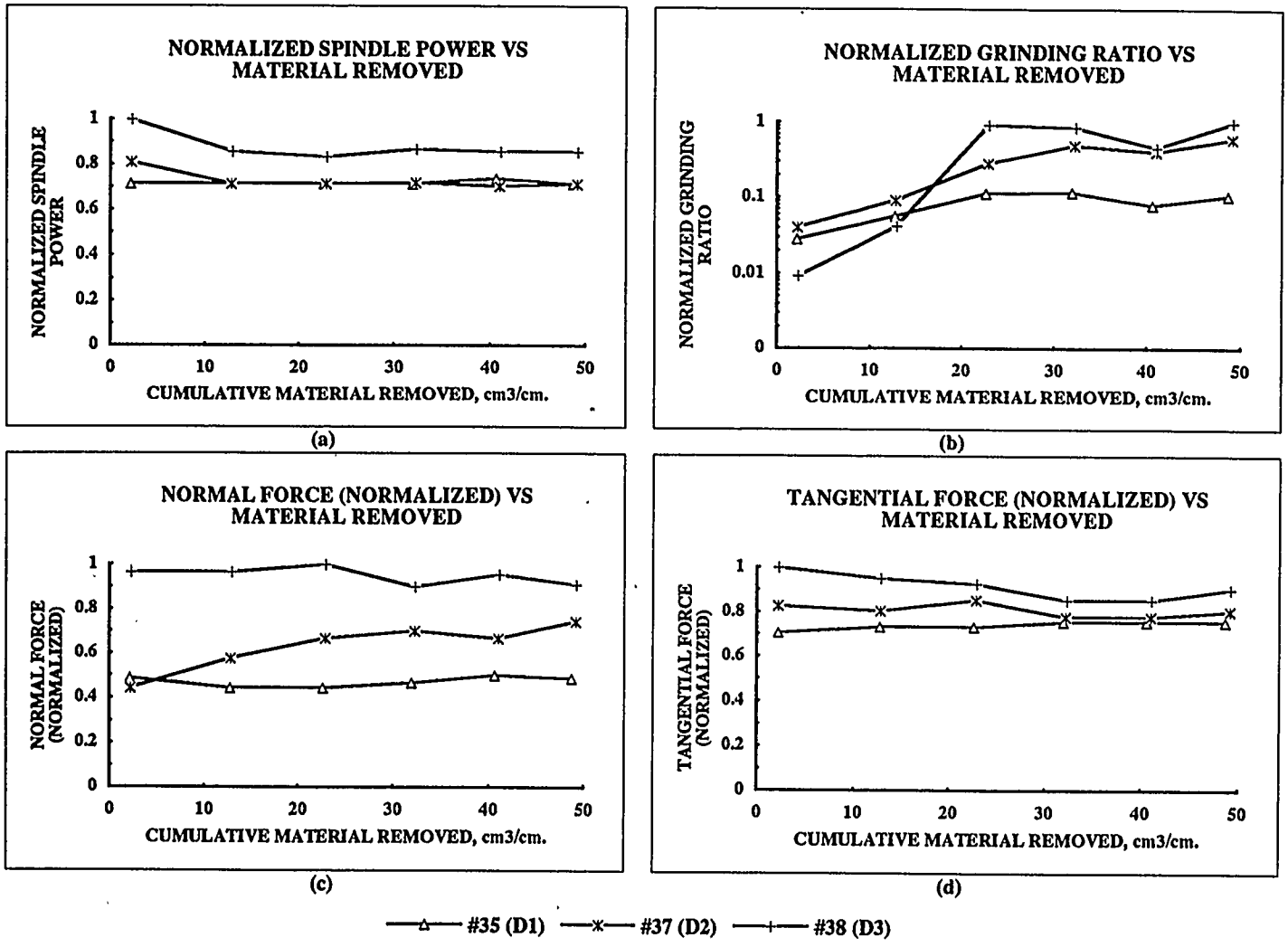

Figure 16. Performances of wheels containing three different diamond types in metal-bond C of Figure 8 are compared. Diamond type D3 provided the highest grinding ratios but also consumed the most power and produced the highest forces. The choice of the diamond types between D1 and D2 were made subsequently based on the larger 203-mm diameter grinding wheel tests.

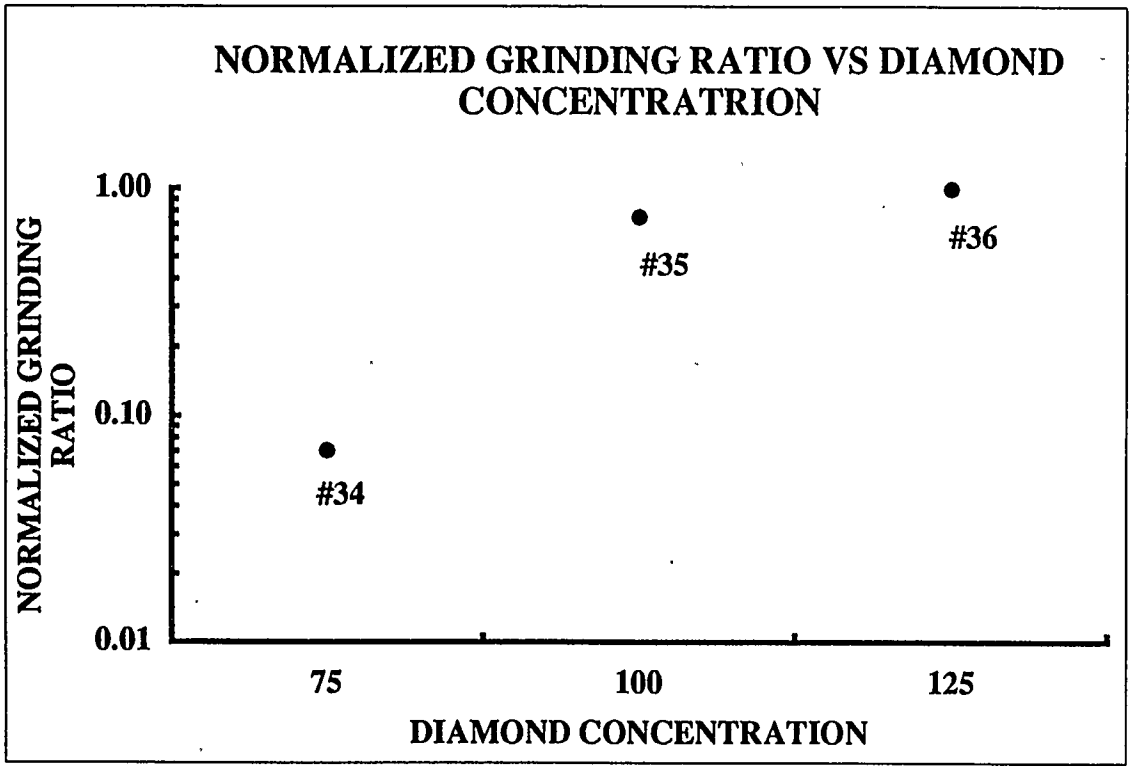

Figure 17. The effect of diamond abrasive concentration (a measure of volume percent) on grinding ratio in metal bond C is shown based on tests using 75-, 100- and 125-concentration diamond wheels. The grinding ratio appears to taper off above 100 concentration.

Test wheels possessing different hardness values were plotted against grinding ratio values obtained in the screening test, seeking the extent of correlation between the two factors. The hardness variation was obtained through change in pore inducer levels in a given bond system. There appears to be a good correlation between the grinding ratio and hardness on a semi-log scale as shown in Figure 18. Such a graph could be used, in principle, to design wheels of given grinding ratios using that bond system, in future.

Figure 19 summarizes all the results of the screening tests. The shaded areas represent the range of power, force and grinding ratio values obtained in grinding with these test wheels at material removal rates of 4.3 to 8.6 mm^3/sec/mm. (0.4 to 0.8 in^3/min/in.). Figure 19 also shows the values obtained using made of resin bond, DB70, and metal bond, DM 17, both using diamond abrasives of type D1 at 100 concentration. As seen earlier in simulated bond wear and 3-point bend strength tests, these results also confirm that it is possible to develop metal bonded wheel specifications that would posses performance characteristics anywhere between the resin (DB70) and metal (DM17) bonds. In subsequent Task 2 of this project, a limited number of 203-mm (8 in.) diameter wheels were tested leading to selection of one optimum wheel specification.

7.1.4.3. CVD Diamond Wheel Screening Test Grinding Results. The first wheel (made in the manner shown in Figure 10) was tested under the conditions listed below on the Okuma CNC cylindrical grinding machine in a plunge grinding mode. The workpiece material was the standard sialon used for the Superabrasive wheel screening tests, except that the disk was 3.8-mm thick. The thinner ceramic disk was to compensate for the slightly thinner CVD wheel, thereby avoiding possible edge effects in the plunge test. The screening test conditions were as follows:

Surface speed	32 m/s (6252 sfpm)
Infeed rate	12 μm/s

The CVD grinding test was disappointing and the configuration was unable to grind effectively. As the wheel encountered the workpiece, the normal force on the workpiece rose rapidly. After 20 s it exceeded 500 N and the test was terminated to avoid damage to the grinding machine.

Optical inspection of the workpiece and the wheel showed little stock removal from the workpiece and significant burning of the wheel face. Also, we observed radial cracks in the wheel face, which were also probably caused by overheating.

Figure 20 shows an electron micrograph of one tooth in the CVD wheel after use. In the center of the picture the molybdenum core of the tooth is visible; the outer end of the tooth core is below the picture. Residual diamond coating is visible over the upper end of the tooth. The rest of the material is the epoxy matrix: the white highlights are instrument artifacts caused by charging of the non-conducting regions.

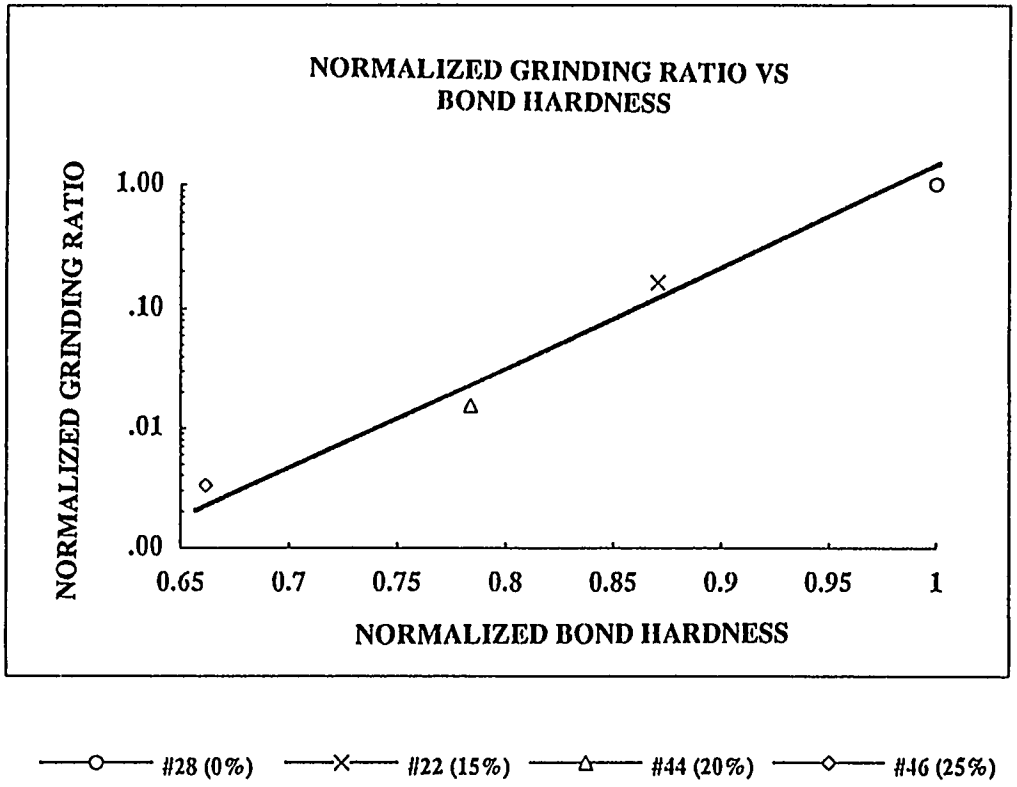

Figure 18. The normalized grinding ratios as a function of bond hardness for a given bond system are shown. The range of values for hardness were obtained by changing the levels of pore inducer from 0 to 25% by volume. Such a graph could be used to design wheels of known grinding ratios in future.

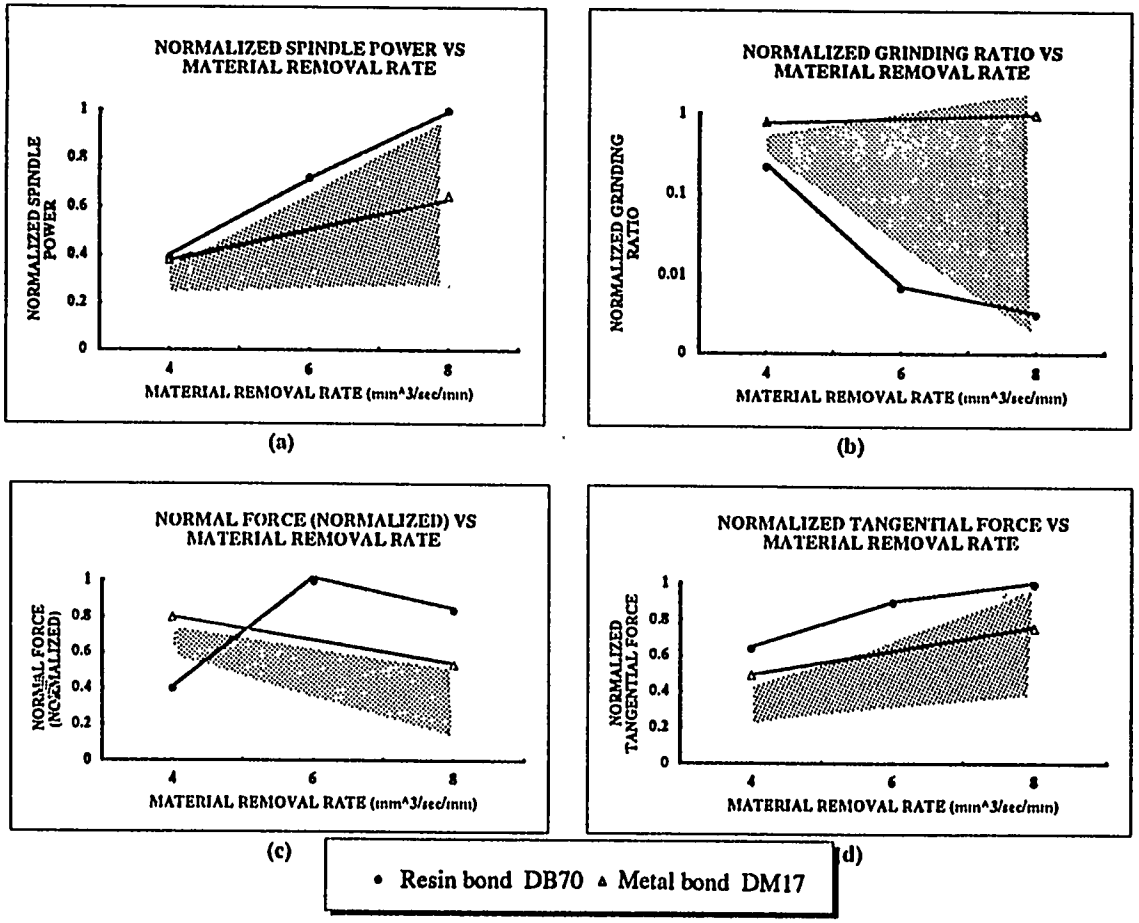

Figure 19. The summary of the results obtained using all the 76-mm (3 in.) diameter wheels on sialon work piece is shown. The results indicate that metal bonds could be designed with a range of characteristics.

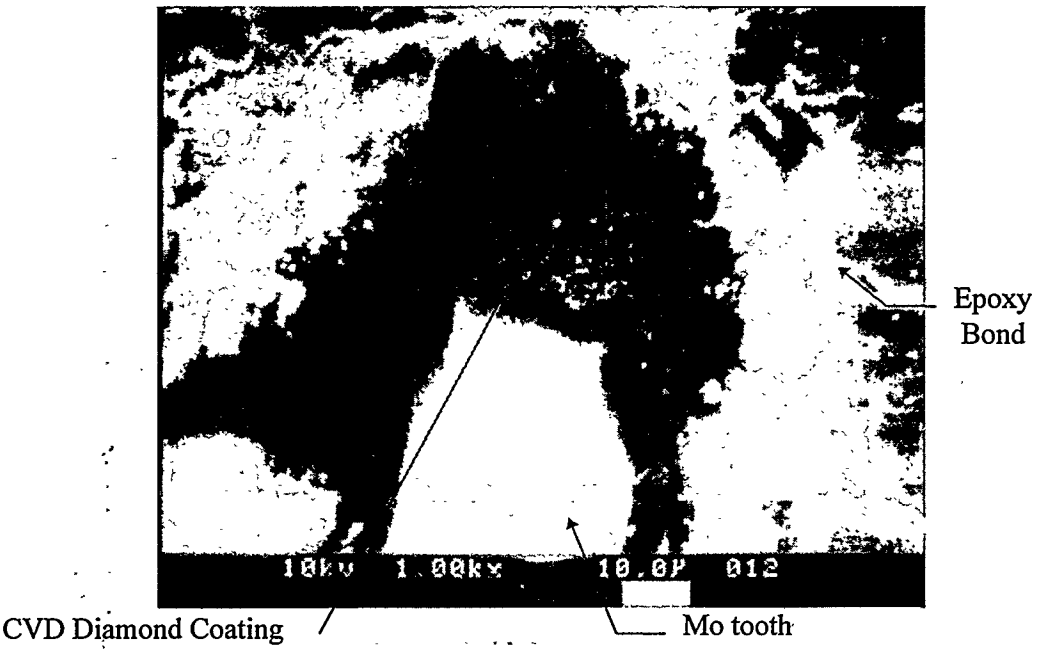

Figure 20. SEM view of a tooth in the first CVD wheel design.

The micrograph suggested that diamond tended to crack away from the tooth cores well below the tip of the tooth. We postulated two reasons for this. First, the strength of the diamond and its bond to the molybdenum may have been insufficient. Second, the long aspect ratio of the tooth and the large difference in flexural modulus between molybdenum, diamond and epoxy (perhaps a factor of 500) may permit the tooth to flex in a manner that led to premature cracking of the diamond. Although we did not appreciate their significance at the time, (after truing, but before testing, the wheel) there was evidence of azimuthal cracks in the diamond down to the visible limit (approximately 100-μm below the surface of the wheel). Figure 20 shows azimuthal cracks in the Mo tooth. We believe that the reason why the wheel did not grind effectively in the test was that diamond prematurely spalled away from the teeth.

Following these tests, the second design was chosen. We initially tried to test the wheels in the configuration shown in Figure 21. This proved not to be useful because the wheels would tear, leading to high wear in the neighborhood of the tear and little wear elsewhere. We could not obtain trustworthy measurements of wear rate under these circumstances.

After some experimentation, a modified geometry shown in Figure 22 was chosen. The Si_3N_4 workpiece had four segments cropped from it to cause interruptions in the cutting process. Experience with other grinding wheel tests indicates that an uninterrupted cut would produce uncharacteristically low wheel wear rates compared to a conventional moving wheel - stationary workpiece situation.

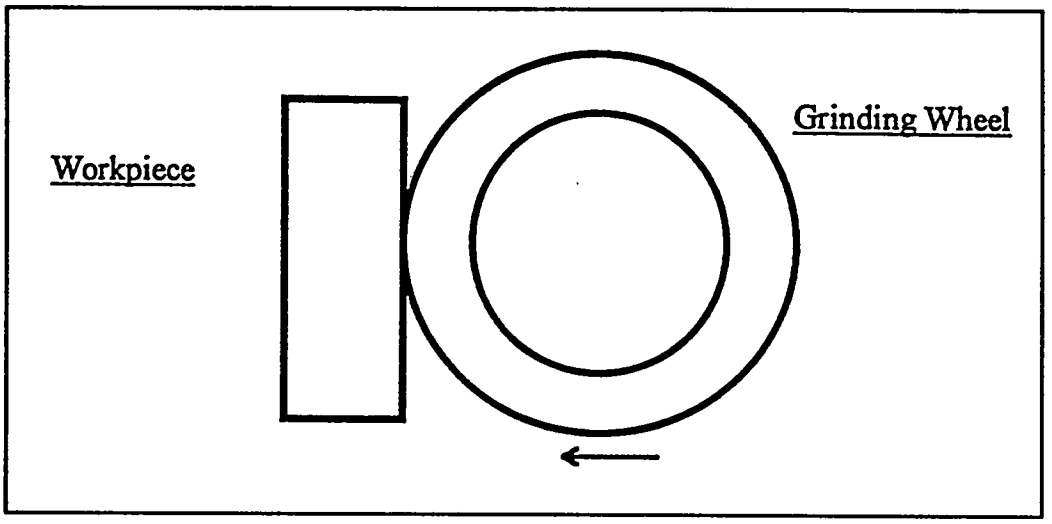

Figure 21. First test arrangement for the second CVD wheel design

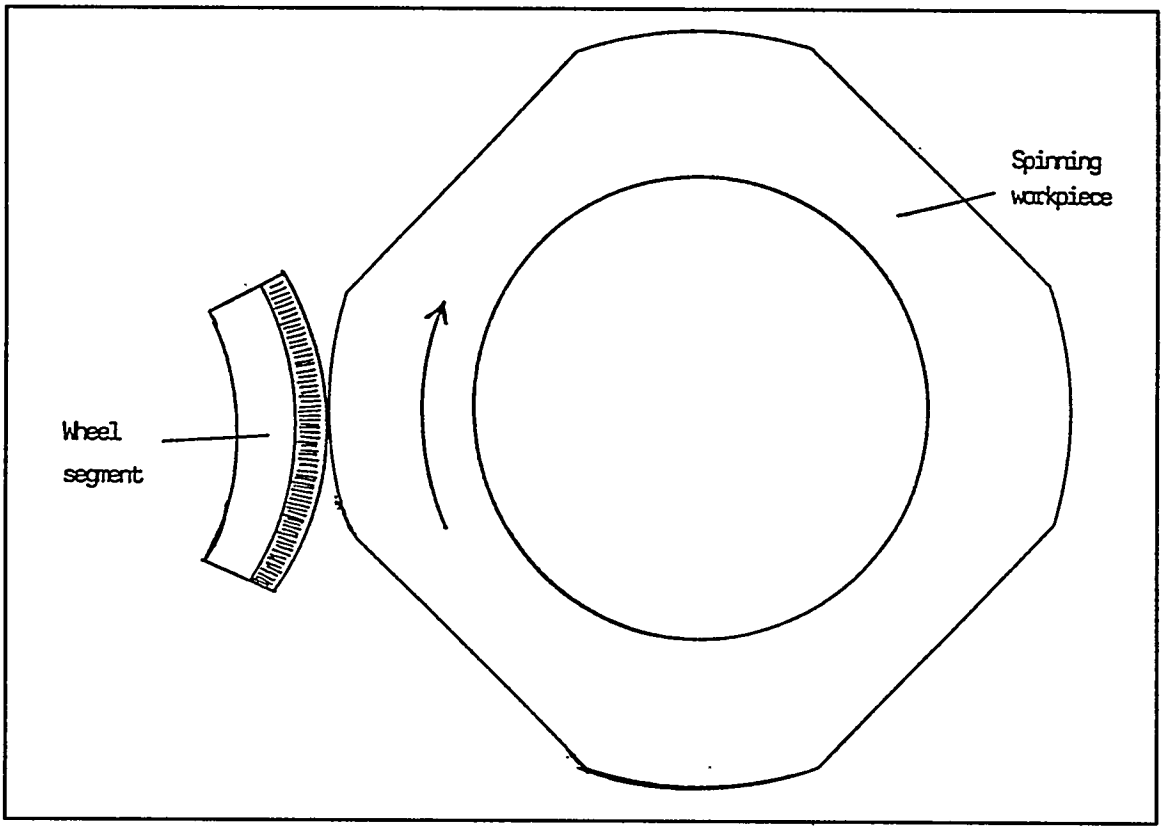

Figure 22. Second test configuration for CVD wheels.

Grinding was done under the conditions listed below:

Surface speed	36 m/s (7092 sfpm)
Infeed rate	1 μm/s.

These conditions are somewhat less aggressive than the first test as we were concerned to avoid wheel damage. Two plunges at different axial locations on the workpiece were made to generate sufficient wear. Each plunge was about 100 μm, although there was uncertainty in defining the precise point at which the workpiece touched the wheel.

Figure 23 shows a view of the top surface of a worn wheel. The molybdenum preform was smeared out over a much larger dimension than its original thickness of approximately 30 μm. On the right side of the micrograph is a small piece of delaminated diamond. Such delaminations were fairly common within about 50 μm of the top surface of the wheel.

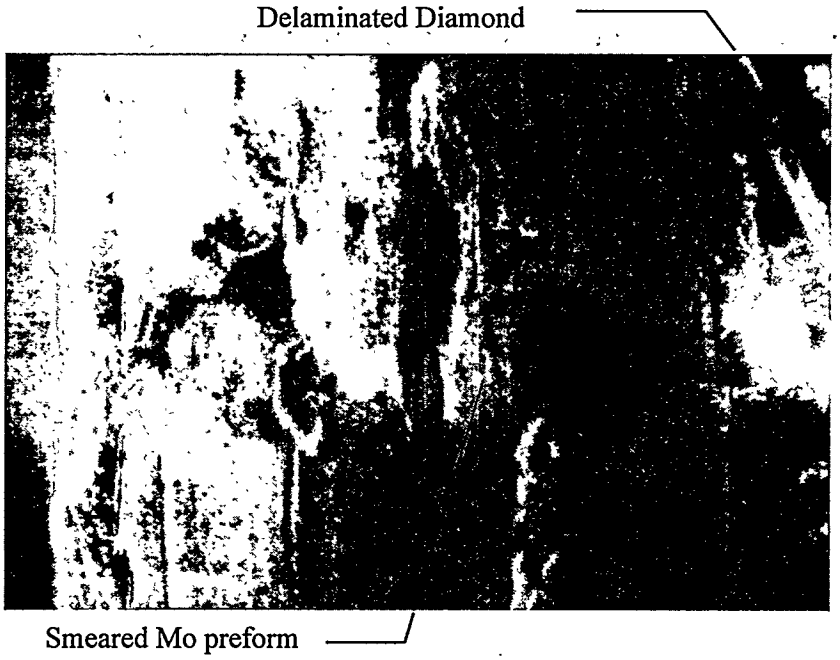

Figure 23. Top surface of worn CVD wheel.

Material removal was measured by tracing a profilometer across two locations of the workpiece wear groove on each of the four curved workpiece sections. For reasons possibly associated with the dynamics of the workpiece, the groove area did vary around the diameter of the workpiece. Wheel wear was measured by measuring the length, d, of the wear scar and computing the area, A_W, worn from the scar length according to the formula:

$$A_W = R_W (\theta_W R_W/2 - d\cos(\theta_W/2)/2) + R_S (\theta_S R_S/2 - d\cos(\theta_S/2)/2)$$

where R_W and R_S are the wheel radii and Si_3N_4 workpiece radii respectively, θ_W and θ_S are the angles subtended by the wear scar at the wheel and workpiece centers respectively.

Table 2 summarizes the wear-test results of the modified cut-off test. G-ratio is the ratio of the volume of stock removed to the volume of wheel wear. Diamond thickness does appear to affect G-ratio. The higher performing run, TC908, had several times the diamond thickness of the other wheels and also performed several times better.

Table 2. CVD Diamond Wheel Test Results

Test run	*Diamond thickness (μm)*	*Stock removal (mm^3)*	*G-ratio*
TC908	14	0.51	9.7
TC910 #1	2.8	0.47	2.0
TC910 #2	2.8	0.54	1.0
TC911	2.8	0.30	3.2
TC912 #1	4.6	0.36	2.4
TC912 #2	4.6	0.27	3.1

For comparison, typical G-ratio values for a Superabrasive cylindrical grinding wheel are several hundred times higher. We believe that local stresses are too high at the grinding face for the polycrystalline CVD diamond to withstand, and fractures at the grain boundaries and at the Mo-diamond interface are causing wheel erosion.

These data indicate that the CVD wheel approach does not appear at this stage to offer promise for cost-effective cylindrical grinding of ceramics.

7.1.4.4. Analysis of Ceramic Grinding Damage. After the screening grinding tests, the sialon disks were examined for unusual visible grinding damage. Optical microscopy did not reveal grinding cracks, or unusual grinding imperfections, in the outer diameters of the screening test disks.

Selected disks were prepared for C-ring compression mechanical tests[17]after they were ground in the screening test with experimental metal bonds. Currently, ASTM is working on a draft standard for diametrically compressed C-ring specimens. The C-ring tests that we performed were meant to identify any unusual grinding damage generated by the experimental and standard wheels in the screening test. These tests evaluated the strength of the ground OD. For the C-ring test, tensile stresses are parallel to the grinding direction. Figure 24 is a finite element analysis of the sialon C ring specimen showing the loading direction and maximum tensile stress. Table 3 lists the grinding conditions for the four disks tested in the C-ring compression test.

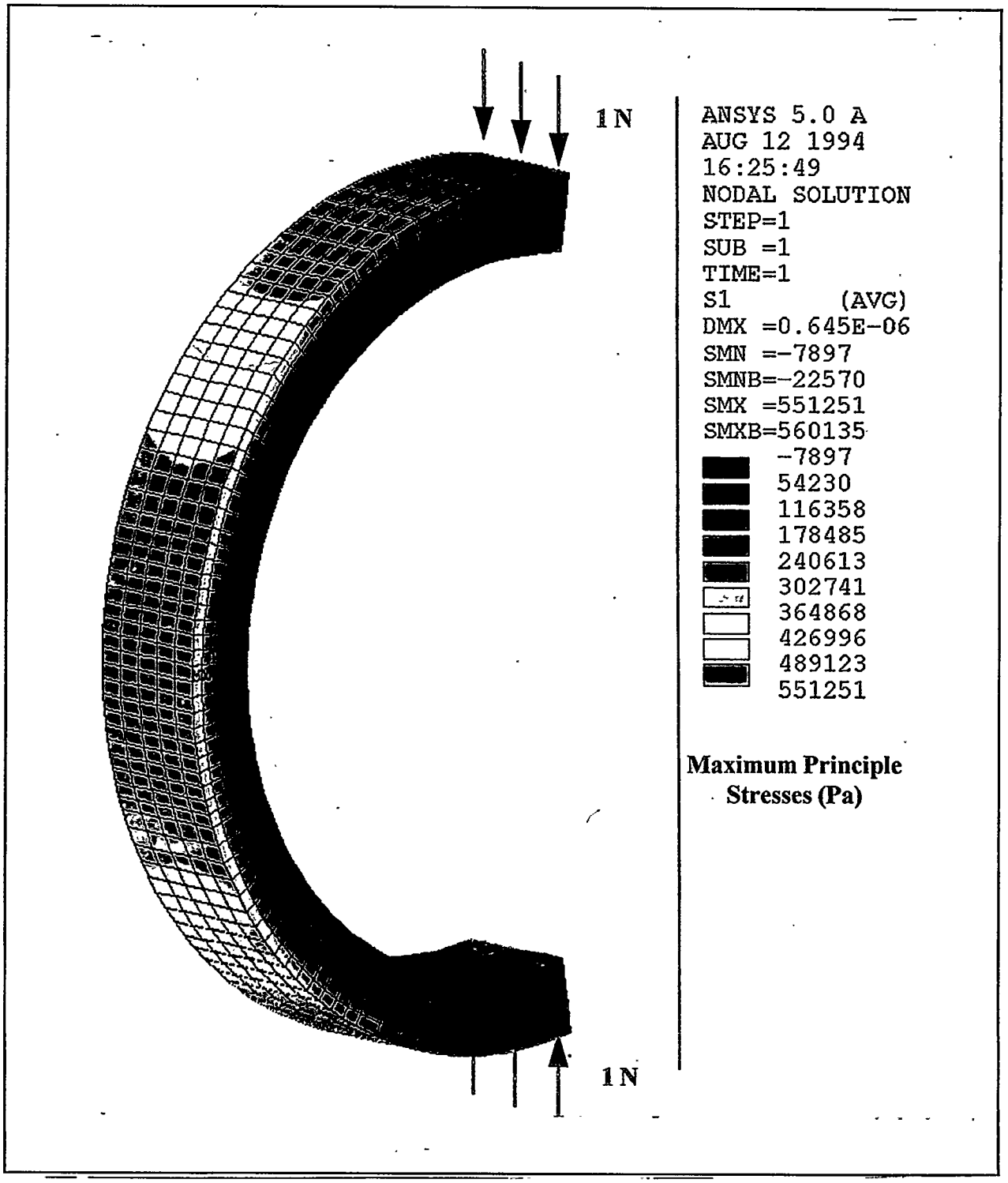

Figure 24. FEA of stresses on a C-ring specimen machined from sialon screening test disks.

Table 3. Grinding conditions for C-ring test.

Sialon Part No.	Wheel No.	Metal Bond No.[a]	Material Removal Rate ($mm^3/s/mm$)[b]	($in^3/min./in.$)
5	7	MXL1970	8.6	0.8
8	10	MXL1941	4.3	0.4
9	10	MXL1941	8.6	0.8
10	12	MXL1981	8.6	0.8

[a] Wheel specification = SD320-100MXL 19XX -⅛; wheel size = 76.2-mm diameter.
[b] All rings were ground to a final diameter of 77.5 mm at this material removal rate.

The following is a description and the results of the C-ring test that we used. Four sialon disks previously circumferentially ground were cut in half and tested under monotonic (continuous nonstop test rate) compressive loading in a C-ring configuration. A schematic of the C-ring is shown in Figure 25. A total of eight tests were performed.

The loading rate was 0.508 mm/min and the testing was performed at room temperature in air. The rings were compressed between articulating steel platens using an Instron 4206 test machine.

The strength results are summarized in Table 4. Parts #8 showed the highest strengths while parts #5 showed the lowest strength although there was no apparent significant difference. Optical fractography revealed that all breaks originated near corners.

The strength data is lower than subsequent measurements on regular flat MOR bars and the rods produced in this study. Corner fractures are hard to avoid in specimens used for this test, and this will lead to a lower strength. Secondly, in this type of test, the volume of the bar under stress is considerably higher than in MOR tests. From a statistical point of view this too will lead to lower strength measured. The corner breaks and the limited number of data points make comparative conclusions suspect. Clearly, the experimental results do not show evidence of unusual grinding damage to the ceramic disks. The test also did not show a significantly lower strength of Wheel No. 10 at the lower material removal rate (specimen 9 vs. 8).

More comprehensive flexure testing was planned and done for the Task 2 rods. Stresses generated during flexural testing was normal to the grinding direction, which resulted in a more meaningful cylindrical grinding damage evaluation. Therefore, the C-ring test in Task 1 was determined to have limited usefulness as a qualitative assessment of grinding damage.

7.1.4.5. Preliminary Wheel Cost Performance Analysis. The superabrasive bond modifications of standard metal bonds in Task 1 would not be expected to increase wheel cost compared to standard metal bond products. This assumes that current acceptable wheel rejection levels during manufacturing can be maintained.

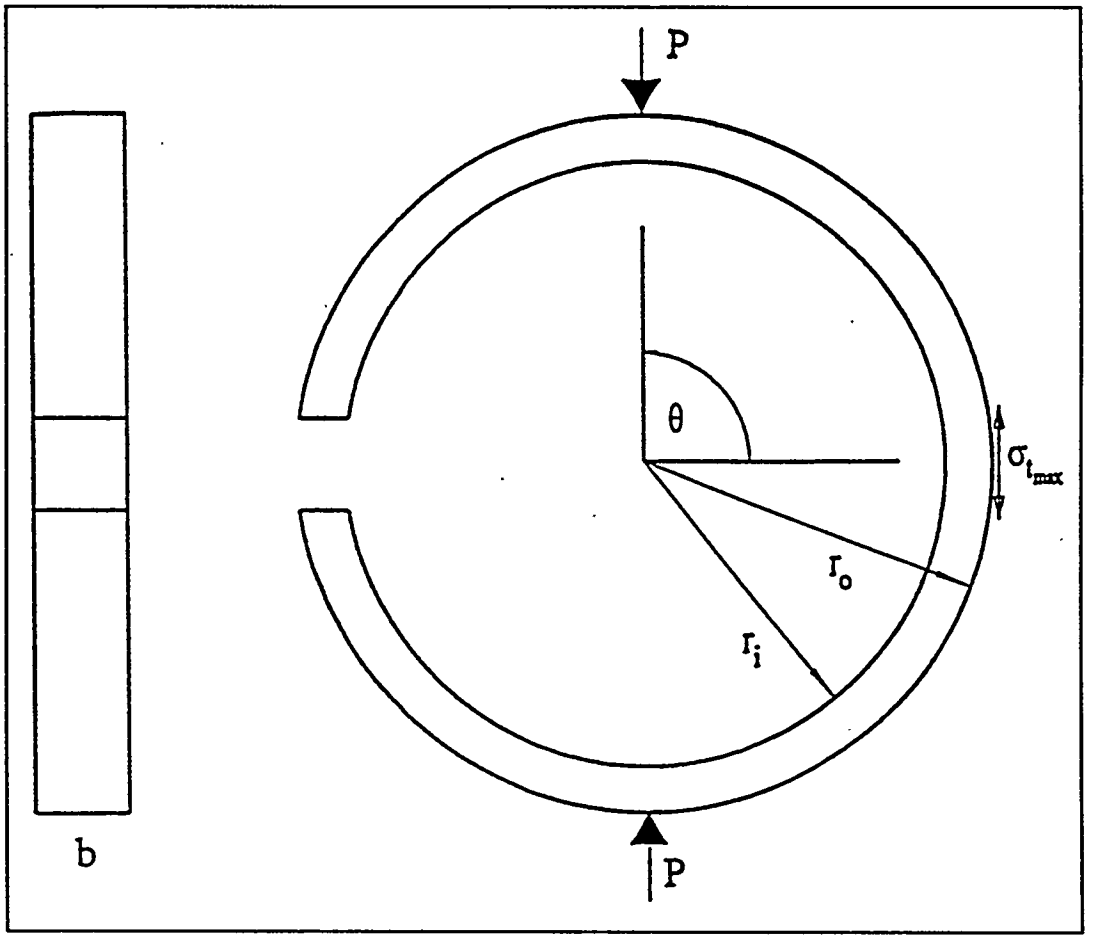

Figure 25. C-ring test geometry with defining geometry and reference angle.

Table 4. Summary of strength data from C-Ring test on sialon test disks.

	Measurements					Calculations						
PART	width	O.D.	thickness	peak load	peak load	outer rad.	inner rad.	term	term	max. stres	max. stres	avg.
No.	"b"		"t"	"P"	"P"	ro	ri	ra	R	Stmax	Stmax	stress
	in.	in.	in.	kg	lb	in.	in.	in.		psi	MPa	MPa
5,1	0.235	3.05	0.144	14.36	31.658	1.525	1.382	1.453	1.452	54,211	374	
5,2	0.235	3.05	0.143	13.15	28.990	1.525	1.382	1.453	1.452	49,862	344	359
8,1	0.236	3.051	0.146	14.36	31.658	1.5255	1.379	1.452	1.451	51,916	358	
8,2	0.236	3.05	0.146	22.15	48.832	1.525	1.379	1.452	1.451	80,166	553	455
9,1	0.236	3.051	0.145	15.97	35.207	1.5255	1.381	1.453	1.452	58,831	406	
9,2	0.236	3.051	0.145	15.57	34.326	1.5255	1.381	1.453	1.452	57,358	395	401
10,1	0.235	3.049	0.141	15.57	34.326	1.5245	1.383	1.454	1.453	60,864	420	
10,2	0.235	3.049	0.141	14.76	32.540	1.5245	1.383	1.454	1.453	57,697	398	409

7.2. DESIGN AND PROTOTYPE DEVELOPMENT -- TASK 2

7.2.1. Task Overview

Task 2, Design and Prototype Development, we down-selected to a few experimental metal-bond wheel types for further design and optimization. The manufacturing process was scaled up from the 76-mm wheels to 203-mm wheels. These 203-mm (8 in.) diameter prototype wheels were tested in a cylindrical mode, grinding ceramic rod specimens similar in geometry to valve stems. Grinding wheel performance was assessed on three types of ceramic specimens: NC-520 sialon, NCX-5102 HIP'ed silicon nitride and AZ67H zirconia-toughened alumina. Wheels were evaluated for grinding parameters such as material removal rate, wheel wear, G ratio, normal force, tangental force and grinding power. Additionally, the grinding wheel influence on ceramic surface integrity characteristics such as surface finish, damage, and retained strength were selectively evaluated. Task 2 culminated with the delivery, to ORNL, of six duplicate wheels of the best specification.

7.2.2. Final Superabrasive Wheel Experimental Design -- Task 2.1

Based on the results of Task 1, the Task 2 experimental design was completed. The test wheel specifications were selected from a short list, determined from the screening tests of 76-mm (3 in.) diameter wheels in Task 1. Approximately 6 wheel variables were selected for further study. The variables included metal composition, induced porosity level, diamond concentration and type. The standard wheel for this test was the standard resin bond product.

The main objective of this task was to extend the results of the 76-mm (3 in.) diameter wheels into larger 203-mm (8 in.) diameter wheels and arrive at an optimum specification for grinding advanced ceramics in external cylindrical grinding mode. A wheel made of the optimum bond composition was expected to consume low power, provide high grinding ratios, is either easy to dress or does not require dressing, and produces acceptable levels of damage to the work piece. The damage level to the ceramic using resin-bonded (DB70) wheel under the same grinding conditions was used as the minimum acceptable value. The best wheel specification was then used to grind three different advanced ceramic materials, seeking range of applicability for the improved metal-bond composition.

7.2.3. Fabrication of 203-mm (8 in.) Wheels and Ceramic Specimens -- Task 2.2

7.2.3.1. Superabrasive Wheel Fabrication. The promising metal-bonded wheel specifications of Task 1 were used to manufacture as series of 203-mm diameter (8 in.) test wheels in a newly designed and developed mold package. The experimental

variables were described in Section 7.2.2. Wheels were manufactured using powder metallurgy techniques, similar to some of our existing products. This permitted the manufacturing costs to be kept low that is essential for cost-effective ceramic machining. All test wheels were made with U.S. mesh 270/325 sized diamond abrasive grits in wheels measuring 203-mm (8 in.) diameter by 12.7-mm (0.5 in.) thick by 22.2-mm (0.875 in.) hole diameter. Manufacturing problems in the scale up from 76-mm to 203-mm diameter were encountered and addressed. Some of these wheels did not meet our quality requirements and had to be manufactured again.

The composition for the core (or hub) of this wheel, designated as CM 17, was selected from among existing, proprietary metal alloys. A similar core was used for the 76-mm diameter screening test wheels. This powder metal core could be sintered under the same processing conditions as the abrasive rim and also provide adequate diffusion bonding between the rim and core. The ingredients in CM 17 are also relatively inexpensive, which helped to maintain the cost-effectiveness of the new wheel system. Bond properties, such as the elastic modulus and the thermal expansion coefficient of CM 17 are similar to the abrasive bond. The use of the CM 17 hub resulted in more than adequate wheel strength for this program and for typical ceramic grinding. The wheels were successfully speed tested to approximately 91 m/s (18,000 surface ft./min.) and rated for at least 61 m/s (12,000 surface ft./min.) grinding speed. The ultimate wheel speed capability of this abrasive rim-core combination was not determined. However, if significantly higher speeds are required for future wheel testing, modifications could be made to the core material to maximize wheel speed capability.

7.2.3.2. Sialon, Silicon Nitride and ZTA Specimen Fabrication. Cylinders of these three materials, approximately 25.4-mm diameter and 79 mm long were produced by CIP'ing and firing. The sialon cylinders were sintered whereas the silicon nitride (NCX-5102) material was glass encapsulation HIP'ed. The ZTA (AZ67) was sintered to closed porosity and then HIP'ed. This material contains 20-vol% Y-TZP with 80-Vol% Al_2O_3. Highly dense material was obtained in all cases and these cylinders were then used directly for machining studies. The AZ67HS zirconia-toughened alumina (ZTA) rods were fabricated by Norton Advanced Ceramics, (Export, PA) and mechanical properties were characterized at NRDC. NRDC fabricated and characterized the NCX-520 sialon and NCX-5102 HIP'ed silicon nitride rods.

The ceramic specimens were qualified by evaluation of MOR flexure tests made from flat tiles at the same time as the rods. Flexure bars were 3 x 4 x 50 mm machined and tested accordance with ASTM Standard C 1161 standard test method for flexural strength of advanced ceramics at ambient temperature[18]. The specimens were longitudinally ground with 320 grit resin bonded wheels.

The same type B specimens were used for indentation fracture toughness, K_{IC}[19]. Indentation loads of 10 kg were used for sialon and silicon nitride and 20 kg for the ZTA. The results of the density, MOR and K_{IC} characterization are listed in Table 5.

Table 5. Average density, K_{IC} and MOR of ceramic materials used in Task 2.

Material	Specification	Density (g/cm^3)	Bars	K_{IC} ($MPa \cdot m^{1/2}$)	Bars	MOR (MPa)
Sialon	NCX-520	3.253	3	6.11	8	655
Silicon Nitride	NCX-5102	3.221	3	6.83	6	921
ZTA	AZ67	4.400	3	4.80	7	782

7.2.4. Grinding Evaluation of 203-mm (8 in.) Wheels -- Task 2.3

7.2.4.1. Grinding Test Description. The grinding test was performed on the same Okuma cylindrical grinder at Norton's World Grinding Technology Center that was used for the Task 1 screening test. The objective of this test was to identify the specification of the one best performing wheel for grinding advanced ceramics such as sialon and Si_3N_4. Ceramics rods of sialon measuring 26 mm in diameter and 84-mm long (32 in.) were ground in external cylindrical plunge grinding mode using 6.25 mm (0.25 in.) of wheel width. Holding it in a three-jaw chuck with 12.7 mm (0.5 in.) of it exposed, the ceramic rod was plunge ground at its end leading to a step diameter of 6.35 mm (0.270 in.). The removal rate was set at 4.5 mm^3/sec/mm (0.42 $in.^3$/min./in.) and maintained by periodically increasing the work speed and radial infeed. After plunge grinding once, the jaws of the chuck were released and the rod indexed axially outwards by 6.35 mm (0.25 in.). This type of part-holding arrangement assured two things; a constant part stiffness for wheel-work combination and removal of any damage caused by the chucking the rod. A total of nine plunges were made with each rod, and several rods were ground using a given wheel.

Some of these rods were subsequently ground transversely by feeding the wheel 0.013-mm radially on one side in several passes to a final diameter of 6.35 mm (0.25 in.). Trimcool, a water based coolant with rust inhibitor was used as the grinding fluid in all tests. Some rods were then tested in flexure at NRDC as described below in Section 7.2.4.3.

The power, forces, wheel wear, and surface finish of the ground rods were measured. Wheel wear was determined through precise micrometer measurements of wheel diameter before and after a grinding cycle. The volume of the wheel wear was calculated from the diametrical wear and the actual wheel face wear zone width. In the plunge mode test the wear zone was approximately half of the wheel face. In the transverse grinding mode the full wheel face was worn and wear volume was calculated from the wheel thickness.

7.2.4.2. Superabrasive Wheel Grinding Results. The composition of the wheel that produced the best performance included metal bond C, with D2 type abrasives of size U.S. mesh 270/325 at 75 concentration. Figure 26 compares the spindle power values drawn as a function of volume of material ground per unit wheel width, using this wheel. The power remained at steady levels during grinding of all three ceramics; sialon, HIP'ed Si_3N_4, and ZTA. The wheel required no dressing in grinding these materials under given test conditions. The power consumed in grinding NCX-5102 HIP'ed Si_3N_4 was about 50% higher than either NC-520 sialon or AZ67H ZTA.

Spindle power drawn when grinding NC-520 sialon, using this improved metal-bonded wheel at 75 diamond concentration versus the resin-bonded (DB70) wheel at 100 concentration, which is typically used in external cylindrical grinding of ceramics, are plotted in Figure 27. Grinding conditions were identical for both the experimental metal and standard resin wheel. While the resin-bonded wheel needed periodic stick dressing every 19 mm3/mm (3 $in.^3/in.$), the metal-bonded wheel did not need any stick dressing over 400 cm^3/cm of material removed. The metal-bonded wheel also consumed up to 30% lower power than the resin bonded wheel.

Figure 28 compares the average spindle power consumed versus diamond concentration with test wheel in metal bond C grinding the three different ceramics. The power values increased with abrasive concentration levels in all cases. NCX-5102 HIP'ed Si_3N_4 continued to consume the most power similar to results from the 75-concentration wheel, while the results on NC-520 sialon and AZ67H ZTA were reversed. The average spindle power consumed by both the resin and metal bonds with 100 concentration were nearly equal. The metal-bonded wheel at 100 concentration required dressing every 45 cm^3/cm (7 $in.^3/in.$) of material removed.

The cumulative wear data against total volume of material removed per unit wheel width is shown in Figure 29. This plot compares the experimental wheel with metal bond C at 75-diamond concentration, and the resin-bonded wheel at 100 concentration in grinding of NC-520 sialon. There is an order of magnitude decrease in wear with the improved metal bond C relative to the resin-bonded wheel. A standard resin-bonded wheel in 75 concentration was not tested because its wheel wear was considered unacceptable for cost-effective ceramics machining. The cumulative wear values as a function of total volume of material removed for a wheel with metal bond C in 75 concentration, grinding the three different ceramics, is plotted in Figure 30. The cumulative wear of the wheel in grinding AZ67H is about three times that in grinding NC-520 sialon and twice in NCX-5102 Si_3N_4. The nearly constant slopes of the three cumulative wear graphs is another indication of controlled and uniform wheel wear with this experimental metal bond at 75 diamond concentration level.

Figure 31 compares the normalized wear of the two 203-mm (8 in.) diameter wheels of metal bond C with 75 and 100 diamond concentration levels grinding the three different ceramics. AZ67H ceramics again are shown to wear the wheel with 100 concentration more than the other two materials, similar to results at 75 concentration. However, the relative wheel wear dropped by about 50% for 100 concentration wheels compared to 75 in all three ceramic workpieces tested.

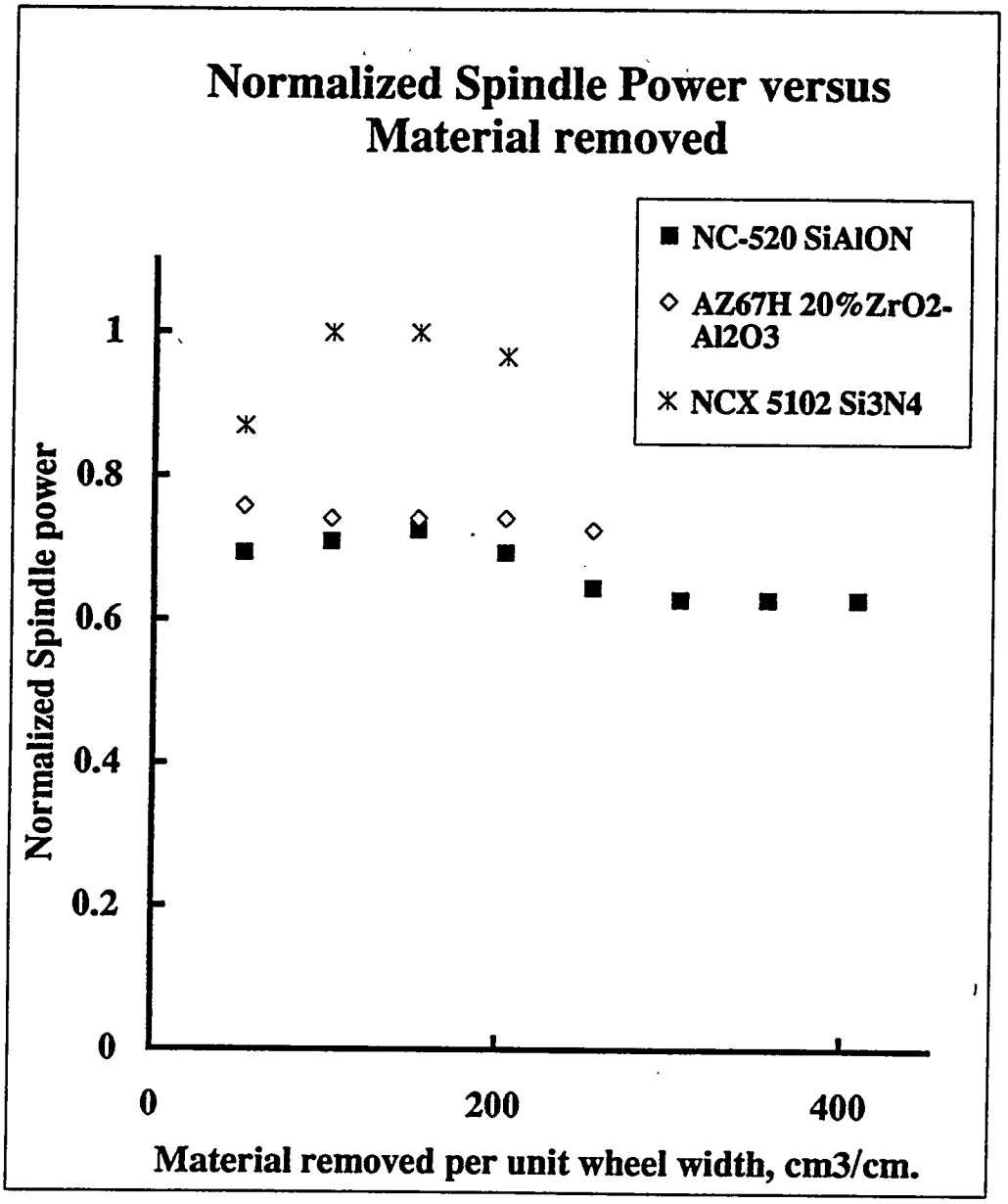

Figure 26. Spindle power drawn during the grinding of three different advanced ceramics using the improved metal bond. The ceramics include NC - 520 Sialon, AZ67H - 20%ZrO_2-Al_2O_3 and NCX-5102 HIP'ed Si_3N_4. The power levels are nearly uniform indicating a controlled wheel wear. The amount of sialon represents nearly 3 hours of continuous grinding.

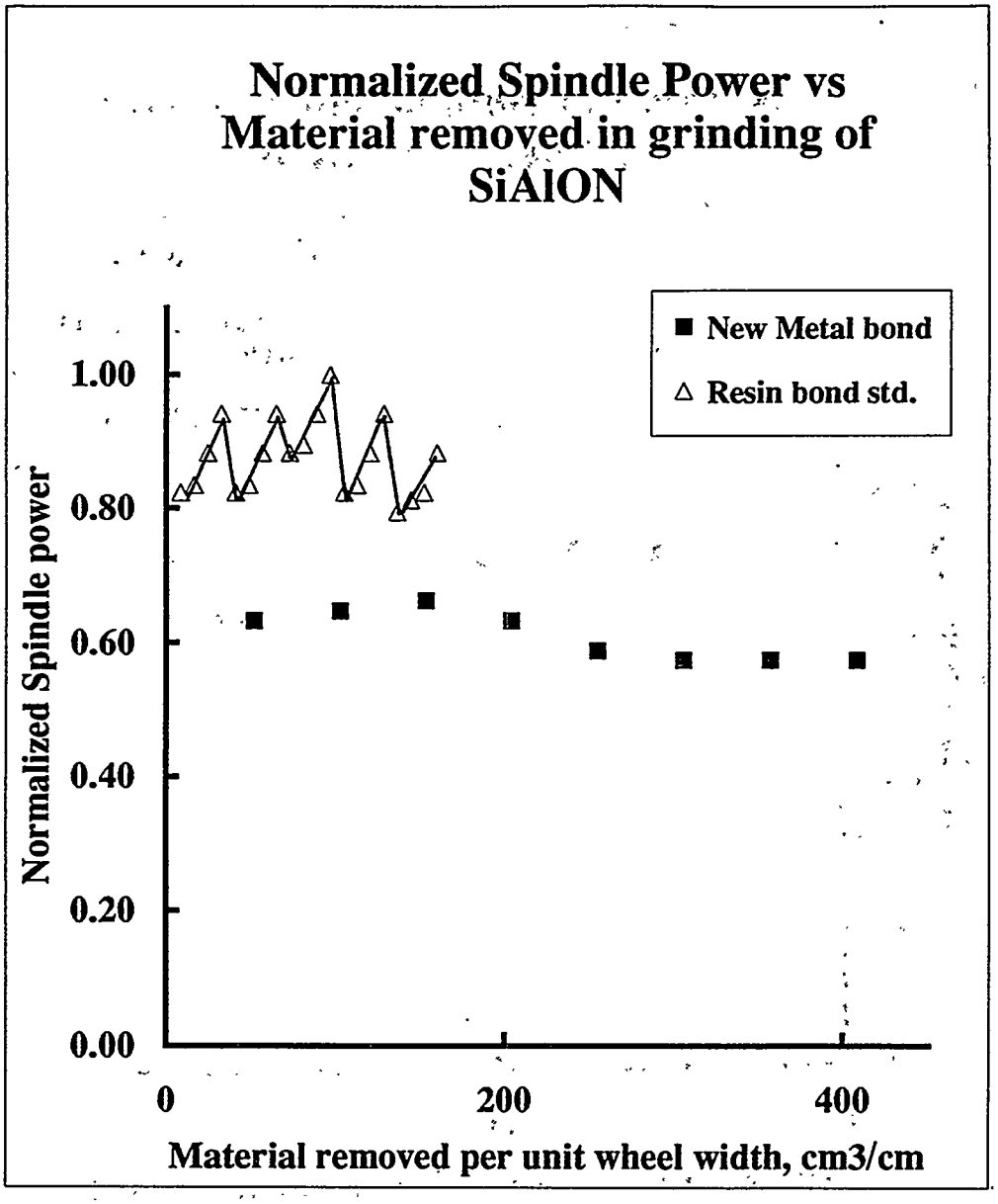

Figure 27. The spindle power drawn during the grinding of NC-520 sialon using the standard 100 diamond concentration resin bond DB70 and the improved metal bond with 75 concentration. The new metal bonded wheel drew lower power than the resin bonded wheel, typically used in grinding of different ceramic materials. The power levels with the metal bond were nearly uniform indicating a controlled wheel wear. The power drawn by the metal bond was nearly constant over 400 cm3/cm or 64in3/in.of wheel width. There was no need for stick dressing with the metal bond. The resin-bonded wheel required periodic stick dressing, every 20 cm3/cm or 3 in3./in., to lower power at acceptable levels.

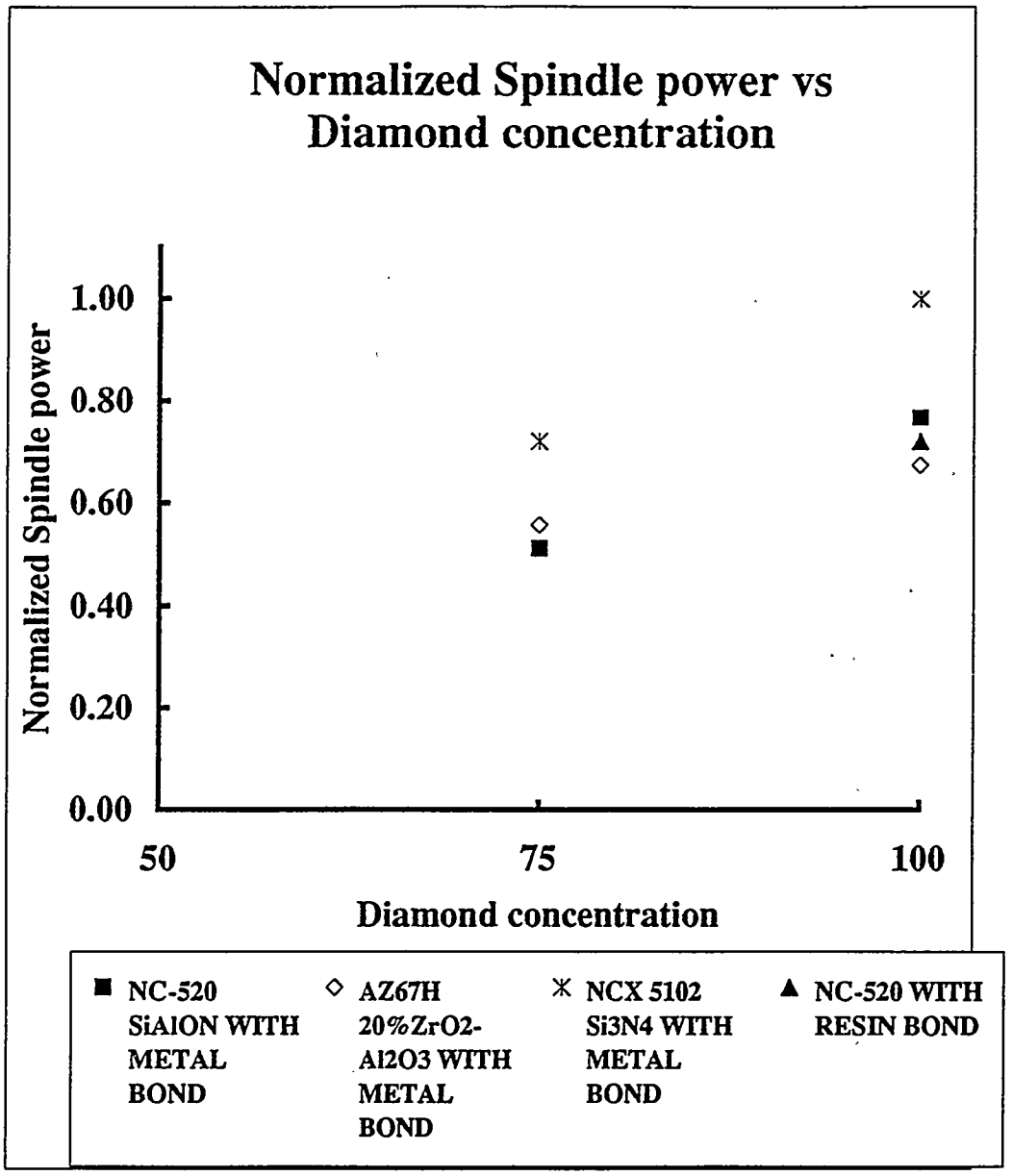

Figure 28. The normalized spindle power drawn in grinding of NC-520 sialon using 203-mm (8 in.) wheels as a function of diamond abrasive concentration. The power drawn increases with concentration with the metal bond with all three ceramics. Power drawn by typical resin-bonded wheel grinding NC-520 sialon is also shown for reference.

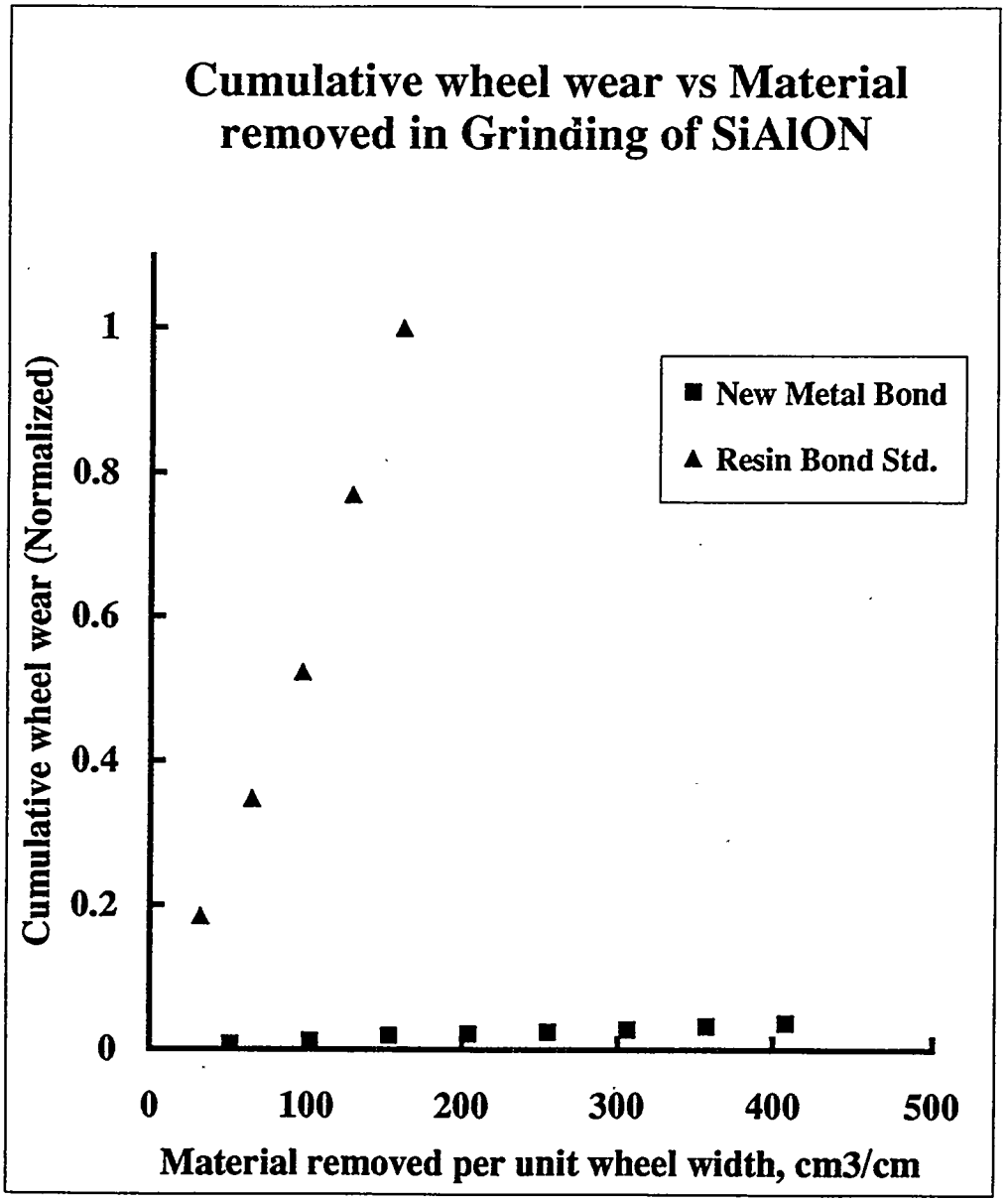

Figure 29. The cumulative wheel wear of the improved metal bond in grinding of sialon is compared with the standard resin bond. Although the diamond concentration in resin bond is 100 and 75 in metal bond, wear rate of the metal bond is an order of magnitude lower than the resin bond.

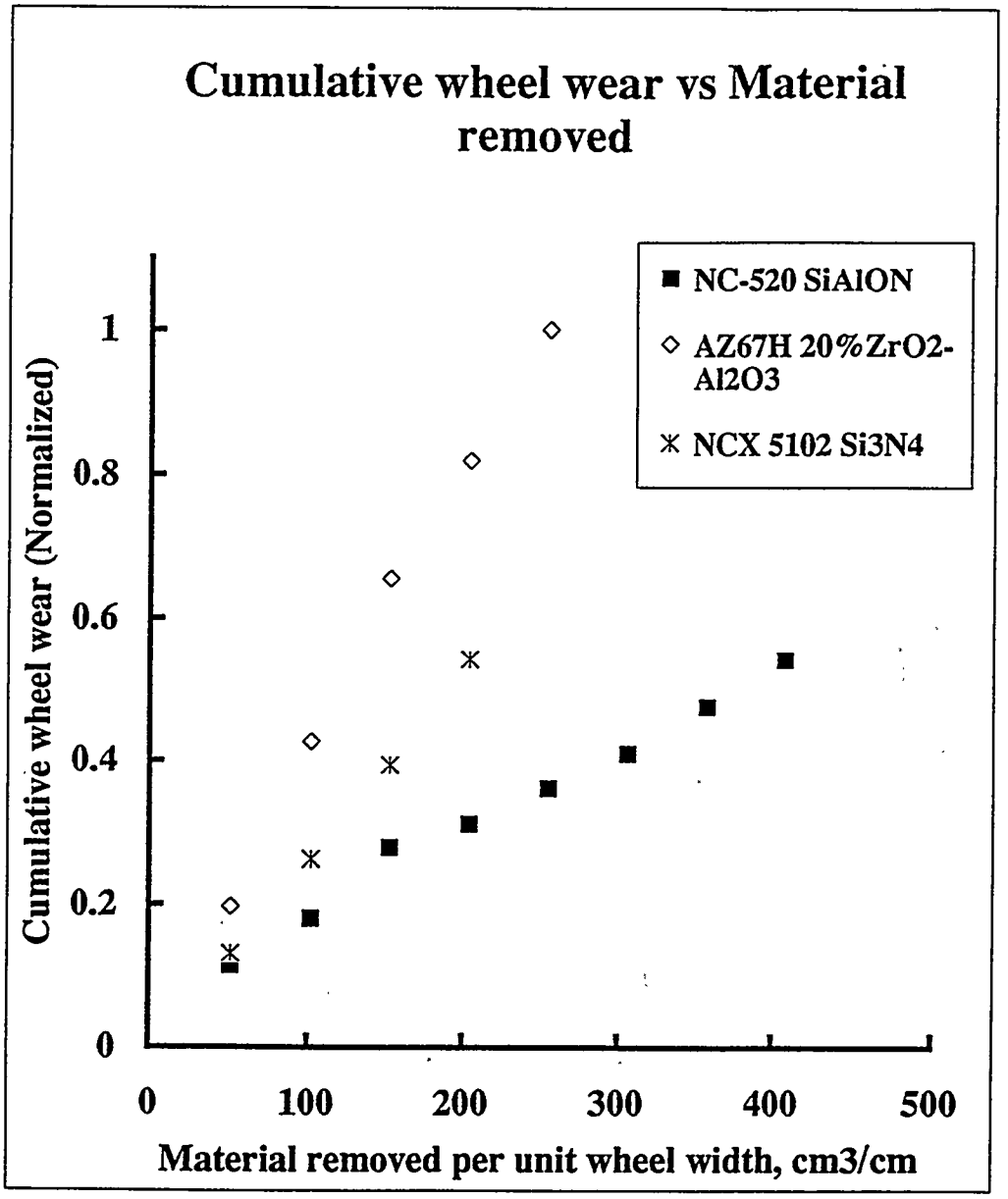

Figure 30. The cumulative wheel wear of the new metal bond in grinding of three ceramics. The constant slopes of the three graphs is another indication of uniform wheel wear. The wear rate of the wheel in grinding AZ67H ZTA is almost three times that of NC-520 sialon.

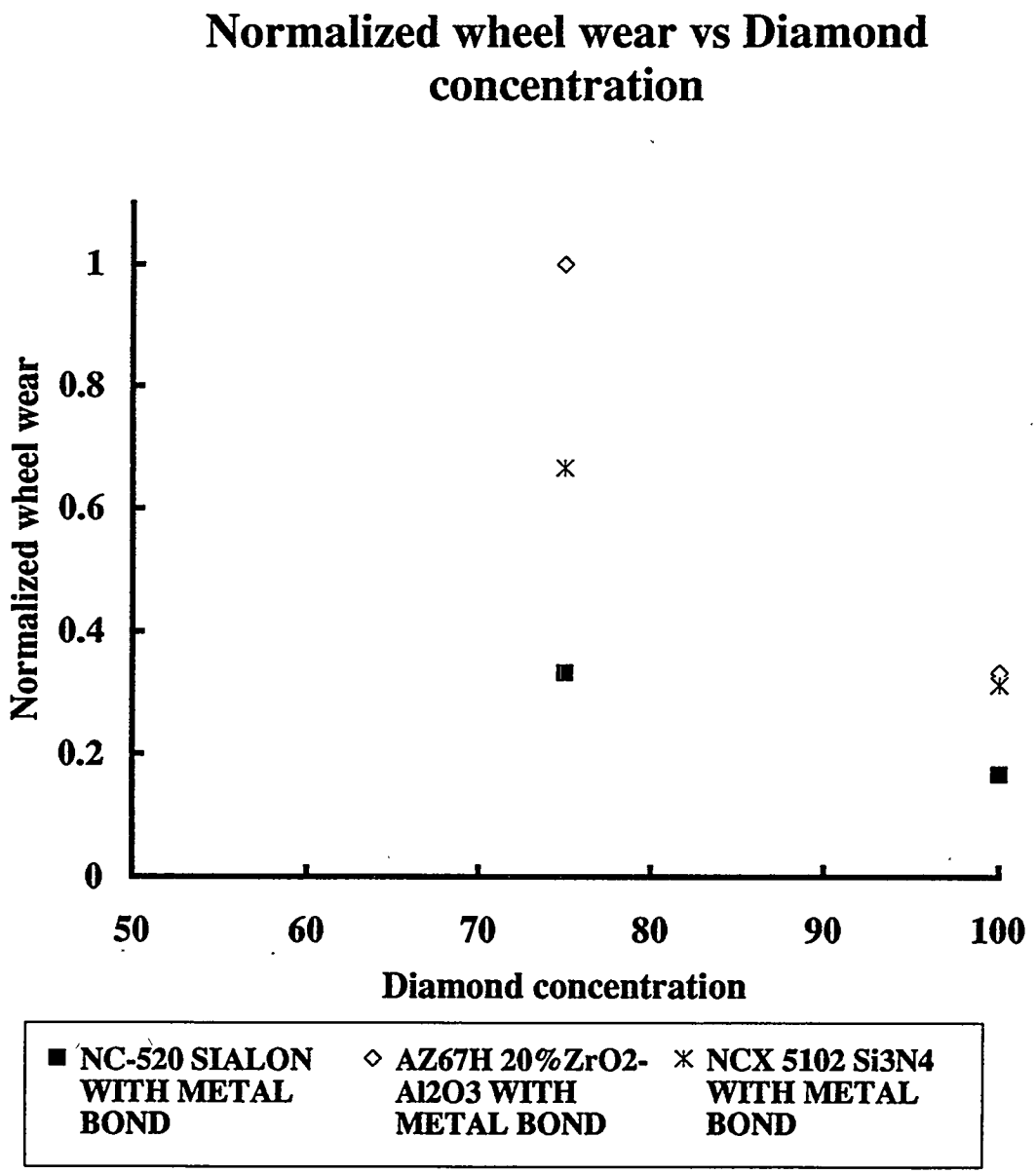

Figure 31. The wheel wear (normalized) in grinding of three ceramics using a 203-mm diameter improved metal-bonded wheel containing 75 and 100 concentration of diamond. The wear decreases with 100-diamond concentration while the wear trends among the different ceramics are similar. The wheel wear volume of in grinding AZ67H ZTA is about three times that of NC-520 sialon and twice that of NCX-5102 HIP'ed Si_3N_4.

"Grindability" values of NC-520 sialon using the improved metal bond at 75 concentration and the standard resin bond at 100 are shown in Figure 32. For a given wheel-work system, grindability is defined here as the grinding ratio of the wheel/specific energy to remove a unit volume of material. A high value of grindability indicates a low wheel wear or energy required for unit volume of material removal and, hence, is desirable.

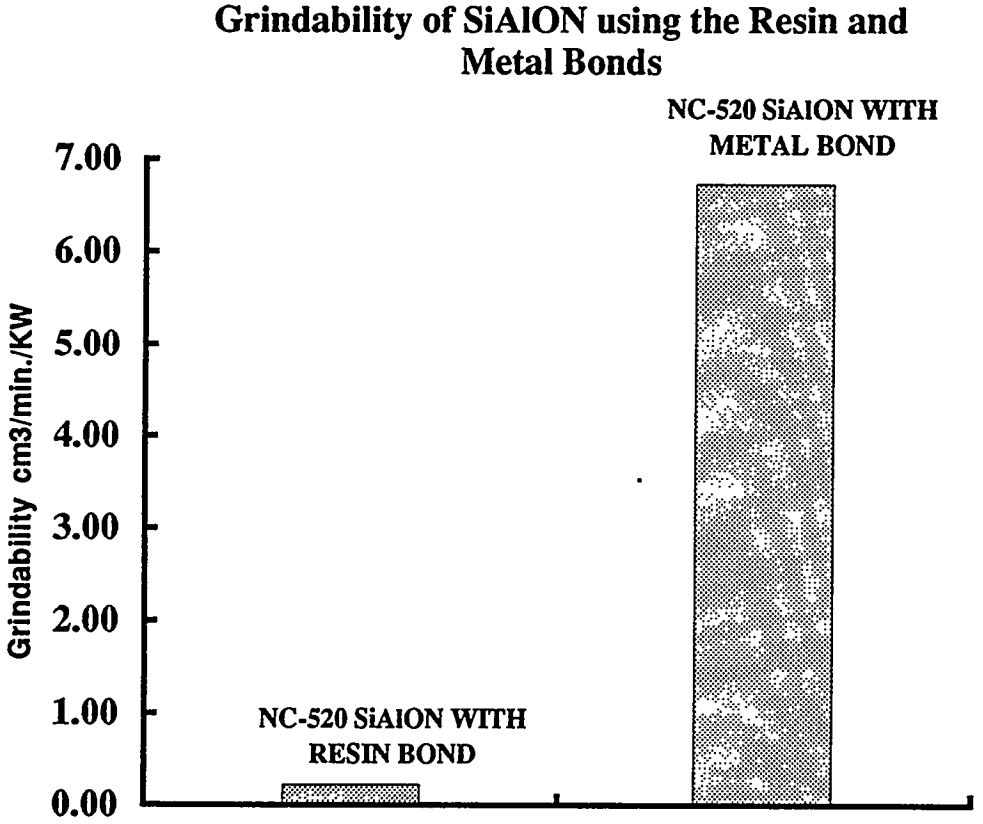

Figure 32. "Grindability" of 203-mm (8 in.) diameter resin- and metal-bonded wheels grinding NC-520 sialon ceramics. Grindability is by definition, Grinding ratio/Specific grinding energy. This is an estimate of wheel consumed removing a unit volume of material over energy required. Higher values imply lower energy needs and/or lower wheel wear. The new metal bond-ceramic combination produced significantly superior results.

Figure 33 compares the grindability of the three ceramic materials with the improved metal bond at 75-diamond concentration. The grindability of sialon is nearly three times that of either ZTA or HIP'ed Si_3N_4.

Some of the other experimental 203-mm wheels resulted in poorer results than the best experimental wheel and in some cases were even poorer than the resin bond. These tests were discontinued. These other experimental wheels would not be considered for cost-effective ceramic machining.

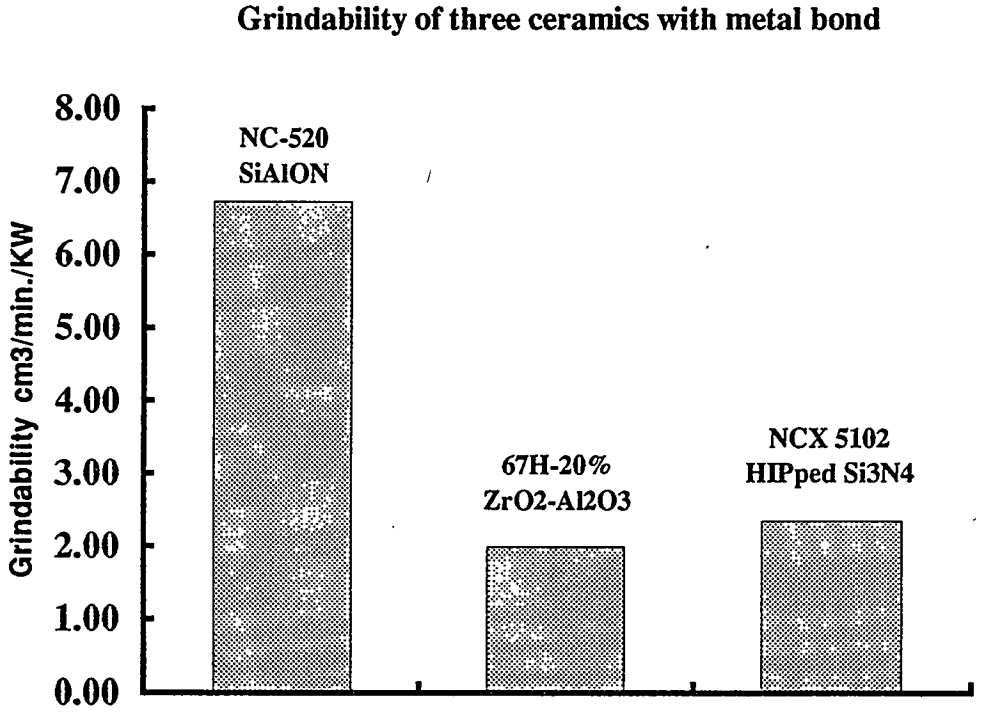

Figure 33. "Grindability" of the 203-mm diameter improved metal-bonded wheel grinding sialon, ZTA and HIP'ed Si_3N_4. The metal bond-NC-520 sialon ceramic combination produced grindability values up to three times that of ZTA or Si_3N_4.

7.2.4.3. Ceramic Rod Specimen Damage Assessment. The cylindrical rods in the Task 2 grinding test were initially plunge ground and subsequently transverse ground to the final 6.35-mm diameter. Figure 34 shows typical rods after grinding tests displaying the original and final diameters (the large diameter end was held in the chuck). These test rods were sent to NRDC for flexure strength and grinding damage evaluation.

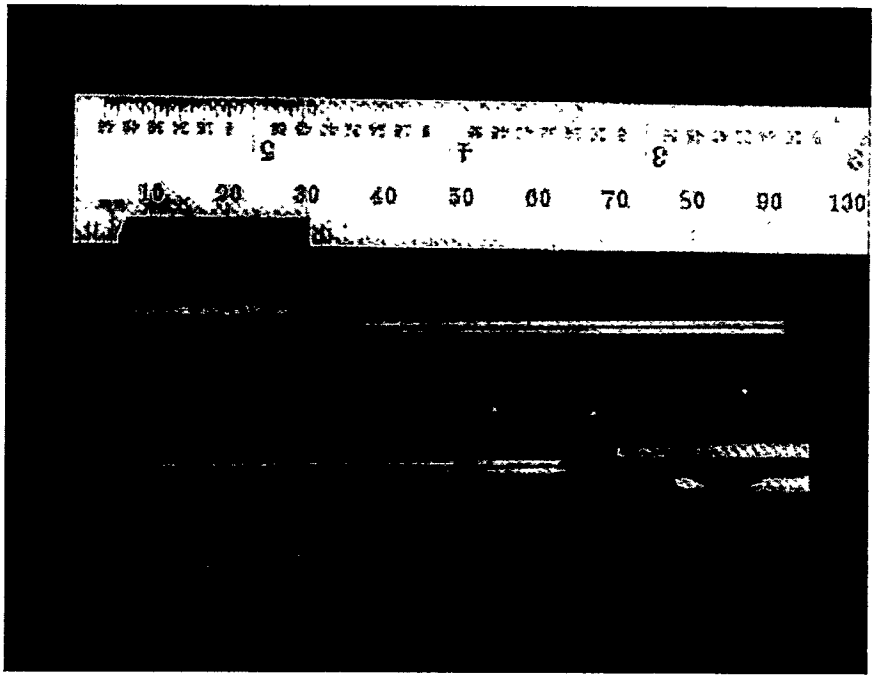

Figure 34. Sialon specimens after cylindrical grinding test and prior to flexural strength testing. Specimens = ~79 mm long. Original diameter = 25.4 mm. Final diameter = 6.35 mm.

Rods from selected grinding tests were next subjected to flexure testing. The flexure stress for three point bending was calculated from the following equation:

$$\sigma = 8\ PL/\pi d^3$$

Where σ is the fracture stress in pascals, P is the fracture load in newtons and L is the span length in meters and D is the rod diameter in meters. The rods used were 6.35-mm diameter and the span was 40 mm.

We compared reciprocal grinding bar strength of our best experimental metal-bonded wheel against a standard resin-bonded wheel for sialon bars. The results are shown in Table 6. Gratifyingly, the experimental metal-bonded wheels gave no significant reduction in strength from that of the standard resin-bonded wheel and the strength is similar to that for flat longitudinal grinding in Table 5. It is somewhat surprising that there is no reduction in strength here with transverse grinding. It is possible that volume flaws are dominating machining flaws, but these are quite high MOR values. In the case of the ZTA material we know from flat transverse grinding studies with 320 resin wheels that the strength can be reduced to 400 MPa, so the numbers here are consistent. The slight tendency for lower strength with the metal bond should be studied in more detail in future work. Unfortunately, the constraints of the contract schedule did not allow a similar study of silicon nitride.

The fracture origins of these fractured sialon bars and the topography of the machined surfaces are of interest. Consequently, we have measured the surface roughness, R_a, for (i) the sialon rods ground with resin- and metal-bonded wheels reciprocally, (ii) plunge ground, and reciprocally ground ZTA. (There was little difference between the two.) A series of profilometry scans are shown in Figures 35-37 for reciprocally ground sialon with the metal-bonded wheel and resin wheel and for ZTA with only the metal wheel. Figures 35 and 36 compare sialon surfaces ground with the standard resin and an experimental metal bond, and shows very little difference. The ZTA material ground with only the metal bond shows significantly rougher surface (Figure 37).

SEM photographs of fracture origins for a sialon rod ground with the resin-bonded wheel and one with a developmental metal-bonded wheel are shown in Figures 38 and 39. In both cases fracture has initiated at the surface with no obvious flaw. The cylindrical shape and three-point bending strongly favor breaking at the surface.

The surfaces of sialon with the two types of grinding wheels are shown in Figures 40 and 41. The two machined surfaces are quite smooth and similar to one another. The harder metal-bonded wheel gave only a slightly rougher surface than the resin-bonded wheel according to the R_a measurements.

In conclusion, the reduction in strength for transverse ground rods of ZTA is about 50% but this has also been found for flat machining. The sialon rods had similar strengths to the resin-bonded wheel flat ground MOR specimens, and there was no noticeable difference between the resin and metal wheel ground specimens. This led us to believe that the innovative metal wheel is performing satisfactorily and not creating unusual or excessive machining damage compared to the standard resin bond product.

7.2.4.4. Wheel Cost Performance Analysis. By applying Norton's existing technology used in the manufacture of other types of production wheels, the wheel costs are kept low and would be acceptable. The price of the metal-bonded wheel is comparable to that of the resin bond even with the order of magnitude improvement in wheel life. Compositional changes to the experimental bond would not increase manufacturing costs compared to standard metal-bonded wheels.

Table 6. Surface Finish and Flexure Strength of Ceramic Rods

ROD NO.	MATERIAL	WHEEL BOND	GRINDING MODE	Ra (μm) 0.08 mm cutoff	Ra (μm) 0.25 mm cutoff	MOR (MPa)
Set-Up Piece	Sialon	Std. Resin	Reciprocal	0.36	0.39	634
18	Sialon	Resin	Reciprocal	0.36	0.41	751
19	Sialon	Resin	Reciprocal	0.38	0.41	581
20	Sialon	Resin	Reciprocal	0.39	.045	780
22	Sialon	Resin	Reciprocal	N/A	N/A	664
23	Sialon	Resin	Reciprocal	0.34	0.37	604
	Sialon	XL Metal	Reciprocal	0.35	.037	628
26	Sialon	XL Metal	Reciprocal	0.40	0.47	575
27	Sialon	XL Metal	Reciprocal	0.41	0.47	609
29	Sialon	XL Metal	Reciprocal	0.49	0.57	717
30B	Sialon	XL Metal	Reciprocal	0.35	0.41	689
23	ZTA	XL Metal	Plunge	0.69	0.89	N/A
34	ZTA	XL Metal	Plunge	0.52	0.62	N/A
25	ZTA	XL Metal	Plunge	0.49	0.60	N/A
27	ZTA	XL Metal	Plunge	0.56	0.67	N/A
?	ZTA	XL Metal	Plunge	0.50	0.62	N/A
23	ZTA	Resin	Reciprocal	-	-	508
34	ZTA	Resin	Reciprocal	-	-	452
25	ZTA	Resin	Reciprocal	-	-	481
27	ZTA	Resin	Reciprocal	-	-	485
?	ZTA	Resin	Reciprocal	-	-	516
1	ZTA	XL Metal	Reciprocal	0.41	-	374
2	ZTA	XL Metal	Reciprocal	0.49	-	381
3	ZTA	XL Metal	Reciprocal	-	-	362
4	ZTA	XL Metal	Reciprocal	-	-	461
5	ZTA	XL Metal	Reciprocal	-	-	412
6	ZTA	XL Metal	Reciprocal	-	-	382
7	ZTA	XL Metal	Reciprocal	-	-	400

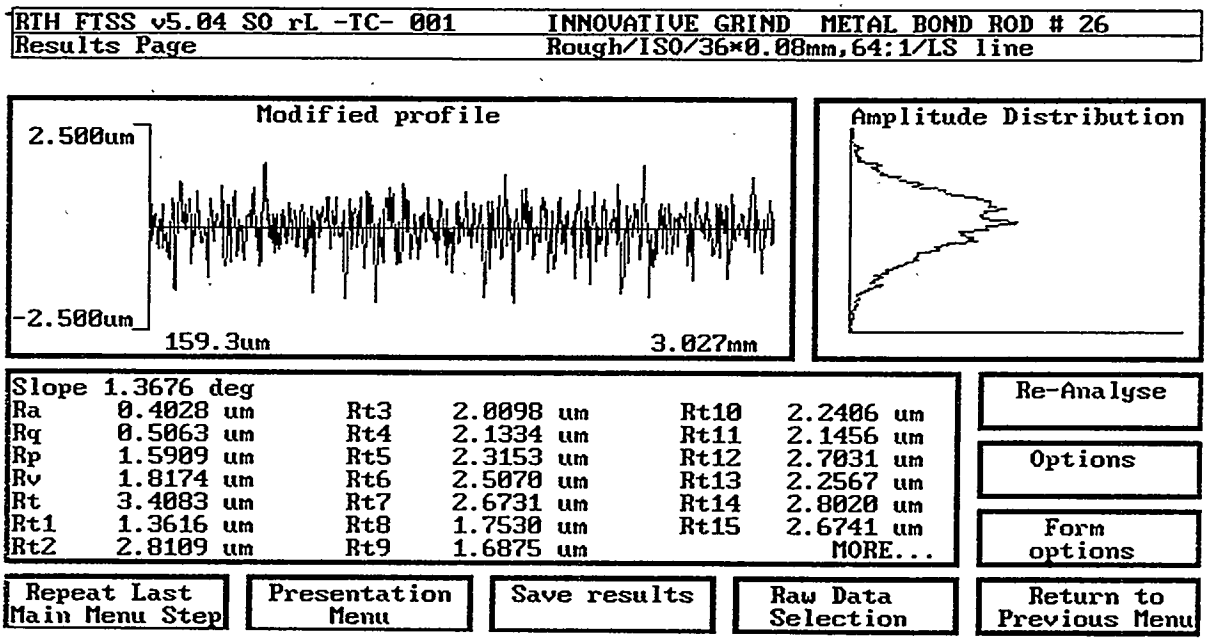

Figure 35. Profilometry scan of reciprocally ground rods. Sialon workpiece ground by experimental metal-bonded wheel.

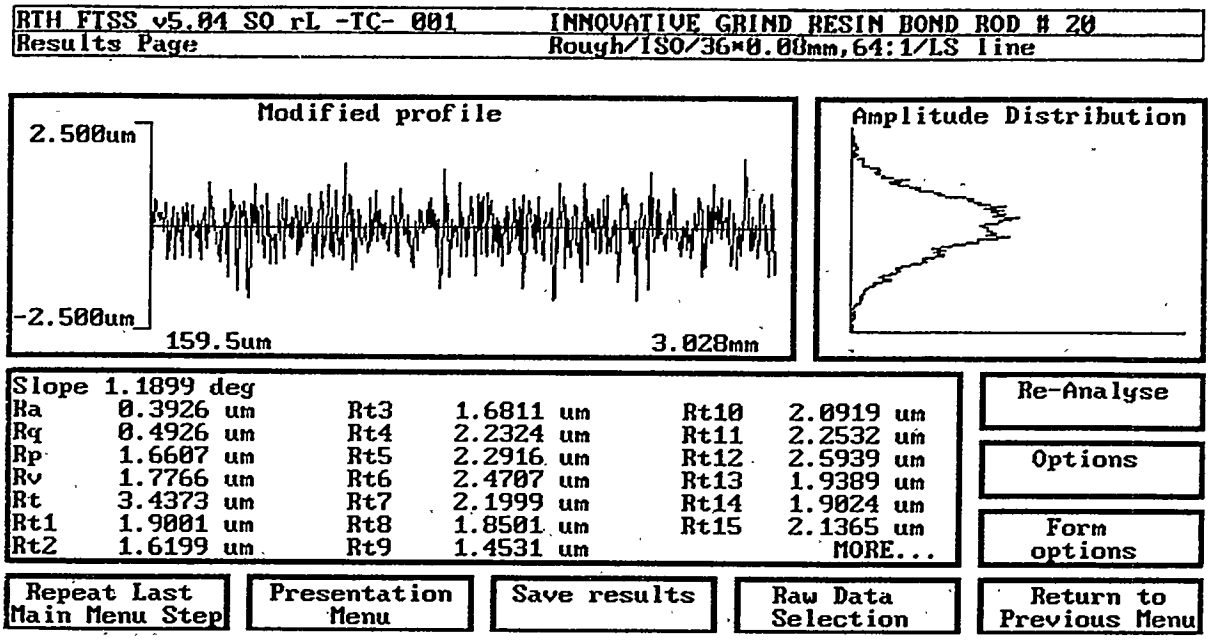

Figure 36. Profilometry scan of reciprocally ground rods. Sialon workpiece ground by standard resin-bonded wheel.

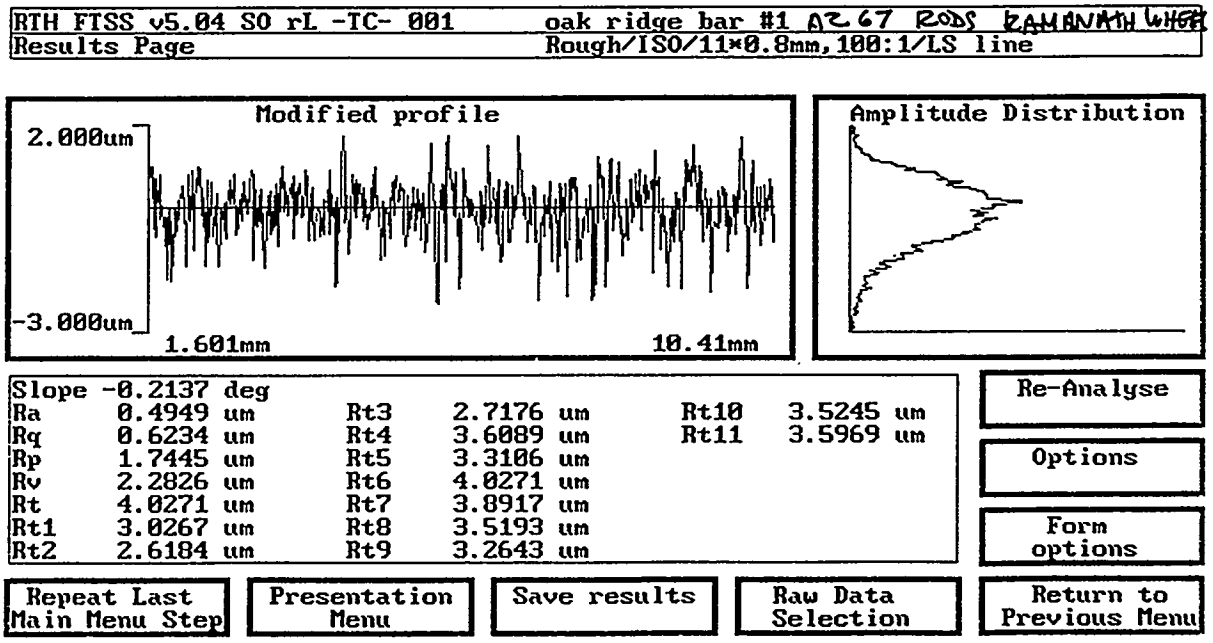

Figure 37. Profilometry scan of reciprocally ground rods. ZTA workpiece ground by experimental metal-bonded wheel.

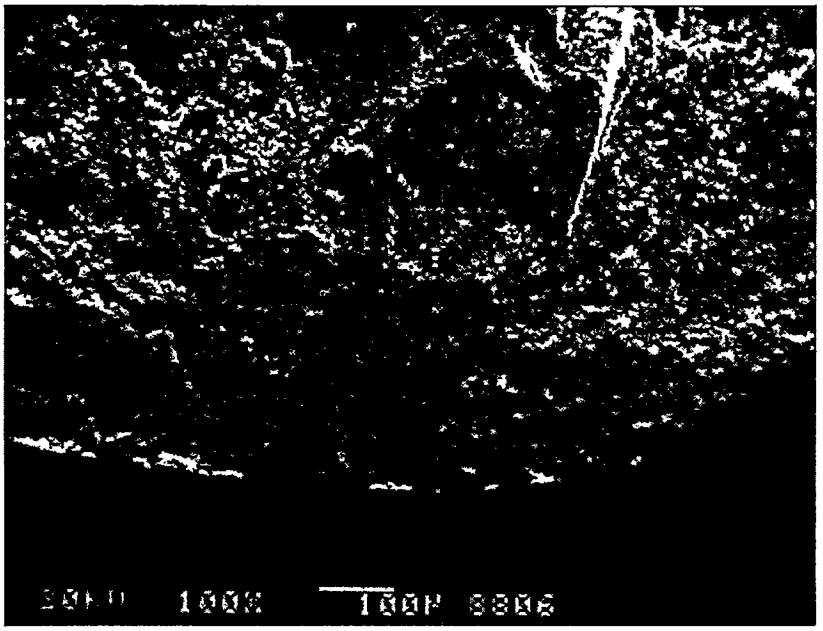

Figure 38. SEM of sialon rod fracture surface ground with resin-bonded wheel.

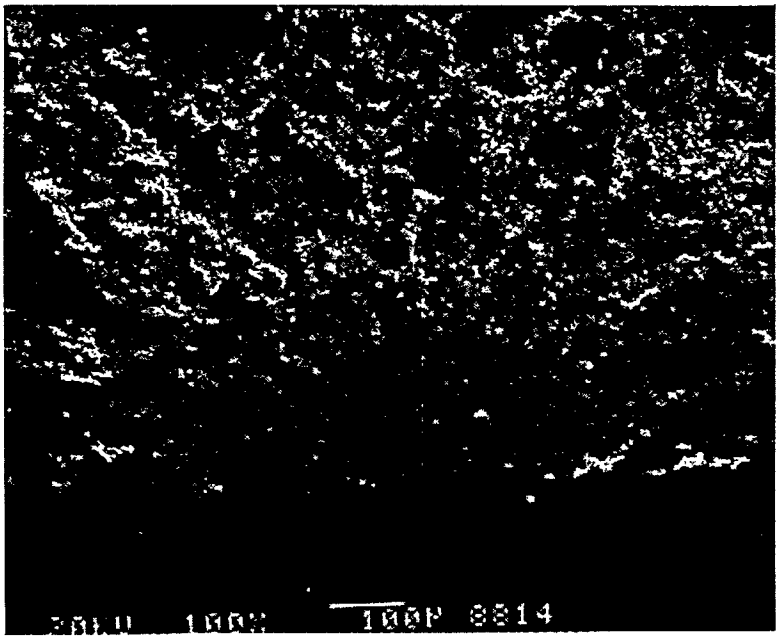

Figure 39. SEM of sialon rod fracture surface ground with metal-bonded wheel.

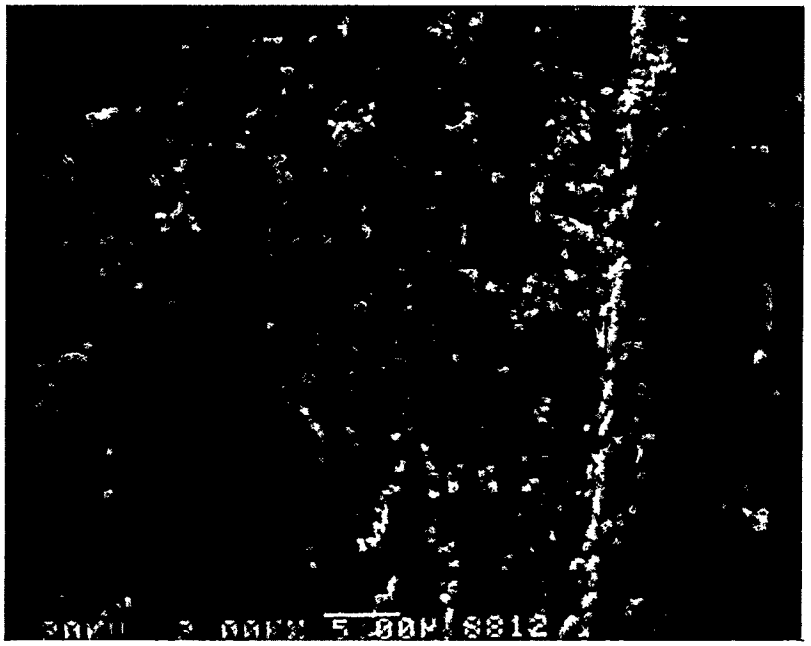

Figure 40. SEM of machined sialon surface ground with resin-bonded wheel.

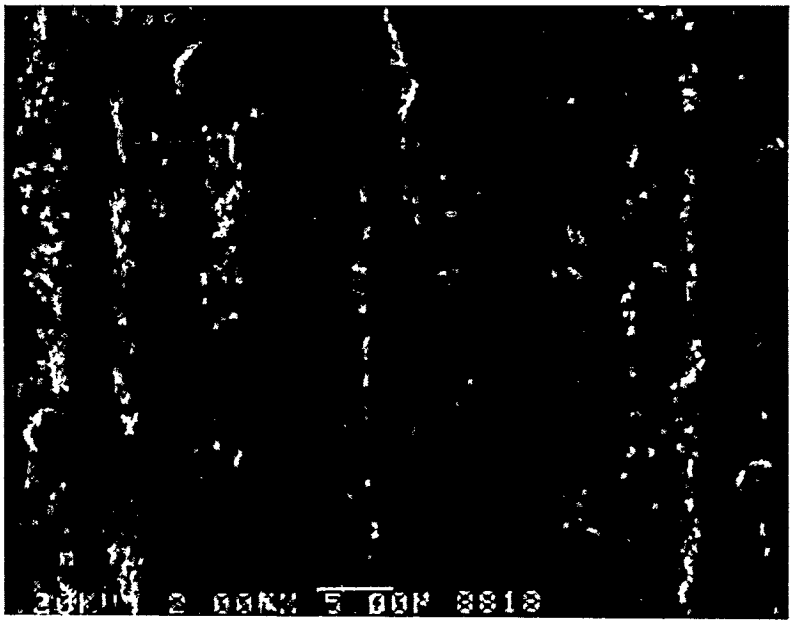

Figure 41. SEM of machined sialon surface ground with metal-bonded wheel.

The order of magnitude improvement in wheel life results in several benefits, some of which are difficult to quantify. The benefits include: increase in components produced per wheel, more components per machine per shift, fewer wheel changes (and lower associated costs), less time/cost spent on dressing the wheel, and finally, better part-to-part consistency. The percentage decrease in the cost of machining using this improved metal-bonded wheel would also depend on such factors as the removal rates used, amount of stock being removed, and the tolerances desired.

7.2.5. Fabrication of Six, 203-mm (8 in.) Wheels for MMES -- Task 2.4

Six duplicate 203 mm diameter wheels of the best experimental specification discussed in Section 7.2.4.2 were fabricated and sent to ORNL as a contract deliverable.

7.3. PROGRAM MANAGEMENT -- TASK 3

7.3.1. Reporting

Norton Company submitted the required bimonthly and semiannual reports to the MMES Project Manager.

7.3.2. Communications/Visits/Travel

R.H. Licht, S. Ramanath and M. Simpson visited the University of Connecticut to consult with Professor Trevor Howes, March 16, 1994.

Trevor Howes and George Bailey, University of Connecticut CGRD visited Norton Company World Grinding Technology Center to perform Harmonic Response (Hammer) Test.

Peter Blau and Ernie Long, ORNL, visited Norton Company to review contract status and next steps, December 1, 1994.

7.3.3. Contract Related Publications/Presentations

R.H. Licht (presenter), S. Ramanath, M. Simpson, E. Lilley, "Development of the Next-Generation Grinding Wheel for Ceramics," Cost-Effective Ceramic Machining Project Review and Coordination Meeting, Oak Ridge, TN, September 8, 1993.

G. M. Caton and J. M. Wyrick, Editors, R. H. Licht, contributor, "Norton to Develop Next Generation Grinding Wheel for Ceramics," *Ceramic Technology Newsletter*, No. 43, April - June 1994, ORNL/DOE.

R.H. Licht (presenter), S. Ramanath, M. Simpson, E. Lilley, "Development of the Next Generation Grinding Wheel," Cost-Effective Machining of Ceramics Workshop, Oak Ridge, TN, August 24, 1994.

R. H. Licht, "Next-Generation Grinding Sets the Stage for Ceramic Breakthroughs", *Ceramic Industry*, 65-67, February 1995.

7.3.4. Schedule and Status of Milestones

Number	Milestone	Due Date	Status
1.1	Requirements Definition and Experimental Design	1/31/94	Completed
1.2	Screening Test Wheel Manufacturing	4/30/94	Completed
1.3-4	Screening Wheel Test and Data Analysis	6/30/94[a]	Completed
2.1	Final Superabrasive Wheel Experimental Design	7/31/94	Completed
2.2	Fabrication of 8" Wheels and Ceramic Specimens	9/15/94	Completed
2.3	Grinding Evaluation, Ceramic Damage Assessment	11/30/94	Completed
2.4	Fabrication of Six, 203 mm Wheels for MMES	12/31/94	Completed
3.1	Delivery of Draft Final Report	1/20/95[b]	Completed
3.2	Delivery of Final Final Report	3/30/95[b]	Completed

[a] CVD Wheel Activity completed 11/94.
[b] Original milestones 12/31/94 and 2/28/95

7.4. PHASE 2 RECOMMENDATIONS

Results of 76-mm (3 in.) and 203-mm (8 in.) diameter test wheels indicate that a superior, next-generation grinding wheel for cylindrical grinding of ceramics has been developed. Most production grinding of cylindrical ceramic parts is done on machines that require 305-mm (12 in.) to 356-mm (14 in.) diameter wheels. We recommend a Phase 2 program to scale up the new Superabrasive wheel specification to the larger diameters and do further in-house wheel specification enhancement. Experimental large test wheels would then be manufactured for independent validation at ceramic manufacturers and ceramic machine shops. The following organizations have expressed interest in performing validation tests: Norton Advanced Ceramics, AlliedSignal Ceramic Components, Chand Kare Technical Ceramics, Caterpillar Inc., and Eaton Manufacturing Technologies Center. Phase 2 validation testing should also include more extensive evaluation of ceramic surface integrity.

8. CONCLUSIONS

Norton Company completed the 16-month Phase 1 technical effort and met the program objectives to define requirements, design, develop and evaluate a next-generation grinding wheel for cost-effective cylindrical grinding of advanced ceramics.

This program was a cooperative effort involving three Norton groups. The Norton Company Abrasives R&D, Norton Diamond Film Division and the Northboro Research and Development Center (NRDC). The program was divided into two technical tasks, Task 1, Analysis of Required Grinding Wheel Characteristics, and Task 2, Design and Prototype Development. In Task 1 we performed a parallel path approach with Superabrasive metal-bond development and the higher technical risk CVD diamond wheel development.

For the Superabrasive approach, Task 1 included bond-only wear and strength tests, which modeled the experimental bonds to give intermediate grinding characteristics between standard resin and metal bonds. Task 1 culminated in a large experimental matrix of 76-mm screening wheels, used to grind sialon disks in a cylindrical plunge test. Some experimental bonds demonstrated significant improvements over standard resin and metal bonds. During screening tests with the conventional metal-bond product, the spindle power and grinding forces increased abruptly after grinding approximately 50 cm^3/cm of material. The wheels required dressing with an abrasive stick. Such abrupt increase in force could cause excessive damage to the ceramic component and would not be acceptable in high-volume production grinding operations. Many experimental metal bonds did not exhibit this tendency. Using this screening test approach, approximately 45 wheel variables were evaluated before down selecting to the most promising bonds for the Task 2, 203-mm diameter tests.

In Task 2, an improved Superabrasive metal bond specification for low-cost machining of ceramics in external cylindrical grinding mode was identified. Under given test conditions, a 203-mm (8 in.) diameter test wheel made in this bond containing 75-concentration diamond abrasives of size U.S. mesh 270/325. The experimental wheel successfully ground three types of advanced ceramics, NC-520 sialon, NCX-5102-HIP'ed Si_3N_4, and AZ67H-20% ZTA, without the need for wheel dressing. The spindle power consumed by this wheel during test grinding of NC-520 sialon is up to 30% lower than with a standard resin-bonded wheel with 100 diamond concentration, that is typically used in this application. The wheel wear with this improved metal bond was an order of magnitude lower than the resin-bonded wheel, which would significantly reduce ceramic grinding costs through fewer wheel changes for retruing and replacements. By applying Norton's existing technology used in the manufacture of other types of production wheels, the wheel costs for this improved metal bond are kept low and is expected to lower the overall machining operation costs. The price of the metal-bonded wheel is comparable to that of the resin bond even with the order of magnitude

improvement in wheel life. The range of application of the improved metal bond was demonstrated in cylindrical grinding of the three advanced ceramics through our in-house tests.

In the Task 1 small-wheel screening test, we performed optical examination and C-ring compression tests of selected sialon disks. For the C-ring compression tests, corner breaks and the limited number of data points made comparative conclusions suspect. However, the experimental results did not show evidence of unusual grinding damage to the ceramic disks. More comprehensive flexure testing was planned and done for the Task 2 rods. Stresses generated during flexural testing was normal to the grinding direction, which resulted in a more meaningful cylindrical grinding damage evaluation. Therefore, the C-ring test in Task 1 was determined to have limited usefulness as a qualitative assessment of grinding damage.

For the Task 2 large-wheel test, optical examination and flexure test of three types of ceramic rods ground by experimental metal-bonded wheels and standard resin wheels did not show any unusual grinding damage. The sialon rods had similar strengths to the resin bonded wheel flat ground MOR specimens, and there was no noticeable difference between the resin and metal wheel ground specimens. The reduction in strength for transverse ground rods of ZTA is about 50% vs. longitudinal grinding, but this has also been found for flat machining. This led us to believe that the innovative metal wheel did not create unusual or excessive machining damage compared to the standard resin-bond product.

The novel CVD diamond wheel approach was incorporated in this program as part of Task 1. Task 1 was designed to include a small-wheel screening test utilizing a parallel path approach to the main Superabrasive metal-type bond approach. The higher risk CVD diamond wheel approach was to be a feasibility study and was not planned for continuation into Task 2, Design and Prototype Development. The CVD approach was considered a higher risk but was considered to have a high potential payoff by applying this new technology to machining of ceramics. The CVD diamond wheel activity was concluded in Task 1 as planned. The initial CVD wheel design was unsuccessful. A thin CVD diamond wheel was redesigned and tested. This test was designed to evaluated the basic grinding characteristics of this new CVD diamond design. Diamond thickness and preform geometry had the greatest impact on performance. While significant grinding improvements were noted from the initial screening test, the results were not promising for this type of operation compared to conventional grinding wheels. The CVD wheel approach does not appear at this stage to offer promise for cost-effective cylindrical grinding of ceramics. Other possible abrasive applications for this approach will be explored.

9. ACKNOWLEDGEMENTS

This research was sponsored by the U.S. Department of Energy, Assistant Secretary for Energy Efficiency and Renewable Energy, Office of Transportation Technologies, as part of the Ceramic Technology Project of the Propulsion System Materials Program, under contract DE-AC05-84OR21400 with Martin Marietta Energy Systems, Inc.

The authors gratefully acknowledge the advice and guidance of Peter Blau, ORNL Program Monitor, and for his support of the need for new grinding products for cost-effective ceramic manufacturing. We are grateful also for the program support given by Ernie Long and Susan Winslow at ORNL. We acknowledge the efforts of D. Ray Johnson, ORNL Manager of the Ceramic Technology Project and Robert B. Schulz, DOE Manager of Materials Development, for their efforts over the years in support of reliable and cost-effective ceramics. The authors wish to thank Professor Trevor Howes and his colleagues at UConn Center of Grinding R&D.

The success of this program was a team effort by many contributors in Norton Company Abrasives, the NRDC of Saint-Gobain-Norton Industrial Ceramics Corporation and Norton Diamond Film. Program guidance and grinding expertise were provided by Tom Buljan, Metal Bond Research Manager, Ron Grieger, Director of Metal Technologies, K. (Subbu) Subramanian, Director of the World Grinding Technology Center and Joseph Picone, Product Engineer for Superabrasives Glass and Ceramic Grinding. Richard Sioui provided valuable information on past product developments. We thank Harold Williston and Jay Stewart for manufacturing of Superabrasive test wheels, Robert Stolberg who ran the grinding tests at the WGTC, Mike White for grinding machine design changes and implementation, and Brad Miller for providing wheel design support.

For Norton Diamond Film, the authors acknowledge the support of Paul Goldman for technical advice during this program, Don Karsberg and Tom Thibaudeau for their patience in assembling wheels and Gordon Cochrane for administration support.

The authors acknowledge the ceramic technical support given at the Northboro Research and Development Center. Kevin Johnston and Peter Pope fabricated the ceramic specimens. We thank Michael Foley and William Hacket for their skill in performing the mechanical property characterization.

The Norton Government Program Group in Northboro provided contract support. We are grateful to Linda Broderick, Senior Contract Administrator, for her support, guidance and diligence. We thank Fred Van Slett, Manager of Compliance, and Colleen Carhart, NRDC Sr. Government Accountant, for supporting the budget tracking effort.

10. REFERENCES

1. G.E. Superabrasives, Worthington, OH., Personal Communication.

2. P. J. Blau, "Report on the Planning Workshop on Cost-Effective Ceramic Machining", November 1991, *ORNL/M* - 1745.

3. DOE/ORNL Workshop, Superabrasives and Grinding Wheel Technology for Machining Ceramics, May 28-29, 1992, Oak Ridge, TN.

4. R. H. Licht, Norton Company presentation at ORNL, White Paper WP-9.12, (1990), from Internal White Paper, "Machining in [Norton Company] Advanced Ceramics".

5. D. Johnson-Walls, A. G. Evans, D. B. Marshall, and M. R. James, "Residual Stresses in Machined Ceramic Surfaces," *J. Am. Ceram. Soc.*, **69** [1] 44-49 (1986).

6. R. Samuel, S. Chandrasekar, T. N. Farris and R. H. Licht, "Effect of Residual Stresses on the Fracture of Ground Ceramics," *J. Am. Ceram. Soc.*, Vol. **72**, No. 10, October 1989.

7. D. J. Snoha and M. R. Foley, "An Investigation of Residual Stresses in Machined Silicon Nitride," *U.S. Army MTL Report MTL TR 92-46*, July 1992, Watertown, MA.

8. K. Subramanian, "Precision Finishing of Ceramic Components with Diamond Abrasives," *American Ceram. Soc. Bull.*, Vol 67 (No 6), June 1988, 1026-1029.

9. K. Subramanian and S. Ramanath, Mechanism of Material Removal in the Precision Grinding of Ceramics, *Proceedings of the Symposium on Precision Machining*, PED -Vol. 58, American Society of Mechanical Engineers, 1-20 (1992).

10. J. A. Kovach and S. Malkin, "High-Speed, Low-Damage Grinding of Advanced Ceramics," *ORNL/TM-12778*, Ceramic Technology Project Semiannual Progress Report for October 1993 Through March 1994, U.S. DOE Office of Transportation Technologies.

11. B. P. Bandyopadhyay and P. J. Blau, *Survey of Ceramic Machining in Japan*, ORNL/M-2881, U.S. DOE Office of Transportation Technologies, July 1993.

12. V. K. Pujari et al., *Development of Improved Processing and Evaluation Methods for High Reliability Structural Ceramics for Advanced Heat Engine Applications, Phase I. Final Report,* ORNL/Sub/98-SB182/1 ORNL Ceramic Technology Project, U.S. DOE Office of Transportation Technologies, August 1993.

13. E. Lilley, G. A. Rossi and P. J. Pelletier, *Tribology of Improved Transformation Toughened Ceramics - Heat Engine Test. Final Report,* ORNL /Sub/90-SG372/1, ORNL Ceramic Technology Project, U.S. DOE Office of Transportation Materials, April 1992

14. J. F. Braza, R. H. Licht, and E. Lilley, "Ceramic Cam Roller Follower Simulation Tests and Evaluation", *STLE Preprint No. 92-AM-2F-1,* 47th Annual Meeting of STLE, Philadelphia, PA, May 4-7, 1992.

15. M. R. Foley, R. H. Licht, L. C. Sales, and D. M. Tracey, "Surface Integrity in Advanced Structural Ceramics," Presented at the Workshop on Superabrasives and Grinding Wheel Technology for Machining Ceramics, ORNL, May, 1992.

16. M. R. Foley and V. K. Pujari, "Tensile Testing in the Development of Processing Methods for High Strength/High Reliability Silicon Nitride," *Ceramic Engineering and Science Proceedings,* Sept. - Oct. 1992, 16th Annual Conference on Composites and Advanced Ceramic Materials.

17. O. M. Jadaan, D. L. Shelleman, J. C. Conway, J. J. Mecholsky, and R. E. Tressler, "Prediction of the Strength of Ceramic Tubular Components: Part I--Analysis," *ASTM J. of Testing and Evaluation,* 19[3], 181-191, May 1991.

18. ASTM Standard C 1161 - 90 "Standard Test Method for Flexural Strength of Advanced Ceramics at Ambient Temperature." *Annual Book of ASTM Standards,* Vol. 15.01.

19. G. R. Anstis, P. Chantikul, B. R. Lawn and D. B. Marshall, "A Critical Evaluation of Indentation Techniques for Measuring Fracture Toughness: I, Direct Crack Measurements," *J. Am. Cer. Soc.*, **64**, 533-538, (1981).

ORNL/Sub/93-SM037/1

INTERNAL DISTRIBUTION

Central Research Library (2)
Document Reference Section
Laboratory Records Department (2)
Laboratory Records, ORNL RC
ORNL Patent Section
M&C Records Office (3)
L. F. Allard, Jr.
L. D. Armstrong
P. F. Becher
R. F. Bernal
T. M. Besmann
P. J. Blau
R. A. Bradley
K. Breder
C. R. Brinkman
V. R. Bullington
G. M. Caton
S. J. Chang
A. Choudhury
D. D. Conger
R. H. Cooper, Jr.
S. A. David
J. L. Ding
M. K. Ferber
R. L. Graves
D. L. Greene
H. W. Hayden, Jr.
E. E. Hoffman
C. R. Hubbard
M. A. Janney
D. R. Johnson (5)
D. Joslin
R. R. Judkins
M. A. Karnitz
B. L. Keyes
H. D. Kimrey, Jr.
W. Y. Lee
K. C. Liu
E. L. Long, Jr.
W. D. Manly
R. W. McClung
D. J. McGuire
T. A. Nolan
A. E. Pasto
K. P. Plucknett
M. H. Rawlins
M. L. Santella
A. C. Schaffhauser
E. J. Soderstrom
D. P. Stinton
R. W. Swindeman
T. N. Tiegs
B. H. West
S. G. Winslow
J. M. Wyrick

EXTERNAL DISTRIBUTION

Pioneering Research Info. Ctr.
E.I. Dupont de Nemours & Co.
Experimental Station
P.O. Box 80302
Wilmington DE 19880-0302

Jeffrey Abboud
U.S. Advanced Ceramics Assoc.
1600 Wilson Blvd., Suite 1008
Arlington VA 22209

James H. Adair
University of Florida
Materials Science & Engineering
317 MAE Bldg.
Gainesville FL 32611-2066

Donald F. Adams
University of Wyoming
Mechanical Engineering Dept.
P.O. Box 3295
Laramie WY 82071

Andrzej Aeamski
Materials Conversion Group
236-B Egidi Drive
Wheeling IL 60090

Jalees Ahmad
AdTech Systems Research Inc.
Solid Mechanics
1342 N. Fairfield Road
Dayton OH 45432-2698

Yoshio Akimune
NISSAN Motor Co., Ltd.
Materials Research Laboratory
1 Natsushima-Cho
Yokosuka 237
JAPAN

Mufit Akinc
Iowa State University
322 Spedding Hall
Ames IA 50011

Ilhan A. Aksay
Princeton University
A313 Engineering Quadrangle
Princeton NJ 08544-5263

Charles Aldridge
Heany Industries, Inc.
249 Briarwood Lane
Scottsville NY 14546

Joseph E. Amaral
Instron Corporation
Corporate Engineering Office
100 Royale Street
Canton MA 02021

Edward M. Anderson
Aluminum Company of America
N. American Industrial Chemical
P.O. Box 300
Bauxite AR 72011

Norman C. Anderson
Ceradyne, Inc.
Ceramic-to-Metal Division
3169 Redhill Avenue
Costa Mesa CA 92626

Don Anson
BCL
Thermal Power Systems
505 King Avenue
Columbus OH 43201-2693

Thomas Arbanas
G.B.C. Materials Corporation
580 Monastery Drive
Latrobe PA 15650-2698

Frank Armatis
3M Company
Building 60-1N-01
St. Paul MN 55144-1000

Everett B. Arnold
Detroit Diesel Corporation
Mechanical Systems Technology
13400 Outer Drive West
Detroit MI 48239-4001

Bertil Aronsson
Sandvik AB
S-12680
Stockholm Lerkrogsvagen 19
SWEDEN

Dennis Assanis
University of Michigan
Dept. of Mechanical Engineering
321 W.E. Lay, N.C.
Ann Arbor MI 48109

V. S. Avva
North Carolina A&T State Univ.
Dept. of Mechanical Engineering
Greensboro NC 27411

Patrick Badgley
Sky Technologies, Inc.
2815 Franklin Drive
Columbus IN 47201

Sunggi Baik
Pohang Institute Sci. & Tech.
P.O. Box 125
Pohang 790-600
KOREA

John M. Bailey
Consultant
Caterpillar, Inc.
P.O. Box 1875
Peoria IL 61656-1875

Bob Baker
Ceradyne, Inc.
3169 Redhill Avenue
Costa Mesa CA 92626

Frank Baker
Aluminum Company of America
Alcoa Technical Center
Alcoa Center PA 15069

Clifford P. Ballard
AlliedSignal Aerospace Company
Ceramics Program
P.O. Box 1021
Morristown NJ 07962-1021

B. P. Bandyopadhyay
ELID Team
Wako Campus
2-1 Hirosawa Wako-shi
Saitama 351-01
JAPAN

P. M. Barnard
Ruston Gas Turbines Limited
P.O. Box 1
Lincoln LN2 5DJ
ENGLAND

Harold N. Barr
Hittman Corporation
9190 Red Branch Road
Columbia MD 21045

Renald D. Bartoe
Vesuvius McDanel
510 Ninth Avenue
Box 560
Beaver Falls PA 15010-0560

David L. Baty
Babcock & Wilcox - LRC
P.O. Box 11165
Lynchburg VA 24506-1165

Donald F. Baxter, Jr.
ASM International
Advanced Materials & Processes
Materials Park OH 44073-0002

M. Brad Beardsley
Caterpillar Inc.
Technical Center Bldg. E
P.O. Box 1875
Peoria IL 61656-1875

John C. Bell
Shell Research Limited
Thornton Research Centre
P.O. Box 1
Chester CH1 3SH
ENGLAND

Larry D. Bentsen
BFGoodrich Company
R&D Center
9921 Brecksville Road
Brecksville OH 44141

Tom Bernecki
Northwestern University
1801 Maple Avenue
Evanston IL 60201-3135

Charles F. Bersch
Institute for Defense Analyses
1801 N. Beauregard Street
Alexandria VA 22311

Ram Bhatt
NASA Lewis Research Center
21000 Brookpark Road
Cleveland OH 44135

Deane I. Biehler
Caterpillar Inc.
Engineering Research Materials
P.O. Box 1875, Bldg. E
Peoria IL 61656-1875

William D. Bjorndahl
TRW, Inc.
One Space Park, MS:R6-2188
Building 01, Room 2040
Redondo Beach CA 90278

Keith A. Blakely
Advanced Refractory Technologies, Inc.
699 Hertel Avenue
Buffalo NY 14207

Edward G. Blanchard
Netzsch Inc.
119 Pickering Way
Exton PA 19341

Bruce Boardman
Deere & Company Technical Ctr.
3300 River Drive
Moline IL 61265

Lawrence P. Boesch
EER Systems Corp.
1593 Spring Hill Road
Vienna VA 22182-2239

Donald H. Boone
Boone & Associates
2412 Cascade Drive
Walnut Creek CA 94598-4313

Tom Booth
AlliedSignal, Inc.
AiResearch Los Angeles Division
2525 West 190th Street
Torrance CA 90509-2960

Raj Bordia
University of Washington
Roberts Hall
Box 35212
Seattle WA 98195-2120

Tibor Bornemisza
Energy Technologies Applications, Inc.
5064 Caminito Vista Lujo
San Diego CA 92130-2846

J.A.M. Boulet
University of Tennessee
Engineering Science & Mechanics
Knoxville TN 37996-2030

Leslie J. Bowen
Materials Systems
53 Hillcrest Road
Concord MA 01742

Steven C. Boyce
Air Force Office of Scientific
Research
AFOSR/NA Bldg. 410
Bolling AFB DC 20332-6448

Steve Bradley
UOP Research Center
50 E. Algonquin Road
Des Plaines IL 60017-6187

Michael C. Brands
Cummins Engine Company, Inc.
P.O. Box 3005, Mail Code 50179
Columbus IN 47201

Raymond J. Bratton
Westinghouse Science & Technology
1310 Beulah Road
Pittsburgh PA 15235

John J. Brennan
United Technologies Corporation
Silver Lane, MS:24
East Hartford CT 06108

Terrence K. Brog
Golden Technologies Company
4545 McIntyre Street
Golden CO 80403

Gunnar Broman
317 Fairlane Drive
Spartanburg SC 29302

Alan Brown
P.O. Box 882
Dayton NJ 08810

Jesse J. Brown
VPI & SU
Ctr. for Adv. Ceram. Mater.
Blacksburg VA 24061-0256

Sherman D. Brown
University of Illinois
Materials Science & Engineering
105 South Goodwin Avenue
Urbana IL 61801

S. L. Bruner
Ceramatec, Inc.
2425 South 900 West
Salt Lake City UT 84119

Walter Bryzik
U.S. Army Tank Automotive Command
R&D Center, Propulsion Systems
Warren MI 48397-5000

Curt V. Burkland
AMERCOM, Inc.
8928 Fullbright Avenue
Chatsworth CA 91311

Bill Bustamante
AMERCOM, Inc.
8928 Fullbright Avenue
Chatsworth CA 91311

Oral Buyukozturk
Massachusetts Institute of Technology
77 Massachusetts Ave., Rm 1-280
Cambridge MA 02139

David A. Caillet
Ethyl Corporation
451 Florida Street
Baton Rouge La 70801

Roger Cannon
Rutgers University
P.O. Box 909
Piscataway NJ 08855-0909

Scott Cannon
P.O. Box 567254
Atlanta GA 30356

Harry W. Carpenter
1844 Fuerte Street
Fallbrook CA 92028

David Carruthers
Kyocera Industrial Ceramics
P.O. Box 2279
Vancouver WA 98668-2279

Calvin H. Carter, Jr.
Cree Research, Inc.
2810 Meridian Parkway
Durham NC 27713

J. David Casey
35 Atlantis Street
West Roxbury MA 02132

Jere G. Castor
J. C. Enterprise
5078 N. 83rd Street
Scottsdale AZ 85250

James D. Cawley
Case Western Reserve University
Materials Science & Engineering
Cleveland OH 44106

Thomas C. Chadwick
Den-Mat Corporation
P.O. Box 1729
Santa Maria CA 93456

Ronald H. Chand
Chand Kare Technical Ceramics
2 Coppage Drive
Worcester MA 01603-1252

William Chapman
Williams International Corp.
2280 W. Maple Road
Walled Lake MI 48390-0200

Ching-Fong Chen
LECO Corporation
3000 Lakeview Avenue
St. Joseph MI 49085

William J. Chmura
Torrington Company
59 Field Street
Torrington CT 06790-4942

Tsu-Wei Chou
University of Delaware
201 Spencer Laboratory
Newark DE 19716

R. J. Christopher
Ricardo Consulting Engineers
Bridge Works
Shoreham-By-Sea W. Sussex
BN435FG ENGLAND

Joel P. Clark
Massachusetts Institute of
Technology
Room 8-409
Cambridge MA 02139

Giorgio Clarotti
Commission of the European Comm
DGXII-C3, MO75, 1-53;
200 Rue de la Loi
B-1049 Brussels
BELGIUM

W. J. Clegg
ICI Advanced Materials
P.O. Box 11, The Heath
Runcorn Cheshire WA7 4QE
ENGLAND

William S. Coblenz
Adv. Research Projects Agency
3701 N. Fairfax Drive
Arlington VA 22203

Gloria M. Collins
ASTM
1916 Race Street
Philadelphia PA 19103

William C. Connors
Sundstrand Aviation Operations
Materials Science & Engineering
4747 Harrison Avenue
Rockford IL 61125-7002

John A. Coppola
Carborundum Company
Niagara Falls R&D Center
P.O. Box 832
Niagara Falls NY 14302

Normand D. Corbin
Norton Company
SGNICC/NRDC
Goddard Road
Northboro MA 01532-1545

Douglas Corey
AlliedSignal, Inc.
2525 West 190th Street, MS:T52
Torrance CA 90504-6099

Keith P. Costello
Chand/Kare Technical Ceramics
2 Coppage Drive
Worcester MA 01603-1252

Ed L. Courtright
Pacific Northwest Laboratory
MS:K3-59
Richland WA 99352

Anna Cox
Mitchell Market Reports
P.O. Box 23
Monmouth Gwent NP5 4YG
UNITED KINGDOM

J. Wesley Cox
BIRL
1801 Maple Avenue
Evanston IL 60201-3135

Art Cozens
Instron Corporation
3414 Snowden Avenue
Long Beach CA 90808

Mark Crawford
New Technology Week
4604 Monterey Drive
Annandale VA 22003

Richard A. Cree
Markets & Products, Inc.
P.O. Box 14328
Columbus OH 43214-0328

Les Crittenden
Vesuvius McDanel
Box 560
Beaver Falls PA 15010

M. J. Cronin
Mechanical Technology, Inc.
968 Albany-Shaker Road
Latham NY 12110

Gary M. Crosbie
Ford Motor Company
20000 Rotunda Drive
MD-2313, SRL Building
Dearborn MI 48121-2053

Floyd W. Crouse, Jr.
U.S. Department of Energy
Morgantown Energy Tech. Ctr.
P.O. Box 880
Morgantown WV 26505

John Cuccio
AlliedSignal Engines
P.O. Box 52180, MS:1302-2Q
Phoenix AZ 85072-2180

Raymond A. Cutler
Ceramatec, Inc.
2425 South 900 West
Salt Lake City UT 84119

Stephen C. Danforth
Rutgers University
P.O. Box 909
Piscataway NJ 08855-0909

Sankar Das Gupta
Electrofuel Manufacturing Co.
9 Hanna Avenue
Toronto Ontario MGK-1W8
CANADA

Frank Davis
AlliedSignal Aerospace Company
7550 Lucerne Drive, #203
Middleburg Heights OH 44130

Robert F. Davis
North Carolina State University
Materials Engineering Department
P.O. Box 7907
Raleigh NC 27695

George C. DeBell
Ford Motor Company
Scientific Research Lab
P.O. Box 2053, Room S2023
Dearborn MI 48121-2053

Michael DeLuca
RSA Research Group
1534 Claas Ave.
Holbrook NY 11741

Gerald L. DePoorter
Colorado School of Mines
Metallurgical & Materials Engr
Golden CO 80401

J. F. DeRidder
Omni Electro Motive, Inc.
12 Seely Hill Road
Newfield NY 14867

Nick C. Dellow
Materials Technology Publications
40 Sotheron Road
Watford Herts WD1 2QA
UNITED KINGDOM

L. R. Dharani
University of Missouri-Rolla
224 M.E.
Rolla MO 65401

Douglas A. Dickerson
Union Carbide Specialty Powders
1555 Main Street
Indianapolis IN 46224

John Dodsworth
Vesuvius Research & Development
Technical Ceramics Group
Box 560
Beaver Falls PA 15010

B. Dogan
Institut fur Werkstofforschung
GKSS-Forschungszentrum Geesthacht
Max-Planck-Strasse
D-2054 Geesthacht
GERMANY

Alan Dragoo
U.S. Department of Energy
ER-131, MS:F-240
Washington DC 20817

Jean-Marie Drapier
FN Moteurs S.A.
Material and Processing
B-4041 Milmort (Herstal)
BELGIUM

Kenneth C. Dreitlein
United Technologies Res. Ctr.
Silver Lane
East Hartford CT 06108

Robin A.L. Drew
McGill University
3450 University Street
Montreal Quebec H3A 2A7
CANADA

Winston H. Duckworth
BCL
Columbus Division
505 King Avenue
Columbus OH 43201-2693

Ernest J. Duwell
3M Abrasive Systems Division
3M Center
St. Paul MN 55144-1000

Chuck J. Dziedzic
GTC Process Forming Systems
4545 McIntyre Street
Golden CO 80403

Robert J. Eagan
Sandia National Laboratories
Engineered Mater. & Proc.
P.O. Box 5800
Albuquerque NM 87185-5800

Harry E. Eaton
United Technologies Corporation
Silver Lane
East Hartford CT 06108

Harvill C. Eaton
Louisiana State University
240 Thomas Boyd Hall
Baton Rouge LA 70803

J. J. Eberhardt
U.S. Department of Energy
Office of Transportation Mater.
CE-34, Forrestal Building
Washington DC 20585

Jim Edler
Eaton Corporation
26201 Northwestern Highway
P.O. Box 766
Southfield MI 48037

G. A. Eisman
Dow Chemical Company
Ceramics and Advanced Materials
52 Building
Midland MI 48667

William A. Ellingson
Argonne National Laboratory
Energy Technology Division
9700 S. Cass Avenue
Argonne IL 60439

Anita Kaye M. Ellis
Machined Ceramics
629 N. Graham Street
Bowling Green KY 42101

Glen B. Engle
Nuclear & Aerospace Materials
16716 Martincoit Road
Poway CA 92064

Kenneth A. Epstein
Dow Chemical Company
2030 Building
Midland MI 48674

Art Erdemir
Argonne National Laboratory
9700 S. Cass Avenue
Argonne IL 60439

E. M. Erwin
Lubrizol Corporation
17710 Riverside Drive
Lakewood OH 44107

John N. Eustis
U.S. Department of Energy
Industrial Energy Efficiency
CE-221, Forrestal Building
Washington DC 20585

W. L. Everitt
Kyocera International, Inc.
8611 Balboa Avenue
San Diego CA 92123

Gordon Q. Evison
332 S. Michigan Avenue
Suite 1730
Chicago IL 60604

John W. Fairbanks
U.S. Department of Energy
Office of Propulsion Systems
CE-322, Forrestal Building
Washington DC 20585

Tim Fawcett
Dow Chemical Company
Advanced Ceramics Laboratory
1776 Building
Midland MI 48674

Robert W. Fawley
Sundstrand Power Systems
Div. of Sundstrand Corporation
P.O. Box 85757
San Diego CA 92186-5757

Jeff T. Fenton
Vista Chemical Company
900 Threadneedle
Houston TX 77079

Larry Ferrell
Babcock & Wilcox
Old Forest Road
Lynchburg VA 24505

Raymond R. Fessler
BIRL
1801 Maple Avenue
Evanston IL 60201

Ross F. Firestone
Ross Firestone Company
188 Mary Street
Winnetka IL 60093-1520

Sharon L. Fletcher
Arthur D. Little, Inc.
15 Acorn Park
Cambridge MA 02140-2390

Michael Foley
Norton Company
Goddard Road
Northboro MA 01532-2527

Thomas F. Foltz
Textron Specialty Materials
2 Industrial Avenue
Lowell MA 01851

Renee G. Ford
Materials and Processing Report
P.O. Box 72
Harrison NY 10528

John Formica
Supermaterials
2020 Lakeside Avenue
Cleveland OH 44114

Edwin Frame
Southwest Research Institute
P.O. Drawer 28510
San Antonio TX 78284

Armanet Francois
French Scientific Mission
4101 Reservoir Road, N.W.
Washington DC 20007-2176

R. G. Frank
Technology Assessment Group
10793 Bentley Pass Lane
Loveland OH 45140

David J. Franus
Forecast International
22 Commerce Road
Newtown CT 06470

Marc R. Freedman
NASA Lewis Research Center
21000 Brookpark Road, MS:49-3
Cleveland OH 44135

Douglas Freitag
Bayside Materials Technology
17 Rocky Glen Court
Brookeville MD 20833

Brian R.T. Frost
Argonne National Laboratory
9700 S. Cass Avenue, Bldg. 900
Argonne IL 60439

Lawrence R. Frost
Instron Corporation
100 Royall Street
Canton MA 02021

Xiren Fu
Shanghai Institute of Ceramics
1295 Ding-xi Road
Shanghai 200050
CHINA

J. P. Gallagher
University of Dayton Research Institute
300 College Park, JPC-250
Dayton OH 45469-0120

Garry Garvey
Golden Technologies Company
4545 McIntyre Street
Golden CO 80403

Richard Gates
NIST
Materials Bldg., A-256
Gaithersburg MD 20899

L. J. Gauckler
ETH-Zurich
Sonneggstrasse 5
CH-8092 Zurich 8092
SWITZERLAND

D. Gerster
CEA-DCOM
33 Rue De La Federation
Paris 75015
FRANCE

John Ghinazzi
Coors Technical Ceramics Co.
1100 Commerce Park Drive
Oak Ridge TN 37830

Robert Giddings
General Electric Company
P.O. Box 8
Schenectady NY 12301

A. M. Glaeser
University of California
Lawrence Berkeley Laboratory
Hearst Mining Building
Berkeley CA 94720

Joseph W. Glatz
510 Rocksville Road
Holland PA 18966

W. M. Goldberger
Superior Graphite Company
R&D
2175 E. Broad Street
Columbus OH 43209

Allan E. Goldman
U.S. Graphite, Inc.
907 W. Outer Drive
Oak Ridge TN 37830

Stephen T. Gonczy
Allied Signal Research
P.O. Box 5016
Des Plaines IL 60017

Robert J. Gottschall
U.S. Department of Energy
ER-131, MS:G-236
Washington DC 20585

Earl Graham
Cleveland State University
Dept. of Chemical Engineering
Euclid Avenue at East 24th St.
Cleveland OH 44115

John W. Graham
Astro Met, Inc.
9974 Springfield Pike
Cincinnati OH 45215

G. A. Graves
U. of Dayton Research Institute
300 College Park
Dayton OH 45469-0001

Robert E. Green, Jr.
Johns Hopkins University
Mater. Sci. and Engineering
Baltimore MD 21218

Alex A. Greiner
Plint & Partners
Oaklands Park
Wokingham Berkshire RG11 2FD
UNITED KINGDOM

Lance Groseclose
Allison Engine Company
P.O. Box 420, MS:W-5
Indianapolis IN 46206

Thomas J. Gross
U.S. Department of Energy
Transportation Technologies
CE-30, Forrestal Building
Washington DC 20585

Mark F. Gruninger
Union Carbide Corporation
Specialty Powder Business
1555 Main Street
Indianapolis IN 46224

Ernst Gugel
Cremer Forschungsinstitut
GmbH&Co.KG
Oeslauer Strasse 35
D-8633 Roedental 8633
GERMANY

John P. Gyekenyesi
NASA Lewis Research Center
21000 Brookpark Road, MS:6-1
Cleveland OH 44135

Nabil S. Hakim
Detroit Diesel Corporation
13400 Outer Drive West
Detroit MI 48239

Philip J. Haley
Allison Engine Company
P.O. Box 420, MS:T12A
Indianapolis IN 46206-0420

Judith Hall
Fiber Materials, Inc.
Biddeford Industrial Park
5 Morin Street
Biddeford ME 04005

Y. Hamano
Kyocera Industrial Ceramics
5713 E. Fourth Plain Blvd.
Vancouver WA 98661-6857

Y. Harada
IIT Research Institute
10 West 35th Street
Chicago IL 60616

Norman H. Harris
Hughes Aircraft Company
P.O. Box 800520
Saugus CA 91380-0520

Alan M. Hart
Dow Chemical Company
1776 Building
Midland MI 48674

Pat E. Hart
Battelle Pacific Northwest Labs
Ceramics and Polymers Development
P.O. Box 999
Richland WA 99352

Michael H. Haselkorn
Caterpillar Inc.
Technical Center, Building E
P.O. Box 1875
Peoria IL 61656-1875

Debbie Haught
U.S. Department of Energy
Off. of Transportation Mater.
EE-34, Forrestal Bldg.
Washington DC 20585

N. B. Havewala
Corning Inc.
SP-PR-11
Corning NY 14831

John Haygarth
Teledyne WAA Chang Albany
P.O. Box 460
Albany OR 97321

Norman L. Hecht
U. of Dayton Research Institute
300 College Park
Dayton OH 45469-0172

Peter W. Heitman
Allison Engine Company
P.O. Box 420, MS:W-5
Indianapolis IN 46206-0420

Robert W. Hendricks
VPI & SU
210 Holden Hall
Blacksburg VA 24061-0237

Thomas P. Herbell
NASA Lewis Research Center
21000 Brookpark Road, MS:49-3
Cleveland OH 44135

Robert L. Hershey
Science Management Corporation
1255 New Hampshire Ave., N.W.
Suite 1033
Washington DC 20036

Hendrik Heystek
Bureau of Mines
Tuscaloosa Research Center
P.O. Box L
University AL 35486

Robert V. Hillery
GE Aircraft Engines
One Neumann Way, M.D. H85
Cincinnati OH 45215

Arthur Hindman
Instron Corporation
100 Royall Street
Canton MA 02021

Shinichi Hirano
Mazda R&D of North America
1203 Woodridge Avenue
Ann Arbor MI 48105

Tommy Hiraoka
NGK Locke, Inc.
1000 Town Center
Southfield MI 48075

Fu H. Ho
5645 Soledad Mtn. Road
San Diego, CA 92037-7256

John M. Hobday
U.S. Department of Energy
Morgantown Energy Tech. Ctr.
P.O. Box 880
Morgantown WV 26507

Clarence Hoenig
Lawrence Livermore National Lab
P.O. Box 808, Mail Code L-369
Livermore CA 94550

Thomas Hollstein
Fraunhofer-Institut fur
Werkstoffmechanik
Wohlerstrasse 11
D-79108 Freiburg
GERMANY

Richard Holt
Natl. Research Council Canada
Structures and Materials Lab
Ottawa Ontario K1A OR6
CANADA

Woodie Howe
Coors Technical Ceramics
1100 Commerce Park Drive
Oak Ridge TN 37830

Stephen M. Hsu
NIST
Gaithersburg MD 20899

Hann S. Huang
Argonne National Laboratory
9700 S. Cass Avenue
Argonne IL 60439-4815

Gene Huber
Precision Ferrites & Ceramics
5576 Corporate Drive
Cypress CA 90630

Fred R. Huettic
Advanced Magnetics Inc.
45 Corey Lane
Mendham NJ 07945

Brian K. Humphrey
Lubrizol Petroleum Chemicals
3000 Town Center, Suite 1340
Southfield MI 48075-1201

Robert M. Humrick
Dylon Ceramic Technologies
3100 Edgehill Road
Cleveland Heights OH 44118

Michael S. Inoue
Kyocera International, Inc.
8611 Balboa Avenue
San Diego CA 92123-1580

Joseph C. Jackson
U.S. Advanced Ceramics Assoc.
1600 Wilson Blvd., Suite 1008
Arlington VA 22209

Osama Jadaan
U. of Wisconsin-Platteville
1 University Plaza
Platteville WI 53818

Said Jahanmir
NIST
Materials Bldg., Room A-237
Gaithersburg MD 20899

Curtis A. Johnson
General Electric Company
P.O. Box 8
Schenectady NY 12301

Sylvia Johnson
SRI International
333 Ravenswood Avenue
Menlo Park CA 94025

Thomas A. Johnson
Lanxide Corporation
P.O. Box 6077
Newark DE 19714-6077

Walter F. Jones
AFOSR/NA
110 Duncan Ave., Ste. B115
Washington DC 20332-0001

Jill E. Jonkouski
U.S. Department of Energy
9800 S. Cass Avenue
Argonne IL 60439-4899

L. A. Joo
Great Lakes Research Corporation
P.O. Box 1031
Elizabethton TN 37643

Adam Jostsons
Australian Nuclear Science &
Technology
New Illawarra Road
Lucas Heightss New South Wales
AUSTRALIA

Lyle R. Kallenbach
Phillips Petroleum
Mail Drop:123AL
Bartlesville OK 74004.

Nick Kamiya
Kyocera Industrial Ceramics Corp.
25 NW Point Blvd., #450
Elk Grove Village IL 60007

Roy Kamo
Adiabatics, Inc.
3385 Commerce Park Drive
Columbus IN 47201

Chih-Chun Kao
Industrial Technology Research
Institute
195 Chung-Hsing Road, Sec. 4
Chutung Hsinchu 31015 R.O.C.
TAIWAN

Keith R. Karasek
AlliedSignal Aerospace Company
50 E. Algonquin Road
Des Plaines IL 60017-5016

Robert E. Kassel
Ceradyne, Inc.
3169 Redhill Avenue
Costa Mesa CA 92626

Allan Katz
Wright Laboratory
Metals and Ceramics Division
Wright-Patterson AFB OH 45433

R. Nathan Katz
Worcester Polytechnic Institute
100 Institute Road
Worcester MA 01609

Ted Kawaguchi
Tokai Carbon America, Inc.
375 Park Avenue, Suite 3802
New York NY 10152

Noritsugu Kawashima
TOSHIBA Corporation
4-1 Ukishima-Cho
Kawasaki-Ku Kawasaki, 210
JAPAN

Lisa Kempfer
Penton Publishing
1100 Superior Avenue
Cleveland OH 44114-2543

Frederick L. Kennard, III
Delphi Energy & Engine Mgmt. Systems
Division of General Motors
1300 N. Dort Highway
Flint MI 48556

David O. Kennedy
Lester B. Knight Cast Metals
549 W. Randolph Street
Chicago IL 60661

George Keros
Photon Physics
3175 Penobscot Building
Detroit MI 48226

Thomas Ketcham
Corning, Inc.
SP-DV-1-9
Corning NY 14831

Pramod K. Khandelwal
Allison Engine Company
P.O. Box 420, MS:T10B
Indianapolis IN 46206

Jim R. Kidwell
AlliedSignal Engines
P.O. Box 52180
Phoenix AZ 85072-2180

Shin Kim
The E-Land Group
19-8 ChangJeon-dong
Mapo-gu, Seoul 121-190
KOREA

W. C. King
Mack Truck, Z-41
1999 Pennsylvania Avneue
Hagerstown MD 21740

Carol Kirkpatrick
MSE, Inc.
P.O. Box 3767
Butte MT 59702

Tony Kirn
Caterpillar Inc.
Defense Products Dept., JB7
Peoria IL 61629

James D. Kiser
NASA Lewis Research Center
21000 Brookpark Road, MS:49-3
Cleveland OH 44135

Max Klein
900 24th Street, N.W., Unit G
Washington DC 20037

Richard N. Kleiner
Golden Technologies Company
4545 McIntyre Street
Golden CO 80403

Stanley J. Klima
NASA Lewis Research Center
21000 Brookpark Road, MS:6-1
Cleveland OH 44135

Albert S. Kobayashi
University of Washington
Mechanical Engineering Dept.
Mail Stop:FU10
Seattle WA 98195

Shigeki Kobayashi
Toyota Central Research Labs
Nagakute Aichi, 480-11
JAPAN

Richard A. Kole
Z-Tech Corporation
8 Dow Road
Bow NH 03304

Joseph A. Kovach
Eaton Corporation
32500 Chardon Road
Willoughby Hills OH 44094

Kenneth A. Kovaly
Technical Insights Inc.
P.O. Box 1304
Fort Lee NJ 07024-9967

Edwin H. Kraft
Kyocera Industrial Ceramics
5713 E. Fourth Plain Boulevard
Vancouver WA 98661

Arthur Kranish
Trends Publishing Inc.
1079 National Press Building
Washington DC 20045

A. S. Krieger
Radiation Science, Inc.
P.O. Box 293
Belmont MA 02178

Pieter Krijgsman
Ceramic Design International Holding B.V.
P.O. Box 68
Hattem 8050-AB
THE NETHERLANDS

Waltraud M. Kriven
University of Illinois
105 S. Goodwin Avenue
Urbana IL 61801

Edward J. Kubel, Jr.
ASM International
Advanced Materials & Processes
Materials Park OH 44073

Dave Kupperman
Argonne National Laboratory
9700 S. Cass Avenue
Argonne IL 60439

Oh-Hun Kwon
North Company
SGNICC/NRDC
Goddard Road
Northboro MA 01532-1545

W. J. Lackey
GTRI
Materials Science and Tech. Lab
Atlanta GA 30332

Jai Lala
Tenmat Ltd.
40 Somers Road
Rugby Warwickshire CV22 7DH
ENGLAND

Hari S. Lamba
General Motors Corporation
9301 West 55th Street
LaGrange IL 60525

Richard L. Landingham
Lawrence Livermore National Lab
P.O. Box 808, L-369
Livermore CA 94550

James Lankford
Southwest Research Institute
6220 Culebra Road
San Antonio TX 78228-0510

Stanley B. Lasday
Business News Publishing Co.
1910 Cochran Road, Suite 630
Pittsburgh PA 15220

S. K. Lau
Carborundum Company
Technology Division
P.O. Box 832, B-100
Niagara Falls NY 14302

J. Lawrence Lauderdale
Babcock & Wilcox
1525 Wilson Blvd., #100
Arlington VA 22209-2411

Jean F. LeCostaouec
Textron Specialty Materials
2 Industrial Avenue
Lowell MA 01851

Benson P. Lee
Technology Management, Inc.
4440 Warrensville Rd., Suite A
Cleveland OH 44128

Burtrand I. Lee
Clemson University
Olin Hall
Clemson SC 29634-0907

June-Gunn Lee
KIST
P.O. Box 131, Cheong-Ryang
Seoul 130-650
KOREA

Stan Levine
NASA Lewis Research Center
21000 Brookpark Road, MS:49-3
Cleveland OH 44135

David Lewis, III
Naval Research Laboratory
Code 6370
Washington DC 20375-5343

Ai-Kang Li
Materials Research Labs., ITRI
195-5 Chung-Hsing Road, Sec. 4
Chutung Hsinchu 31015 R.O.C.
TAIWAN

Robert H. Licht
Norton Company
SGNICC/NRDC
Goddard Road
Northboro MA 01532-1545

E. Lilley
Norton Company
SGNICC/NRDC
Goddard Road
Northboro MA 01532-1545

Chih-Kuang Lin
National Central University
Dept. of Mechanical Engineering
Chung-Li 32054
TAIWAN

Laura J. Lindberg
AlliedSignal Aerospace Company
Garrett Fluid Systems Division
P.O. Box 22200
Tempe AZ 85284-2200

Hans A. Lindner
Cremer Forschungsinstitut
GmbH&Co.KG
Oeslauer Strasse 35
D-8633 Rodental 8866
GERMANY

Ronald E. Loehman
Sandia National Laboratories
Chemistry & Ceramics Dept. 1840
P.O. Box 5800
Albuquerque NM 87185

Bill Long
Babcock & Wilcox
P.O. Box 11165
Lynchburg VA 24506

L. A. Lott
EG&G Idaho, Inc.
Idaho National Engineering Lab
P.O. Box 1625
Idaho Falls ID 83415-2209

Raouf O. Loutfy
MER Corporation
7960 S. Kolb Road
Tucson AZ 85706

Lydia Luckevich
Ortech International
2395 Speakman Drive
Mississauga Ontario L5K 1B3
CANADA

James W. MacBeth
Carborundum Company
Structural Ceramics Division
P.O. Box 1054
Niagara Falls NY 14302

George Maczura
Aluminum Company of America
3450 Park Lane Drive
Pittsburgh PA 15275-1119

David Maginnis
Tinker AFB
OC-ALC/LIIRE
Tinker AFB OK 73145-5989

Frank Maginnis
Aspen Research, Inc.
220 Industrial Boulevard
Moore OK 73160

Tai-il Mah
Universal Energy Systems, Inc.
4401 Dayton-Xenia Road
Dayton OH 45432

Kenneth M. Maillar
Barbour Stockwell Company
83 Linskey Way
Cambridge MA 02142

S. G. Malghan
NIST
I-270 & Clopper Road
Gaithersburg MD 20899

Lars Malmrup
United Turbine AB
Box 13027
Malmo S-200 44
SWEDEN

John Mangels
Ceradyne, Inc.
3169 Redhill Avenue
Costa Mesa CA 92626

Murli Manghnani
University of Hawaii
2525 Correa Road
Honolulu HI 96822

Russell V. Mann
Matec Applied Sciences, Inc.
75 South Street
Hopkinton MA 01748

William R. Manning
Champion Aviation Products Div
P.O. Box 686
Liberty SC 29657

Ken Marnoch
Amercom, Inc.
8928 Fullbright Avenue
Chatsworth CA 91311

Robert A. Marra
Aluminum Company of America
Alcoa Technical Center
Alcoa Center PA 15069

Steve C. Martin
Advanced Refractory Technologies
699 Hertel Avenue
Buffalo NY 14207

Kelly J. Mather
William International Corp.
2280 W. Maple Road
Walled Lake MI 48088

James P. Mathers
3M Company
3M Center, Bldg. 201-3N-06
St. Paul MN 55144

Ron Mayville
Arthur D. Little, Inc.
15-163 Acorn Park
Cambridge MA 02140

F. N. Mazadarany
General Electric Company
Bldg. K-1, Room MB-159
P.O. Box 8
Schenectady NY 12301

James W. McCauley
Alfred University
Binns-Merrill Hall
Alfred NY 14802

Colin F. McDonald
McDonald Thermal Engineering
1730 Castellana Road
La Jolla CA 92037

B. J. McEntire
Norton Company
10 Airport Park Road
East Granby CT 06026

Chuck McFadden
Coors Ceramics Company
600 9th Street
Golden CO 80401

Thomas D. McGee
Iowa State University
110 Engineering Annex
Ames IA 50011

James McLaughlin
Sundstrand Power Systems
4400 Ruffin Road
P.O. Box 85757
San Diego CA 92186-5757

Matt McMonigle
U.S. Department of Energy
Improved Energy Productivity
CE-231, Forrestal Building
Washington DC 20585

J. C. McVickers
AlliedSignal Engines
P.O. Box 52180, MS:9317-2
Phoenix AZ 85072-2180

D. B. Meadowcroft
"Jura," The Ridgeway
Oxshott
Leatherhead Surrey KT22 OLG
UNITED KINGDOM

Joseph J. Meindl
Reynolds International, Inc.
6603 W. Broad Street
P.O. Box 27002
Richmond VA 23261-7003

Michael D. Meiser
AlliedSignal, Inc.
Ceramic Components
P.O. Box 2960, MS:T21
Torrance CA 90509-2960

George Messenger
National Research Council of Canada
Building M-7
Ottawa Ontario K1A OR6
CANADA

Arthur G. Metcalfe
Arthur G. Metcalfe & Assoc.
2108 East 24th Street
National City CA 91950

R. Metselaar
Eindhoven University
P.O. Box 513
Endhoven 5600 MB
THE NETHERLANDS

David J. Michael
Harbison-Walker Refractories
P.O. Box 98037
Pittsburgh PA 15227

Ken Michaels
Chrysler Motors Corporation
P.O. Box 1118, CIMS:418-17-09
Detroit MI 48288

Bernd Michel
Institute of Mechanics
P.O. Box 408
D-9010 Chemnitz
GERMANY

D. E. Miles
Commission of the European Community
rue de la Loi 200
B-1049 Brussels
BELGIUM

Carl E. Miller
AC Rochester
1300 N. Dort Highway, MS:32-31
Flint MI 48556

Charles W. Miller, Jr.
Centorr Furnaces/Vacuum Industries
542 Amherst Street
Nashua NH 03063

R. Minimmi
Enichem America
2000 Cornwall Road
Monmouth Junction NJ 08852

Michele V. Mitchell
AlliedSignal, Inc.
Ceramic Components
P.O. Box 2960, MS:T21
Torrance CA 90509-2960

Howard Mizuhara
WESGO
477 Harbor Boulevard
Belmont CA 94002

Helen Moeller
Babcock & Wilcox
P.O. Box 11165
Lynchburg VA 24506-1165

Francois R. Mollard
Concurrent Technologies Corp.
1450 Scalp Avenue
Johnstown PA 15904-3374

Phil Mooney
Panametrics
221 Crescent Street
Waltham MA 02254

Geoffrey P. Morris
3M Company
3M Traffic Control Materials
Bldg. 209-BW-10, 3M Center
St. Paul MN 55144-1000

Jay A. Morrison
Rolls-Royce, Inc.
2849 Paces Ferry Rd., Suite 450
Atlanta GA 30339-3769

Joel P. Moskowitz
Ceradyne, Inc.
3169 Redhill Avenue
Costa Mesa CA 92626

Brij Moudgil
University of Florida
Material Science & Engineering
Gainesville FL 32611

Christoph J. Mueller
Sprechsaal Publishing Group
P.O. Box 2962, Mauer 2
D-8630 Coburg
GERMANY

Thomas W. Mullan
Vapor Technologies Inc.
345 Route 17 South
Upper Saddle River NJ 07458

Theresa A. Mursick-Meyer
Norton Company
SGNICC/NRDC
Goddard Road
Northboro MA 01532-1545

M. K. Murthy
MkM Consultants International
10 Avoca Avenue, Unit 1906
Toronto Onntario M4T 2B7
CANADA

David L. Mustoe
Custom Technical Ceramics
8041 W I-70 Service Rd. Unit 6
Arvada CO 80002

Curtis V. Nakaishi
U.S. Department of Energy
Morgantown Energy Tech. Ctr.
P.O. Box 880
Morgantown WV 26507-0880

Yoshio Nakamura
Faicera Research Institute
3-11-12 Misono
Sagamihara, Tokyo
JAPAN

K. S. Narasimhan
Hoeganaes Corporation
River Road
Riverton NJ 08077

Robert Naum
Applied Resources, Inc.
P.O. Box 241
Pittsford NY 14534

Malcolm Naylor
Cummins Engine Company, Inc.
P.O. Box 3005, Mail Code 50183
Columbus IN 47202-3005

Fred A. Nichols
Argonne National Laboratory
9700 S. Cass Avenue
Argonne IL 60439

H. Nickel
Forschungszentrum Juelich (KFA)
Postfach 1913
D-52425 Juelich
GERMANY

Dale E. Niesz
Rutgers University
Center for Ceramic Research
P.O. Box 909
Piscataway NJ 08855-0909

Paul W. Niskanen
Lanxide Corporation
P.O. Box 6077
Newark DE 19714-6077

David M. Nissley
United Technologies Corporation
Pratt & Whitney Aircraft
400 Main Street, MS:163-10
East Hartford CT 06108

Daniel Oblas
50 Meadowbrook Drive
Bedford MA 01730

Don Ohanehi
Magnetic Bearings, Inc.
1908 Sussex Road
Blacksburg VA 24060

Hitoshi Ohmori
ELID Team
Itabashi Branch
1-7 13 Kaga Itabashi
Tokyo 173
JAPAN

Robert Orenstein
General Electric Company
55-112, River Road
Schenectady NY 12345

Richard Palicka
Cercom, Inc.
1960 Watson Way
Vista CA 92083

Joseph N. Panzarino
379 Howard Street
P. O. Box 652
Northboro MA 01532-1545

Pellegrino Papa
Corning Inc.
MP-WX-02-1
Corning NY 14831

Terry Paquet
Boride Products Inc.
2879 Aero Park Drive
Traverse City MI 49684

E. Beth Pardue
MPC
8297 Williams Ferry Road
Lenior City TN 37771

Soon C. Park
3M Company
Building 142-4N-02
P.O. Box 2963
St. Paul MN 55144

Vijay M. Parthasarathy
Caterpillar/Solar Turbines
2200 Pacific Highway
P.O. Box 85376
San Diego CA 92186-5376

Harmut Paschke
Schott Glaswerke
Christoph-Dorner-Strasse 29
D-8300 Landshut
GERMANY

James W. Patten
Cummins Engine Company, Inc.
P.O. Box 3005, Mail Code 50183
Columbus IN 47202-3005

Robert A. Penty
Penty & Associates
38 Oakdale Drive
Rocester NY 14618

Robert W. Pepper
Textron Specialty Materials
2 Industrial Avenue
Lowell MA 01851

Peter Perdue
Detroit Diesel Corporation
13400 Outer Drive West,
Speed Code L-04
Detroit MI 48239-4001

John J. Petrovic
Los Alamos National Laboratory
Group MST-4, MS:G771
Los Alamos NM 87545

Frederick S. Pettit
University of Pittsburgh
Pittsburgh PA 15261

Richard C. Phoenix
Ohmtek, Inc.
2160 Liberty Drive
Niagara Falls NY 14302

Bruce J. Pletka
Michigan Technological Univ.
Metallurgical & Materials Engr.
Houghton MI 49931

John P. Pollinger
AlliedSignal, Inc.
Ceramic Components
P.O. Box 2960, MS:T21
Torrance CA 90509-2960

P. Popper
High Tech Ceramics Int. Journal 22
Pembroke Drive - Westlands
Newcastle-under-Lyme
Staffs ST5 2JN
ENGLAND

F. Porz
Universitat Karlsruhe
Institut fur Keramik Im
Maschinendau
Postfach 6980
D-76128 Karlsruhe
GERMANY

Harry L. Potma
Royal Netherlands Embassy
Science and Technology
4200 Linnean Avenue, N.W.
Washington DC 20008

Bob R. Powell
General Motors Corporation
Metallurgy Department
Box 9055
Warren MI 48090-9055

Stephen C. Pred
Biesterfeld U.S., Inc.
500 Fifth Avenue
New York NY 10110

Karl M. Prewo
United Technologies Res. Ctr.
411 Silver Lane, MS:24
East Hartford CT 06108

Vimal K. Pujari
Norton Company
SGNICC/NRDC
Goddard Road
Northboro MA 01532-1545

Fred Quan
Corning Inc.
Sullivan Park, FR-02-08
Corning NY 14831

George Quinn
NIST
Ceramics Division, Bldg. 223
Gaithersburg MD 20899

Ramas V. Raman
Ceracon, Inc.
1101 N. Market Blvd., Suite 9
Sacramento CA 95834

Charles F. Rapp
Owens Corning Fiberglass
2790 Columbus Road
Granville OH 43023-1200

Dennis W. Readey
Colorado School of Mines
Metallurgy and Materials Engr.
Golden CO 80401

Wilfred J. Rebello
PAR Enterprises, Inc.
12601 Clifton Hunt Lane
Clifton VA 22024

Harold Rechter
Chicago Fire Brick Company
7531 S. Ashland Avenue
Chicago IL 60620

Robert R. Reeber
U.S. Army Research Office
P.O. Box 12211
Research Triangle Park NC
27709-2211

K. L. Reifsnider
VPI & SU
Engineering Science and Mechanics
Blacksburg VA 24061

Paul E. Rempes
McDonnell Douglass Aircraft Co.
P.O. Box 516, Mail Code:0642263
St. Louis MO 63166-0516

Gopal S. Revankar
John Deere Company
3300 River Drive
Moline IL 61265

K. Y. Rhee
Rutgers University
P.O. Box 909
Piscataway NJ 08854

James Rhodes
Advanced Composite Materials
1525 S. Buncombe Road
Greer SC 29651

Roy W. Rice
W. R. Grace and Company
7379 Route 32
Columbia MD 21044

David W. Richerson
2093 E. Delmont Drive
Salt Lake City UT 84117

Tomas Richter
J. H. France Refractories
1944 Clarence Road
Snow Shoe PA 16874

Michel Rigaud
Ecole Polytechnique
Campus Universite De Montreal
P.O. Box 6079, Station A
Montreal, P.Q. Quebec H3C 3A7
CANADA

John E. Ritter
University of Massachusetts
Mechanical Engineering Department
Amherst MA 01003

W. Eric Roberts
Advanced Ceramic Technology
990 "F" Enterprise Street
Orange CA 92667

Y. G. Roman
TNO TPD Keramick
P.O. Box 595
Einhoven 5600 AN
HOLLAND

Michael Rossetti
Arthur D. Little, Inc.
15 Acorn Park
Cambridge MA 01240

Barry Rossing
Lanxide Corporation
P.O. Box 6077
Newark DE 19714-6077

Steven L. Rotz
Lubrizol Corporation
29400 Lakeland Boulevard
Wickliffe OH 44092

Robert Ruh
Wright Laboratory
WL/MLLM
Wright-Patterson AFB OH 45433

Robert J. Russell
Riverdale Consulting, Inc.
24 Micah Hamlin Road
Centerville MA 02632-2107

Jon A. Salem
NASA Lewis Research Center
21000 Brookpark Road
Cleveland OH 44135

W. A. Sanders
NASA Lewis Research Center
21000 Brookpark Road, MS:49-3
Cleveland OH 44135

J. Sankar
North Carolina A&T State Univ.
Dept. of Mechanical Engineering
Greensboro NC 27406

Yasushi Sato
NGK Spark Plugs (U.S.A.), Inc.
1200 Business Center Dr., #300
Mt. Prospect IL 60056

Maxine L. Savitz
AlliedSignal, Inc.
Ceramic Components
P.O. Box 2960, MS:T21
Torrance CA 90509-2960

Ashok Saxena
GTRI
Materials Engineering
Atlanta GA 30332-0245

David W. Scanlon
Instron Corporation
100 Royall Street
Canton MA 02021

Charles A. Schacht
Schacht Consulting Services
12 Holland Road
Pittsburgh PA 15235

Robert E. Schafrik
Natl Materials Advisory Board
2101 Constitution Ave., N.W.
Washington DC 20418

James Schienle
AlliedSignal Engines
P.O. Box 52180, MS:1302-2P
Phoenix AZ 85072-2180

Gary Schnittgrund
PyroPacific Processes
16401 Knollwood Drive
Granada Hills, CA 91344

Mark Schomp
Lonza, Inc.
17-17 Route 208
Fair Lann NJ 07410

Joop Schoonman
Delft University of Technology
P.O. Box 5045
2600 GA Delft
THE NETHERLANDS

Robert B. Schulz
U.S. Department of Energy
Office of Transportation Mater.
CE-34, Forrestal Building
Washington DC 20585

Murray A. Schwartz
Materials Technology Consulting
30 Orchard Way, North
Potomac MD 20854

Peter Schwarzkopf
SRI International
333 Ravenswood Avenue
Menlo Park CA 94025

William T. Schwessinger
Multi-Arc Scientific Coatings
1064 Chicago Road
Troy MI 48083-4297

W. D. Scott
University of Washington
Materials Science Department
Mail Stop:FB10
Seattle WA 98195

Nancy Scoville
Thermo Electron Technologies
P.O. Box 9046
Waltham MA 02254-9046

Thomas M. Sebestyen
U.S. Department of Energy
Advanced Propulsion Division
CE-322, Forrestal Building
Washington DC 20585

Brian Seegmiller
Coors Ceramics Company
600 9th Street
Golden CO 80401

T. B. Selover
AICRE/DIPPR
3575 Traver Road
Shaker Heights OH 44122

Charles E. Semler
Semler Materials Services
4160 Mumford Court
Columbus OH 43220

Thomas Service
Service Engineering Laboratory
324 Wells Street
Greenfield MA 01301

Kish Seth
Ethyl Corporation
P.O. Box 341
Baton Rouge LA 70821

William J. Shack
Argonne National Laboratory
9700 S. Cass Avenue, Bldg. 212
Argonne IL 60439

Peter T.B. Shaffer
Shaffer Associates
3225 Chimney Cove Drive
Cumming GA 30131

Richard K. Shaltens
NASA Lewis Research Center
21000 Brookpark Road, MS:302-2
Cleveland OH 44135

Robert S. Shane
1904 NW 22nd Street
Stuart FL 34994-9270

Ravi Shankar
Chromalloy
Research and Technology
Blaisdell Road
Orangeburg NY 10962

Terence Sheehan
Alpex Wheel Company
727 Berkley Street
New Milford NJ 07646

Dinesh K. Shetty
University of Utah
Materials Science and Engineering
Salt Lake City UT 84112

Masahide Shimizu
New Ceramics Association
Shirasagi 2-13-1-208, Nakano-ku
Tokyo, 165
JAPAN

Thomas Shreves
American Ceramic Society, Inc.
735 Ceramic Place
Westerville OH 43081-8720

Jack D. Sibold
Coors Ceramics Company
4545 McIntyre Street
Golden CO 80403

Johann Siebels
Volkswagen AG
Werkstofftechnologie
Postfach 3180
Wolfsburg 1
GERMANY

George H. Siegel
Point North Associates, Inc.
P.O. Box 907
Madison NJ 07940

Richard Silberglitt
FM Technologies, Inc.
10529-B Braddock Road
Fairfax VA 22032

Mary Silverberg
Norton Company
SGNICC/NRDC
Goddard Road
Northboro MA 01532-1545

Gurpreet Singh
Department of the Navy
Code 56X31
Washington DC 20362-5101

Maurice J. Sinnott
University of Michigan
5106 IST Building
Ann Arbor MI 48109-2099

John Skildum
3M Company
3M Center
Building 224-2S-25
St. Paul MN 55144

Richard H. Smoak
Smoak & Associates
3554 Hollyslope Road
Altadena CA 91001-3923

Jay R. Smyth
AlliedSignal Engines
111 S. 34th Street, MS:503-412
Phoenix AZ 85034

Rafal A. Sobotowski
British Petroleum Company
Technical Center, Broadway
3092 Broadway Avenue
Cleveland OH 44115

S. Somiya
Nishi Tokyo University
3-7-19 Seijo, Setagaya
Tokyo, 157
JAPAN

Boyd W. Sorenson
DuPont Lanxide Composites
1300 Marrows Road
Newark DE 19711

Charles A. Sorrell
U.S. Department of Energy
Advanced Industrial Concepts
CE-232, Forrestal Building
Washington DC 20585

C. Spencer
EA Technology
Capenhurst Chester CH1 6ES
UNITED KINGDOM

Allen Spizzo
Hercules Inc.
Hercules Plaza
Wilmington DE 19894

Richard M. Spriggs
Alfred University
Ctr. for Advanced Ceramic Tech.
Alfred NY 14802

Charles Spuckler
NASA Lewis Research Center
21000 Brookpark Road, MS:5-11
Cleveland OH 44135-3191

Gordon L. Starr
Cummins Engine Company, Inc.
P.O. Box 3005, Mail Code:50182
Columbus IN 47202-3005

Tom Stillwagon
AlliedSignal, Inc.
Ceramic Components
P.O. Box 2960, MS:T21
Torrance CA 90509-2960

H. M. Stoller
TPL Inc.
3754 Hawkins, N.E.
Albuquerque NM 87109

Paul D. Stone
Dow Chemical USA
1776 "Eye" Street, N.W.,#575
Washington DC 20006

F. W. Stringer
Aero & Industrial Technology
P.O. Box 46, Wood Top
Burnley Lancashire BB11 4BX
UNITED KINGDOM

Thomas N. Strom
NASA Lewis Research Center
21000 Brookpark Road, MS:86-6
Cleveland OH 44135

M. F. Stroosnijder
Institute for Advanced Materials
Joint Research Centre
21020 Ispra (VA)
ITALY

Karsten Styhr
30604 Ganado Drive
Rancho Palos Verdes CA 90274

T. S. Sudarshan
Materials Modification, Inc.
2929-P1 Eskridge Center
Fairfax VA 22031

M. J. Sundaresan
University of Miami
P.O. Box 248294
Coral Gables FL 33124

Patrick L. Sutton
U.S. Department of Energy
Office of Propulsion Systems
CE-322, Forrestal Building
Washington DC 20585

Willard H. Sutton
United Technologies Corporation
Silver Lane, MS:24
East Hartford CT 06108

Robert E. Swanson
Metalworking Technology, Inc.
1450 Scalp Avenue
Johnstown PA 15904

Yo Tajima
NGK Spark Plug Company
2808 Iwasaki
Komaki-shi Aichi-ken, 485
JAPAN

Fred Teeter
5 Tralee Terrace
East Amherst NY 14051

Victor J. Tennery
113 Newell Lane
Oak Ridge TN 37830

Monika O. Ten Eyck
Carborundum Microelectronics
P.O. Box 2467
Niagara Falls NY 14302-2467

David F. Thompson
Corning Glass Works
SP-DV-02-1
Corning NY 14831

T. Y. Tien
University of Michigan
Materials Science & Engineering
Dow Building
Ann Arbor MI 48103

D. M. Tracey
Norton Company
SGNICC/NRDC
Goddard Road
Northboro MA 01532-1545

Marc Tricard
Norton Company, WGTC
1 New Bond Street, MS-413-201
Worcester MA 01615-0008

L. J. Trostel, Jr.
Box 199
Princeton MA 01541

W. T. Tucker
General Electric Company
P.O. Box 8, Bldg. K1-4C35
Schenectady NY 12301

Masanori Ueki
Nippon Steel Corporation
1618 Ida
Nakahara-Ku Kawasaki, 211
JAPAN

Filippo M. Ugolini
ATA Studio
Via Degli Scipioni, 268A
ROMA, 00192
ITALY

Donald L. Vaccari
Allison Gas Turbines
P.O. Box 420, Speed Code S49
Indianapolis IN 46206-0420

Carl F. Van Conant
Boride Products, Inc.
2879 Aero Park Drive
Traverse City MI 49684

John F. Vander Louw
3M Company
3M Center, Bldg. 60-1N-01
Saint Paul MN 55144

Marcel H. Van De Voorde
Commission of the European
Community
P.O. Box 2
1755 ZG Petten
THE NETHERLANDS

O. Van Der Biest
Katholieke Universiteit Leuven
Dept. Metaalkunde en Toegepaste
de Croylaan 2
B-3030 Leuven
BELGIUM

Michael Vannier
Washington University,
St. Louis
510 S. Kings Highway
St. Louis MO 63110

Stan Venkatesan
Southern Coke & Coal Corp.
P.O. Box 52383
Knoxville TN 37950

V. Venkateswaran
Carborundum Company
Niagara Falls R&D Center
P.O. Box 832
Niagara Falls NY 14302

Ted Vojnovich
U.S. Department of Energy
Office of Energy Research, 3F077P
Washington DC 20585

John D. Volt
E.I. Dupont de Nemours & Co.
P.O. Box 80262
Wilmington DE 19880

John B. Wachtman
Rutgers University
P.O. Box 909
Piscataway NJ 08855

Shigetaka Wada
Toyota Central Research Labs
Nagakute Aichi, 480-11
JAPAN

Janet Wade
AlliedSignal Engines
P.O. Box 52180, MS:1303-2
Phoenix AZ 85072-2180

Richard L. Wagner
Ceramic Technologies, Inc.
537 Turtle Creek South Dr.
Indianapolis IN 46227

J. Bruce Wagner, Jr.
Arizona State University
Center for Solid State Science
Tempe AZ 85287-1704

Daniel J. Wahlen
Kohler, Co.
444 Highland Drive
Kohler WI 53044

Ingrid Wahlgren
Royal Institute of Technology
Studsvik Library
S-611 82 Nykoping
SWEDEN

Ron H. Walecki
AlliedSignal, Inc.
Ceramic Components
P.O. Box 2960, MS:T21
Torrance CA 90509-2960

Michael S. Walsh
Vapor Technologies Inc.
6300 Gunpark Drive
Boulder CO 80301

Chien-Min Wang
Industrial Technology Research Institute
195 Chung-Hsing Road, Sec. 4
Chutung Hsinchu 31015 R.O.C.
TAIWAN

Robert M. Washburn
ASMT
11203 Colima Road
Whittier CA 90604

Kevin Webber
Toyota Technical Center, U.S.A.
1410 Woodridge, RR7
Ann Arbor MI 48105

Karen E. Weber
Detroit Diesel Corporation
13400 Outer Drive West
Detroit MI 48239-4001

James K. Weddell
Du Pont Lanxide Composites Inc.
P.O. Box 6100
Newark DE 19714-6100

R. W. Weeks
Argonne National Laboratory
MCT-212
9700 S. Cass Avenue
Argonne IL 60439

Ludwig Weiler
ASEA Brown Boveri AG
Eppelheimer Str. 82
D-6900 Heidelberg
GERMANY

James Wessel
127 Westview Lane
Oak Ridge TN 37830

Robert D. West
Therm Advanced Ceramics
P.O. Box 220
Ithaca NY 14851

Thomas J. Whalen
1845 Cypress Pointe Court
Ann Arbor MI 48108

Ian A. White
Hoeganaes Corporation
River Road
Riverton NJ 08077

Sheldon M. Wiederhorn
NIST
Building 223, Room A329
Gaithersburg MD 20899

John F. Wight
Alfred University
McMahon Building
Alfred NY 14802

D. S. Wilkinson
McMaster University
1280 Main Street, West
Hamilton Ontario L8S 4L7
CANADA

James C. Williams
General Electric Company
Engineering Materials Tech.
One Neumann Way, Mail Drop:H85
Cincinnati OH 45215-6301

Steve J. Williams
RCG Hagler Bailly, Inc.
1530 Wilson Blvd., Suite 900
Arlington VA 22209-2406

Thomas A. Williams
National Renewable Energy Lab
1617 Cole Boulevard
Golden CO 80401

Craig A. Willkens
Norton Company
SGNICC/NRDC
Goddard Road
Northboro MA 01532-1545

Roger R. Wills
Ohio Aerospace Institute (OAI)
22800 Cedar Point Road
Brook Park OH 44142

David Gordon Wilson
Massachusetts Institute of
Technology
77 Massachusetts Ave., Rm 3-455
Cambridge MA 02139

J. M. Wimmer
AlliedSignal Ceramic Components
Department 27000, MS:T21
2525 W. 190th Street
Torrance CA 90509

Matthew F. Winkler
Seaworthy Systems, Inc.
P.O. Box 965
Essex CT 06426

Gerhard Winter
Hermann C. Starck Berlin GmbH
P.O. Box 25 40
D-3380 Goslar 3380
GERMANY

Thomas J. Wissing
Eaton Corporation
Engineering and Research Center
P.O. Box 766
Southfield MI 48037

James C. Withers
MER Corporation
7960 S. Kolb Road
Building F
Tucson AZ 85706

Dale E. Wittmer
Southern Illinois University
Mechanical Engineering Dept.
Carbondale IL 62901

Warren W. Wolf
Owens Corning Fiberglass
2790 Columbus Road, Route 16
Granville OH 43023

Egon E. Wolff
Caterpillar Inc.
Technical Center
P.O. Box 1875
Peoria IL 61656-1875

George W. Wolter
Howmet Turbine Components Corp.
Technical Center
699 Benston Road
Whitehall MI 49461

Wayne L. Worrell
University of Pennsylvania
3231 Walnut Street
Philadelphia PA 19104

John F. Wosinski
Corning Inc.
ME-2 E-5 H8
Corning NY 14830

Ruth Wroe
ERDC
Capenhurst Chester CH1 6ES
ENGLAND

Bernard J. Wrona
Advanced Composite Materials
1525 S. Buncombe Road
Greer SC 29651

Carl C. M. Wu
Naval Research Laboratory
Ceramic Branch, Code 6373
Washington DC 20375

David C. Wu
AlliedSignal Engines
P.O. Box 52181, MS:301-227
Phoenix AZ 85072-2181

John C. Wurst
U. of Dayton Research Institute
300 College Park
Dayton OH 45469-0101

Neil Wyant
ARCH Development Corp.
9700 S. Cass Avenue, Bldg. 202
Argonne IL 60439

Roy Yamamoto
Texaco Inc.
P.O. Box 509
Beacon NY 12508-0509

John Yamanis
AlliedSignal Aerospace Company
P.O. Box 1021
Morristown NJ 07962-1021

Harry C. Yeh
AlliedSignal, Inc.
Ceramic Components
P.O. Box 2960, MS:T21
Torrance CA 90509-2960

Hiroshi Yokoyama
Hitachi Research Lab
4026 Kuji-Cho
Hitachi-shi Ibaraki 319-12
JAPAN

Thomas M. Yonushonis
Cummins Engine Company, Inc.
P.O. Box 3005, Mail Code 50183
Columbus IN 47202-3005

Jong Yung
Sundstrand Aviation Operations
4747 Harrison Avenue
Rockford IL 61125

C. S. Yust
106 Newcrest Lane
Oak Ridge TN 37830

A. L. Zadoks
Caterpillar Inc.
Technical Center, Building L
P.O. Box 1875
Peoria IL 61656-1875

Avi Zangvil
University of Illinois
104 S. Goodwin Avenue
Urbana IL 61801

Charles H. Zenuk
Transtech
6662 E. Paseo San Andres
Tucson AZ 85710-2106

Carl Zweben
General Electric Company
P. O Box 8555, VFSC/V4019
Philadelphia PA 19101

Department of Energy
Oak Ridge Operations Office
Asst. Manager for Energy
Research and Development
P.O. Box 2001
Oak Ridge, TN 37871-8600

Department of Energy
Office of Scientific and
Technical Information
Office of Information Services
P.O. Box 62
Oak Ridge, TN 37831?